

© Copyright by Aparna Balasubramani 2017
All Rights Reserved

CARBON-BASED TECHNOLOGIES FOR REMEDIATING POLYCHLORINATED
BIPHENYLS IN CONTAMINATED SEDIMENT

A Dissertation

Presented to

the Faculty of the Department of Civil & Environmental Engineering

University of Houston

In Partial Fulfillment

of the Requirements for the Degree

Doctor of Philosophy

in Environmental Engineering

by

Aparna Balasubramani

May 2017

CARBON-BASED TECHNOLOGIES FOR REMEDIATING POLYCHLORINATED
BIPHENYLS IN CONTAMINATED SEDIMENT

Aparna Balasubramani

Approved:

Chair of the Committee
Hanadi S. Rifai, Professor
Civil & Environmental Engineering
University of Houston

Committee Members:

Upal Ghosh, Professor
Chemical, Biochemical, &
Environmental Engineering
University of Maryland, Baltimore County

William Rixey, Associate Professor
Civil & Environmental Engineering
University of Houston

Jeffrey Rimer, Associate Professor
Chemical & Biomolecular Engineering
University of Houston

Yandi Hu, Assistant Professor
Civil & Environmental Engineering
University of Houston

Suresh K. Khator, Associate Dean
Cullen College Engineering

Hanadi S. Rifai, Director
Environmental Graduate Program
Civil & Environmental Engineering

Acknowledgements

I would like to thank all those who have helped me along this challenging yet wonderful journey over the last five and a half years, and would like to extend a special thanks to the following people:

Dr. Hanadi S. Rifai, my advisor, for having the confidence in me and accepting me into the PhD in Environmental Engineering program. She has continually provided me with numerous research projects that have helped me to learn and grow as a researcher. Her constant guidance, encouragement, and support have helped me realize goals in life that seemed impossible at the beginning.

My committee members: Dr. Upal Ghosh, Dr. William Rixey, Dr. Jeffrey Rimer, and Dr. Yandi Hu, for agreeing to serve on my committee and being available whenever I needed their input and expertise with certain aspects of my research.

Dr. Pradeep Sharma and Dr. Fritz Claydon, for providing me with the opportunity to teach ENGI 1100: Introduction to Engineering in Fall 2015 and Spring 2016, thereby helping me gain experience as an instructor.

My lab mates over the years: Cagla Akat, Brad Beless, Dan Burleson, Taylour Burton, Brandon Georgetown, Adithya Govindarajan, Nathan Howell, Amin Kiaghadi, Maria Modelska, Emily Sappington, Catherine Santos, Tiffany Schmidt, Rose Sobel, and Taft Tucker, who have all helped me during various instances over the years with my research work and opened their hearts to my friendship.

My Houston family: Iswarhya, Megha, Viji, Rishi, and Shyam, who have defined my life in Houston over the past years, and have become my life-long friends.

My family: Amma, Appa, and Anand for their unconditional love and support.

CARBON-BASED TECHNOLOGIES FOR REMEDIATING POLYCHLORINATED
BIPHENYLS IN CONTAMINATED SEDIMENT

An Abstract
of a
Dissertation
Presented to
the Faculty of the Department of Civil & Environmental Engineering
University of Houston

In Partial Fulfillment
of the Requirements for the Degree
Doctor of Philosophy
in Environmental Engineering

by
Aparna Balasubramani

May 2017

Abstract

Polychlorinated biphenyls (PCBs) are persistent hydrophobic compounds that are present widely in the environment. Due to poorly maintained hazardous waste sites, electrical equipment leakage, and illegal disposal, compounds like PCBs were deposited in sediments present in bays and estuaries. PCBs continuously partition into the overlying water posing a long-term exposure risk to the environment and human health. This dissertation demonstrates the efficacy of carbon-based materials in reducing the partitioning of PCBs from sediment to the water column and analyzes their efficiency for managing PCBs in sediment in the Houston Ship Channel and Galveston Bay System (HSC-GBS) using the Environmental Fluid Dynamics Code (EFDC) water quality model. Both existing carbon-based materials [activated carbon (AC), black carbon (BC)] and emerging nanomaterials [graphene (GE), graphene oxide (GO), carbon nanotube (CNT)] were tested to determine their efficacy to bind PCBs in sediment. The comparison between the sorbents was accomplished by examining their distribution coefficient (K_s). The magnitude of K_s provides an idea about the bioavailable fraction of PCBs in the system; the higher the K_s , the greater the strength of sorption by the sorbent and therefore, the lower the PCB bioavailability. The EFDC model grid was developed for the HSC-GBS and the Toxics module was used to simulate the fate and transport of five PCB congeners (PCB-1, PCB-3, PCB-11, PCB-17, and PCB-25). Model sensitivity was examined and the model was most sensitive to sediment PCB concentrations and partitioning properties. Results from the sorption experiment indicated that CNT performed the best overall followed by AC, BC, GO and GE. Results indicated that the K_s value for CNT was 1.16, 1.15, 1.13 and 1.04 log

units greater than GE, GO, BC, and AC. The EFDC results showed a significant dependence between the change in organic carbon in sediment and the partitioning coefficients in the sediment bed, against the concentration of PCBs in the water column. Modeling results also demonstrated that there was an average reduction of 35% in the concentrations in the HSC-GBS when carbon-based materials were added to sediment.

Table of Contents

Acknowledgements	v
Abstract	vii
Table of Contents.....	ix
List of Figures	xii
List of Tables.....	xvi
Chapter 1. Introduction and Objectives	1
Chapter 2. Background	5
2.1 Polychlorinated biphenyls (PCBs).....	5
2.1.1 Physico-chemical properties of PCBs	6
2.1.2 PCBs in the environment.....	9
2.1.3 Degradation of PCBs	10
2.2 Sediment remediation of PCBs.....	13
2.2.1 Current sediment remediation technologies	13
2.2.2 Carbon-based technologies for remediation of PCBs.....	20
2.3 PCBs in the Houston Ship Channel and Galveston Bay System (HSC-GBS)	22
2.3.1 Description of the HSC-GBS	23
2.3.2 Occurrence and distribution of PCBs in the HSC-GBS	23
2.3.3 Partitioning of PCBs in the HSC-GBS	28
2.3.4 Modeling of PCBs in bays and estuaries	30

Chapter 3. Materials and Methods	32
3.1 Effluent sampling methods and analyses.....	32
3.1.1 Sample collection	32
3.1.2 Chemical analyses	35
3.2 Sorbent experimental methods and materials.....	36
3.2.1 Chemicals and lab materials	36
3.2.2 Carbon-based materials	37
3.2.3 Experimental setup	38
3.2.4 Determination of K_s	40
3.3 Model development	41
3.3.1 Model setup	42
3.3.2 Model calibration.....	54
3.3.3 Model output.....	56
3.3.4 Model predictions	57
Chapter 4. Results and Discussion	60
4.1 PCBs in industrial and municipal effluents in the HSC-GBS	60
4.1.1 PCB congener patterns	60
4.1.2 Total PCB ($\Sigma 209$) concentrations	63
4.1.3 Suspended mass concentrations.....	66
4.1.4 PCB homolog concentrations in dissolved and suspended phases...	66
4.1.5 Distribution of PCBs between dissolved and suspended media.....	68
4.1.6 Suspended fraction as a function of $\log(K_{ow})$	70
4.1.7 Estimating organic carbon partitioning coefficients in effluents.....	75

4.1.8	Discussion.....	79
4.2	Experimental results	81
4.2.1	Sorbent characteristics	81
4.2.2	Quality assurance (QA)/Quality control (QC).....	83
4.2.3	Appropriate use of PDMS fibers	84
4.2.4	Distribution coefficients (K_s) and comparison between sorbents.....	85
4.2.5	Discussion.....	89
4.3	Modeling results	89
4.3.1	Calibration run.....	89
4.3.2	Model calibration/validation.....	93
4.3.3	Sensitivity analyses.....	93
4.3.4	Sediment remediation using carbon-based materials	97
4.3.5	Discussion.....	100
Chapter 5. Summary and Conclusions		102
References.....		104

List of Figures

Figure 2-1. Chemical structure of a PCB molecule	7
Figure 2-2. Chemical structure of PCDD/Fs.....	8
Figure 2-3. PCB clean-up criteria in sediment based on type of waterbody	15
Figure 2-4. Schematic honeycomb structure of a graphene sheet (adapted from Wang et al. [85])	21
Figure 2-5. Schematic structure of graphene oxide (adapted from Nasrollahzadeh et al. [88])	21
Figure 2-6. Schematic structure of single and multi-walled CNTs (adapted from Choudhary and Gupta [90])	22
Figure 2-7. HSC-GBS segments that exhibit PCBs and dioxin in edible tissue (Source: TCEQ 2014 303(d) List).....	24
Figure 2-8. Locations sampled for PCBs in the various sampling campaigns	26
Figure 2-9. Total PCBs ($\Sigma 209$) in sediment (ng/g) over time (totals represent all 209 congeners for all the years and stations).....	27
Figure 2-10. Conceptual framework of EFDC model setup and field sampling measurements	29
Figure 3-1. Locations of the effluent outfalls sampled for PCBs	34
Figure 3-2. The HSC-GBS grid used in EFDC with boundary conditions.....	43
Figure 3-3. Fraction of clay, silt and sand in the sediment bed measured in the HSC-GBS	45
Figure 3-4. Locations of USGS gages that were used to obtain flows for the model.....	47
Figure 3-5. Structure of toxic module (adapted from Ji [120]).....	49

Figure 3-6. PCB water and sediment sampling locations in 2002-2003.....	51
Figure 3-7. Evaluation of spin-up time for the model	53
Figure 4-1. Total PCBs ($\Sigma 209$) and distribution of PCB homolog concentration at each of the effluent outfalls in the suspended phase. Non-detects = $\frac{1}{2}$ MDL.....	64
Figure 4-2. Total PCBs ($\Sigma 209$) and distribution of PCB homolog concentrations at each of the effluent outfalls in the dissolved phase. Non-detects = $\frac{1}{2}$ MDL	64
Figure 4-3. Total mass concentration of the PCBs and the average detected congener concentration of the PCBs in the suspended phase at each of the outfalls	67
Figure 4-4. Distribution of all detected PCB congener concentrations between the dissolved and suspended phases at the sampled wastewater treatment plants (except for WWTP2 that had a very low detection rate)	69
Figure 4-5. Suspended fraction of PCBs in water at each of the municipal wastewater treatment plant outfall locations plotted against the $\log K_{ow}$ for the detected concentrations in the suspended and dissolved phases.....	71
Figure 4-6. Suspended fraction in water at each of the industrial effluent outfall locations plotted against the $\log K_{ow}$ for the detected concentrations in the suspended and dissolved phases.....	73
Figure 4-7. Suspended fraction in water at the two industrial wastewater treatment plants (O3 and O4), refuse system (O1), and special warehousing and storage facility (O2) plotted against the $\log K_{ow}$	74
Figure 4-8. Comparison of HSC-GBS $\log K_{toc,adj}$ values of industries and wastewater treatment plants with data obtained from Seth et al. [126] model and Hansen et al. [127]. Error bars represent standard deviation.....	78

Figure 4-9. SEM images of activated carbon, black carbon, zoomed in image of graphene, graphene oxide particles, and non-functionalized carbon nanotubes	82
Figure 4-10. Line graph of $\log(K_s)$ values for each of the 11 PCB congeners and five sorbent materials. Each point represents the average measured $\log(K_s)$ value for that congener-sorbent combination.....	86
Figure 4-11. Comparison of $\log(K_s)$ values of PCB-4 and PCB-2	88
Figure 4-12. Spatial distribution of PCB-1 in the water column after 30 days of simulation time	90
Figure 4-13. Spatial distribution of PCB-3, PCB-11, PCB-17, and PCB-25 in the water column after 30 days	91
Figure 4-14. Temporal distribution of PCB-1 in the water column at five different locations in the HSC-GBS.....	92
Figure 4-15. Results of sensitivity analysis for OC for PCB-1 at Buffalo Bayou	94
Figure 4-16. Results of sensitivity analysis of K_{poc} and K_{doc} for PCB-1 at the HSC-SJR confluence.....	95
Figure 4-17. Percent change in the cumulative mass loading of PCBs into Galveston Bay	96
Figure 4-18. Temporal distribution of PCB-1 in the HSC-GBS between run 9 and calibration run.....	97
Figure 4-19. Spatial difference in PCB-1 concentration in the water column between run 9 and the calibration run	98
Figure 4-20. Spatial distribution of PCB-1 concentration in the water column between the	

calibration run and the carbon run.....	99
-----------------------------------------	----

Figure 4-21. Time series comparison at area of higher contamination (Burnett Bay) for

PCB-1	100
-------------	-----

List of Tables

Table 2-1. List of Aroclors and percent chlorine (by mass): ^a ATSDR [34]	6
Table 2-2. Summary of WHO 2005 TEF value for dioxin-like PCBs: ^a van den Berg et al. [38]	8
Table 2-3. Physical properties of the 11 PCB congeners used in the current study: ^a Hawker and Connell [49], ^b Mackay et al. [50], ^c Brodsky and Ballschmiter [51], and ^d Sinkkonen and Paasivirta [52]	11
Table 2-4. <i>In situ</i> sediment PCB remediation technologies used at specific sites: ^a Effectiveness in some studies is based on how the technology performed in the field (the material retained a strong stabilization capacity to reduce aqueous concentrations) and in the laboratory for certain studies	17
Table 3-1. Physical properties of PCB congeners used in the EFDC model	50
Table 3-2. PCB concentrations at stations sampled in 2003 within the time period of EFDC calibration run	55
Table 3-3. Description of sensitivity analysis runs	55
Table 3-4. Partitioning coefficients used in the model for the carbon-based materials....	59
Table 4-1. Number of detects and the three congeners which show maximum concentrations in the dissolved and suspended phases for all effluents	61
Table 4-2. Atomic mass fractions determined using EDS elemental analysis	82
Table 4-3. Average log (K_s) values calculated for each sorbent with each of the 11 PCB congeners used in the experiment. The \pm values indicate the standard deviation from the average.....	86
Table 4-4. Rankings of the five sorbent materials based on their K_s values	87

Table 4-5. Total water concentrations obtained from the EFDC model compared to the	
sampling data	93

Chapter 1. Introduction and Objectives

Polychlorinated biphenyls (PCBs) ($C_{12}H_{10-x}Cl_x$) are anthropogenic organic chemical compounds that consist of two benzene rings (biphenyl ring) with chlorine atoms attached to the benzene rings and are a family of 209 congeners (chemical substances that are related to one another through origin, structure, or function). PCBs have been manufactured in numerous industries in the U.S. since 1929. Due to their high chemical stability and electrical insulating properties, PCBs were manufactured commercially and used in a wide range of electrical equipment such as transformers, capacitors, regulators, hydraulic fluids, plasticizers, and lubricants [1] until their ban in 1979 [2]. Within two to three decades after their introduction, PCBs were found in several environmental media around the world [3-19]. Being chemically stable, PCBs are not readily biodegradable and thus, tend to persist in the environment for relatively long periods of time earning the designation of being persistent organic pollutants (POPs). Their removal from environmental media, as will be seen later in this dissertation, has proven to be challenging.

The United States Environmental Protection Agency (USEPA) currently lists 527 sites in the Superfund program that have PCBs as their contaminant of concern (COC), including major water bodies such as the Great Lakes and the Hudson River [20]. While the Superfund list does not include the Houston Ship Channel and Galveston Bay System (HSC-GBS) studied in this research, Patrick Bayou, one of the tributaries of the HSC is on the Superfund List with PCBs as one of the COCs. Additionally, the HSC-GBS is listed on the Texas 303d list of water bodies [21] that exhibit water quality concentrations in excess of established standards; in this case, not only for PCBs but also for other POPs,

including dioxins, chlordane, and dieldrin. Several studies have documented the presence and distribution of PCBs in HSC-GBS sediment, water, fish tissue and effluent discharges [22-26].

Because of its presence in air, water, soils, and sediment; PCB exposure is via ingestion, inhalation, and/or dermal pathways throughout the life of an individual [1]. Negative health effects include chloracne, liver disorders, damage to the immune and reproductive systems, and even cancer [1]. Once in the environment, PCBs move relatively easily between media (e.g., partitioning from sediment to water and water to air). Current remediation practices include dredging and *in situ* or *ex situ* treatment; these technologies are costly, in some cases limited in their effectiveness, and in other cases mobilize the pollution and increase the exposure risk [27-29]. Hence, there is a critical need for less invasive, and environmentally friendly longer term solutions for PCB pollution in natural water systems that limit its bioavailability (the degree and rate at which a contaminant is absorbed into a living organism or made available at the contaminated site), thereby lowering the risk of exposure while allowing sufficient time for eventual breakdown and biodegradation.

The study presented in this research addresses the aforementioned needs and investigates carbon-based materials as sorbents to manage PCBs in sediment and reduce their partitioning into the water column. The materials studied include: activated carbon (AC), black carbon (BC), graphene (GE), graphene oxide (GO), and carbon nanotube (CNT). Laboratory experiments were undertaken to quantify the partitioning coefficients associated with 11 representative PCB congeners (PCB-1, PCB-2, PCB-4, PCB-8, PCB-15, PCB-52, PCB-72, PCB-77, PCB-138, PCB-156, and PCB-169) and compare the

efficacies of the studied materials in sequestering the 11 PCBs. The efficiency of the carbon-based materials for restoring water quality in a natural water system was demonstrated using an Environmental Fluid Dynamics Code (EFDC) water quality model that was specifically developed for the HSC-GBS. The model was calibrated to measured PCB concentrations and was used to simulate the mixing of the carbon-based materials into the sediment and predict future PCB concentrations over time.

The overall goal of the dissertation was to demonstrate the efficacy of carbon-based materials in reducing the partitioning of PCBs from sediment to water column and analyzing their efficiency for managing PCBs in sediment in natural water systems.

Specific objectives included:

1. Characterizing the distribution of PCBs in effluents in the HSC-GBS and understanding their partitioning behavior in the estuary;
2. Determining K_s , the distribution coefficient between sorbent and water for AC, BC, GE, GO, and CNT;
3. Developing an EFDC water quality model to simulate the measured distribution of PCBs in the HSC-GBS;
4. Simulating the mixing of the carbon-based materials into the HSC-GBS sediment and associated change in partitioning from the sediment to the water column;
5. Understanding the efficiency associated with using the studied carbon-based materials in reducing PCB concentrations in water in the HSC-GBS over time.

The research approach involves understanding the physical and chemical properties of PCBs and how they behave (partition) in the environment, thereby aiding in the

evaluation of remediating PCBs in sediments using carbon-based materials. The next chapter (Chapter 2) provides background information that has been published on PCBs in the environment, current sediment remediation technologies, and the status of PCB contamination in the HSC-GBS. Chapter 3 provides a detailed description of the sample collection of effluents, and the chemical analyses performed to obtain the concentration of PCBs. Additionally, both the experimental methods to evaluate the efficacy of the various carbon-based materials, and the EFDC model development for simulating the distribution of PCBs in the HSC-GBS and their remediation via the carbon-based materials under study are provided in Chapter 3. Results are provided in Chapter 4 with emphasis on the potential for carbon-based materials to control the truly dissolved (freely available concentration present in the porewater of sediments) concentration of PCBs in the HSC-GBS. Conclusions are discussed in Chapter 5.

Chapter 2. Background

2.1 Polychlorinated biphenyls (PCBs)

As stated in Chapter 1, PCBs are hydrophobic compounds that belong to the class of compounds referred to as POPs. POPs are chemical compounds that are extremely resistant to various degradation processes occurring in the environment. The estimated half-life of a PCB in the environment is approximately eight to 15 years, depending upon the congener [30], and up to twenty years in a human body [31]. Thus, if 2ng/L of PCB is present in water in the HSC-GBS studied in this dissertation, it would take approximately 14-28 years depending on the congener type for the concentration to attenuate to below the Texas Commission on Environmental Quality (TCEQ) surface water quality standard of 0.64ng/L [32].

PCBs were commercially produced as mixtures called Aroclors between 1930 and 1979. Different types of Aroclors were manufactured, and the first two digits in the numbering of the Aroclor mixture represents the number of carbon atoms in the phenyl ring, and the last two digits represent the percentage of chlorine (by mass) present in the mixture [33]. Table 2-1 gives the list of Aroclor mixtures and their percent weight of chlorine, when available (the percent chlorine for the Aroclor mixtures was obtained from ATSDR [34]). As can be seen in the Table, PCBs can contain as little as 20% all the way to more than 60% chlorine by weight. Prior to the development of an improved PCB quantitation method to identify individual PCB congeners (USEPA method 1668A in 1995), analytical methods were only available to quantify Aroclors.

This section will focus on the physical and chemical properties of PCBs, their presence in the environment due to legacy contamination, their biodegradability, and

their fate and transport in the environment.

Table 2-1. List of Aroclors and percent chlorine (by mass): ^aATSDR [34]

IUPAC Name	Percent Chlorine (by mass)^a
Aroclor 1016	41.50%
Aroclor 1210	<i>n/a</i>
Aroclor 1216	<i>n/a</i>
Aroclor 1221	21%
Aroclor 1231	<i>n/a</i>
Aroclor 1232	32%
Aroclor 1240	<i>n/a</i>
Aroclor 1242	41.50%
Aroclor 1248	48%
Aroclor 1250	<i>n/a</i>
Aroclor 1252	<i>n/a</i>
Aroclor 1254	54%
Aroclor 1260	60%
Aroclor 1262	61.5%-62.5%
Aroclor 1268	68%

2.1.1 Physico-chemical properties of PCBs

PCBs ($C_{12}H_{10-x}Cl_x$) are man-made organic chemical compounds that consist of two benzene rings (biphenyl ring) with chlorine atoms attached to the benzene rings as shown in Figure 2-1. The number of chlorine atoms attached to the biphenyl ring ranges between one and ten. Depending on the positions to which the chlorine atoms are attached on the biphenyl ring, 209 different congeners of PCBs can be formed. The structure and toxicity of these congeners varies depending on the position to which the chlorine atoms are attached [35], and they exist in varying consistencies as liquids (light-colored) or waxy solids (light-colored to black) [2]. In addition, the position and number of chlorine atoms also affects the partitioning of PCBs from sediment into the water column, with the heavier congeners preferentially remaining in the sediment.

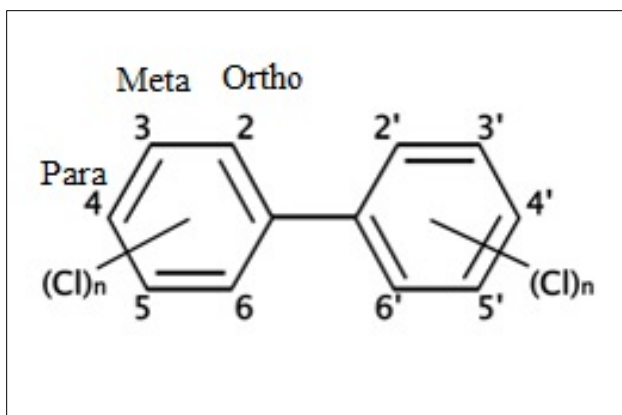


Figure 2-1. Chemical structure of a PCB molecule

Also based on the number of chlorine atoms and position to which they are attached, PCBs can be either planar or non-planar; a characteristic that determines their toxicity [35]. The dihedral angle between the two-phenyl rings is used to determine the planarity: the smaller the dihedral angle, the higher the planarity of the PCB congener. The dihedral angles for non-, mono-, and di-ortho-PCBs are approximately 40°, 60°, and 90°, respectively [36, 37]. When the two-phenyl rings of a PCB congener are in the same plane, they are termed to be coplanar, and this makes the PCB structurally similar to polychlorinated dibenzo-p-dioxins and dibenzo-furans (PCDD/Fs) (see Figure 2-2), causing them to be termed dioxin-like PCBs. The 4 non-ortho (PCB-77, PCB-81, PCB-126, PCB-169), and 8 mono-ortho (PCB-105, PCB-114, PCB-118, PCB-123, PCB-156, PCB-157, PCB-167, PCB-189), constitute the 12 dioxin-like PCBs [38]; these are included when the exposure risk for dioxins are estimated. Table 2-2 gives the toxic equivalency factors (TEF): “or the factor that indicates the degree of toxicity in comparison to the most toxic compound which is given a reference value of 1” of the 12 dioxin-like PCBs set by the World Health Organization (WHO) in 2005 that range from 0.00003 to 0.10 with PCB-126 exhibiting the highest TEF of 0.10.

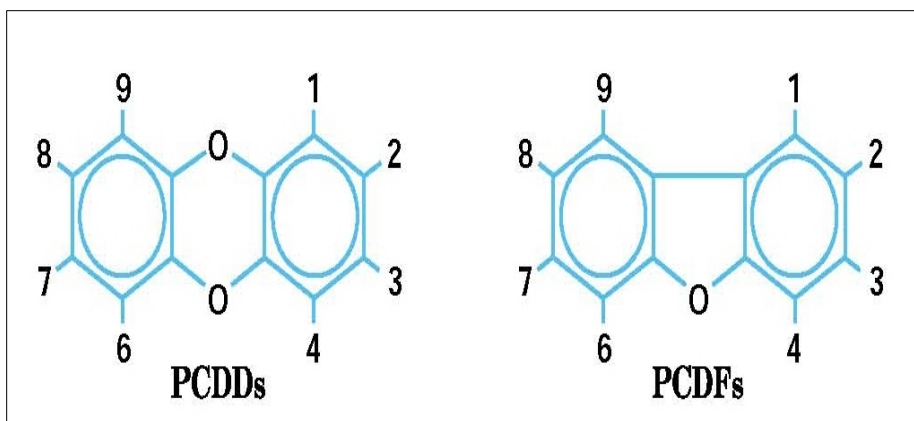


Figure 2-2. Chemical structure of PCDD/Fs

Table 2-2. Summary of WHO 2005 TEF value for dioxin-like PCBs: ^avan den Berg et al. [38]

Compound	WHO 2005 TEF ^a
<i>Non-ortho-substituted PCBs</i>	
PCB-77	0.0001
PCB-81	0.0003
PCB-126	0.10
PCB-169	0.03
<i>Mono-ortho-substituted PCBs</i>	
PCB-105	0.00003
PCB-114	0.00003
PCB-118	0.00003
PCB-123	0.00003
PCB-156	0.00003
PCB-157	0.00003
PCB-167	0.00003
PCB-189	0.00003

The International Agency for Research on Cancer (IARC) classified PCBs as carcinogenic to humans based on acceptable evidence of carcinogenicity in both humans and experimental animals [39]. Lauby-Secretan et al. [39] also termed dioxin-like PCBs to be carcinogenic, but claimed that the carcinogenicity of PCBs is not solely attributed to the dioxin-like PCB congeners. In addition, the USEPA has performed several studies to support the evidence that PCBs can cause cancer in both animals and humans [40]. In the

U.S., the human-health criterion for PCBs in fish tissue was set at 47ng/g [41], and in water was set at 0.64ng/L [32] by TCEQ for Texas. In addition, some states in the U.S. have sediment based standards for clean-up of PCBs, but many do not (Texas is among these).

2.1.2 PCBs in the environment

Although the manufacture of PCBs was banned in 1979, PCBs found their way into the environment, prior to the ban in the U.S. Even today, PCBs can still be released into the environment due to grandfathered stockpiles of PCBs produced before 1979, poorly maintained hazardous waste sites contaminated with PCBs, illegal disposal of PCB wastes and improper handling of consumer products containing PCBs into landfills not designed to manage hazardous waste, leaks from electrical equipment that contain PCBs, and incineration of waste [2]. Rauner [1] suggested that more than 50% of the PCBs that have been commercially produced have found their way into the environment. It should also be noted that while their ban was enacted in the U.S., PCBs remain in production and in use in many other countries around the world [42, 43].

Current sources of PCBs also include direct discharges to water bodies via permitted or unpermitted flows. Municipal and industrial effluents have been found to contain measurable concentrations of PCBs as will be seen later in section 4.1 of this dissertation. At present, there are no PCB limits for effluent that are associated with a National Pollutant Discharge Elimination System (NPDES) permit.

Of most concern are the presence of PCBs in numerous water bodies due to their associated ecological impacts, increased risk of exposure via consumption of contaminated seafood, and the difficulty of remediating natural water systems. The Great

Lakes, one of the most studied waterbodies in the U.S. for example, has PCB contamination in Lake Michigan from a release of 100,000 tons of PCBs in 1954 [30]. Sludge concentrations were as high as 500,000mg/kg and PCB concentrations in water were approximately 3µg/L [44]. Despite extensive remediation efforts and the recent establishment of The Great Lakes Restoration Initiative (GLRI) in 2010, which designated 42 areas of concern around the Great Lakes and careful monitoring of PCBs at those sites, the Great Lakes remain heavily polluted [11]. Other examples of PCB contaminated natural water systems include the New Bedford Harbor in Bristol County, Massachusetts [45] that has more than 900,000 cubic yards of contaminated sediment, the Hudson River in New York with more than 1.3 million pounds of PCBs that were released between 1947 and 1977 [46], and Twelve Mile Creek in Pickens, South Carolina where 400,000 pounds of PCB-laden wastewater was discharged into the Creek between 1955 and 1977 [47]. All three have been the subject of sediment remediation studies as will be seen in section 2.2.

2.1.3 Degradation of PCBs

As discussed above, the unique physical and chemical properties of PCBs have made them popular for use in various industrial applications. These same unique properties, however, are the main reasons behind their persistence. PCBs are largely insoluble in water, but highly soluble in lipids. As solubility plays a very important role in the degradation of a compound, the low aqueous solubility of PCBs makes its degradation by microorganisms difficult [48]. But, it should be understood here that different PCB congeners exist in the environment as a mixture, and hence, the solubility of a PCB congener in water would be lower than its actual solubility listed in Table 2-3. To take

Table 2-3. Physical properties of the 11 PCB congeners used in the current study: ^aHawker and Connell [49], ^bMackay et al. [50], ^cBrodsky and Ballschmiter [51], and ^dSinkkonen and Paasivirta [52]

PCB Congener	IUPCA Name	# of Chlorine Substitutions	Ortho-Positions	Octanol-Water Partitioning Coefficient ^a	Molecular Weight	Molecular Volume ^b	Solubility ^c	Half-life in Sediment ^d
				log (K _{ow})	MW (g/mol)	V _m (cm ³ /mol)	S _w (µg/L)	t _{1/2} (years)
PCB-1	2-Chlorobiphenyl	1	mono	4.46	188.66	205.50	1431.10	No data
PCB-2	3-Chlorobiphenyl	1	non	4.69	188.66	205.50	768.55	No data
PCB-4	4-Chlorobiphenyl	2	di	4.65	223.10	226.40	417.83	No data
PCB-8	2,4'-Dichlorobiphenyl	2	mono	5.07	223.10	226.40	769.14	No data
PCB-15	4-4'-Dichlorobiphenyl	2	non	5.30	223.10	226.40	94.08	No data
PCB-52	2,2',5,5'-Tetrachlorobiphenyl	4	di	5.84	291.99	268.20	29.20	10
PCB-72	2,3',5,5'-Tetrachlorobiphenyl	4	mono	6.26	291.99	268.20	24.28	10
PCB-77	3,3',4,4'-Tetrachlorobiphenyl	4	non	6.36	291.99	268.20	0.99	10
PCB-138	2,2',3,4,4',5'-Hexachlorobiphenyl	6	di	6.83	360.88	310.00	1.50	19
PCB-156	2,3,3',4,4',5-Hexachlorobiphenyl	6	mono	7.18	360.88	310.00	1.70	19
PCB-169	3,3',4,4',5,5'-Hexachlorobiphenyl	6	non	7.42	360.88	310.00	0.50	19

this into consideration, the experiments undertaken in this research were set up with a mixture of 11 PCB congeners, and Table 2-3 (adapted from Beless [53]) provides the physical properties of the 11 PCB congeners used in the study experiments that exhibit different chlorination and solubility levels. As can be seen in the Table, chlorination levels varied from one to six and solubility levels ranged from 0.50 μ g/L to 1431.10 μ g/L.

Effluent discharges, air deposition, and illegal dumping are among the sources that [22] have caused PCBs to be present in waterbodies. The total PCB concentration in water is the sum of the dissolved and suspended fractions, and the partitioning of PCBs is a function of organics in the system (organic elements in water, organic carbon fractions, etc.). Partitioning of PCBs from sediment to water will be discussed in detail in section 2.3.3. The PCBs dissolved in water adsorb on sediments and organic matter due to their inherently hydrophobic nature, and deposit onto the sediment bed while continually partitioning into the porewater within the sediment. Further, PCBs continue to move to the water by means of desorption, bioturbation, erosion, etc., which in turn can lead to their transport into air [18]. Table 2-3 provides data on half-lives ($t_{1/2}$) for some of the PCBs studied in this dissertation, and it can be observed that $t_{1/2}$ increases with the increase in chlorination, thereby indicating that higher chlorinated congeners tend to remain in the sediment for longer periods of time. The strength of sorption of the different PCB congeners is based on water solubility and the octanol-water partition coefficient (K_{ow}) of the congener (see Table 2-3 that shows $\log(K_{ow})$ ranging from 4.46 to 7.42 for the studied congeners). Although the more water soluble lower chlorinated congeners have higher potential to desorb from the sediments and move into the water column, the sedimentation rate can still heavily reduce the concentration of PCBs in the

water by causing the PCBs to bind to particulates [18]. Hence, the PCBs tend to accumulate in the sediments, rather than move into the water column [54].

Only a fraction of the PCBs present in sediment are typically available as truly dissolved molecules in the porewater, i.e., freely available for sorption/uptake by micro/macro-organisms [55] (see section 2.3.3 for more information). The bioavailable fraction of PCBs is taken up directly by benthic organisms thereby allowing the PCBs to further progress into the food chain [18]. A long-term elimination study conducted by De Boer et al. [56] with eel exposed to PCBs showed that the half-lives of tetra- and penta-PCBs ranged from one to four years in the eel, and that no elimination of hexa- and octa-PCBs occurred, concluding that once accumulated, PCBs never leave the organism. For example, the lifespan of an American eel is 43 years, and hence, for the eel to be free (really low concentrations) of the lower chlorinated PCBs (assume the eel consumed a concentration of 1ng/L when it was 20 years old), it would be approximately 48 years for the concentration to go to 0.00785ng/L, assuming that there was no further PCB ingestion by the eel during this time period.

Hence, in this study, the focus of the experiments is on the determination of the concentration of PCBs in the truly dissolved phase, and this will be discussed in detail in sections 3.2 and 4.2.

2.2 Sediment remediation of PCBs

2.2.1 Current sediment remediation technologies

Conventionally, dredging has been used in the U.S. to remove hundreds of millions of cubic yards of sediment [57] to keep waterways and channels navigable for movement of ship and barge traffic. Therefore, it was logical to also use dredging to physically remove

contamination from a location.

The USEPA has implemented varying PCB clean-up criteria in sediment based on the type of waterbody (see Figure 2-3). It is important to note here that these clean-up criteria are developed based on existing/available conventional technologies at sites where remediation has begun, and might not be consistent with applicable water quality standards and/or tissue consumption standards. This is an important consideration and is one of the main reasons for exploring technologies in this dissertation that limit the bioavailability of PCBs. It is also important to note from Figure 2-3 that no PCB sediment clean-up criteria are available for Texas at present.

Recent evidence suggests that dredging may cause further resuspension and mobilization of PCBs [3, 7, 19, 58-61]. As a result, alternative *in situ* technologies and strategies have been explored and are discussed in the next section.

In situ sediment remediation technologies can be broadly categorized into five types (Table 2-4): monitored natural recovery (MNR), enhanced monitored natural recovery (EMNR), conventional capping, amendment capping, and *in situ* treatment. MNR is the process where natural sediment deposition or other risk attenuation processes are used to manage the contamination while EMNR applies a physical thin layer of confining material (typically sand) on the contamination, thereby reducing the bio-uptake of contamination by benthic organisms and fish. When a cap made of sand, or clay, or sediment is used to both physically and chemically isolate the contamination, it is termed conventional capping. Amendment capping is the process whereby activated carbon (AC), or carbon, or natural carbon is co-placed along with an inert cap material like sand, to isolate the contamination in the sediment. The placement of various adsorbents like

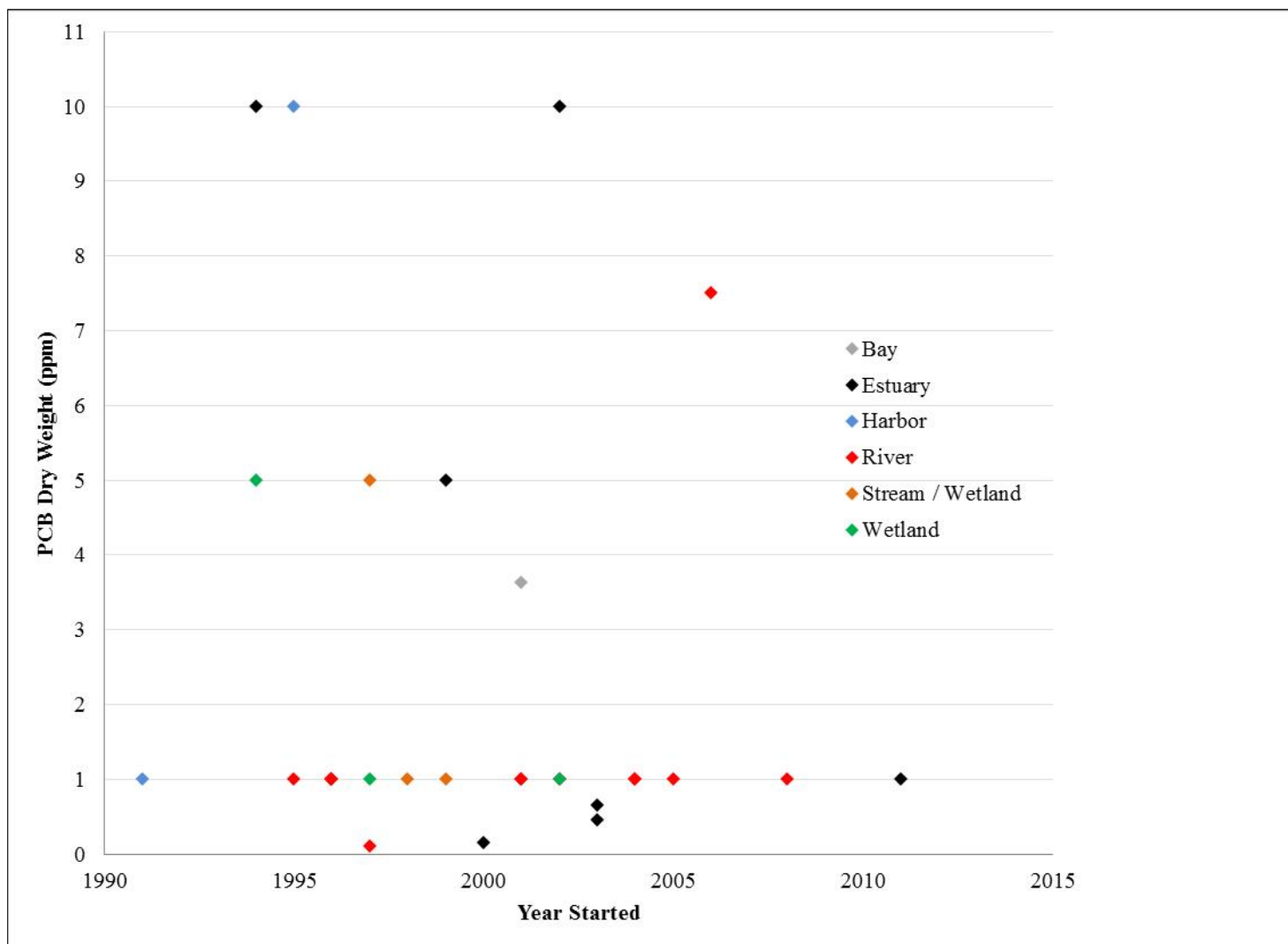


Figure 2-3. PCB clean-up criteria in sediment based on type of waterbody

AC or natural carbon directly on the contaminated sediments to reduce exposure and bioavailability is the principle behind *in situ* treatment, and is the most favorable choice to remediate contaminated sediments at present. Table 2-4 provides more details about the use of the aforementioned technologies to manage PCBs, along with the expected reduction in risk. These details in the Table provide valuable information about the specific technologies that can be used depending on the site where remediation needs to be performed. Other *in situ* technologies that have been explored include iron catalyzed degradation, and direct redox control reactions using electrodes [62]; these will not be discussed here as they are not related to the topic of the dissertation.

While AC has been demonstrated as an effective carbon-based sorbent via capping, other carbon-based materials have yet to be explored for use in caps or when mixed into the sediment. For natural systems like the HSC-GBS that also serve as navigation water bodies, the stability and sustainability of amended caps would be of concern as would be the changing hydrodynamic environment particularly during floods and hurricanes and diurnal tidal influences. Replacing amended caps on a regular basis would be cost-prohibitive whereas the ability to amend the sediment with mixed-in carbon-based materials may be more sustainable and effective.

Table 2-4. *In situ* sediment PCB remediation technologies used at specific sites: ^aEffectiveness in some studies is based on how the technology performed in the field (the material retained a strong stabilization capacity to reduce aqueous concentrations) and in the laboratory for certain studies

Technology	Cap Material	Technology Advantages	Technology Limitations	Appropriate Site Conditions	Locations/Applications	References	Effectiveness/ Expected Risk Reduction ^a
MNR		Minimally invasive, minimal cost	Dependent upon availability and consistency of natural attenuation processes; Significant long-term monitoring costs	Typically stable, depositional environment	- Twelve-Mile Creek/Lake Hartwell (PCBs), Pickens County, South California - Bremerton Naval Complex Superfund Site (PCBs) - Washington's Puget Sound	[63, 64]	Variable
EMNR		Minimally invasive, minimal cost	Thickness should exceed depth of expected substantial bioturbation; Erosional and/or mixing processes could negate effectiveness over time	Typically stable, depositional environment due to lack of other dioxin fate processes	- Peninsular Harbor (PCBs), Canada - Bremerton Naval Complex (PCBs) - Washington's Puget Sound	[65, 66]	50-90%
Conventional Capping	Sand	Relatively inexpensive and implementable with readily available equipment and can be quite	May not be effective in active environments (e.g. rapid groundwater upwelling or location subject to significant erosion)	Potentially applicable in most sediment environments, particularly with armoring to manage	- Sheboygan River, Wisconsin (PCBs) - Convair Lagoon (PCBs) San Diego, CA	[63]	50-90%

Table 2-4 continued

		effective for the strongly sorbing, low mobility dioxin		potential resuspension			
Conventional Capping	Clay/Sediment	Relatively inexpensive and implementable with readily available equipment; Presence of natural organic matter can significantly increase performance	Clay and fines more difficult to place than sand and potentially more subject to resuspension and loss	Generally applicable only in stable depositional environments except where the cap is armored to protect against erosive events	- Simpson-Tacoma, Washington (cresote, PAHs and Dioxins) Denny Way - Washington (PAHs and PCBs)	[67]	>90%
Amendment Capping	Activated Carbon	Extremely effective in that exhibits advantages of both carbon treatment and a cap	May be difficult to place uniformly with more dense inert material such as sand. Non-uniform placement impacts performance (thin concentrated layers much less effective than uniformly mixed)	Potentially applicable in most sediment environments, particularly with armoring to manage potential resuspension	- Olympic view resource area(PCBs and Dioxins) - WA Trondheim Harbour(PAHs and PCBs), Norway - Grenlandfjords (Dioxins/Furans), Norway	[68, 69]	>95%
		Easier, demonstrated placement of activated carbon	Thin layer of active material less effective than uniformly mixed amendments	Potentially applicable in most sediment environments	- Anacostia River, (PAHs and PCBs), Washington D.C.	[70]	>90%

Table 2-4 continued

<i>In Situ</i> Treatment	Activated Carbon	Theoretically effective at reducing bioavailability and exposure	Fouling of AC or resuspension in active environment could reduce effectiveness over time; Concerns over mixing over biologically active zone due to potential for resuspension and loss of contaminants and/or AC	Typically stable, depositional environment to minimize effects of resuspension and loss of AC	- Hunters point (PCBs), San Francisco, CA	[71, 72]	90-95%
		Better placement and retention	Potential reduction in performance initially due to containing matrix; Same concerns as direct placement of AC long-term	Potentially wider variety of site conditions could be treated with AC in this manner	- Hunters point (PCBs), San Francisco, CA	[69]	50-90%

2.2.2 Carbon-based technologies for remediation of PCBs

As noted in the previous section, AC is the most common material for sediment caps and its efficacy for reducing the concentrations in the overlying water column has been demonstrated [69, 71, 73-76]. Cho et al. [71], however, reported uneven distribution of AC when applied in the field that resulted in low mass transfer of PCBs onto AC, and Choi et al. [73] reported that as AC capping is only a physical amendment, changes in the hydrodynamics of the environment can erode the AC cap, leading to resuspension of PCBs. Hence, other sorbents like natural carbon [77, 78], and fly ash [79] have been tested as alternatives, but they have not been applied as widely as AC because they are not as effective [77]. Fly ash also releases heavy metals into the aqueous phase [79] and soil [80]. Beless et al. [81] and others [82-84] have proposed the use of carbon-based nanomaterials for sequestering PCBs in lieu of natural carbon and fly ash to address the aforementioned limitations.

Graphene (GE), a two-dimensional form of carbon with a honeycomb like structure (see Figure 2-4 from Wang et al. [85]), has been gaining popularity in various applications [86]. Single-layer graphene of one atom thickness was first created by Novoselov et al. [87]. Despite the fact that graphene serves as the starting material for most of the other commonly used carbon-based materials like AC, natural carbon, etc., very limited laboratory studies [81] have been performed to test its effectiveness in the management of PCB contamination. The oxidized form of graphene, graphene oxide (GO), has not been studied in any detail in this context. Figure 2-5 illustrates one possible structure of GO proposed by Nasrollahzadeh et al. [88].

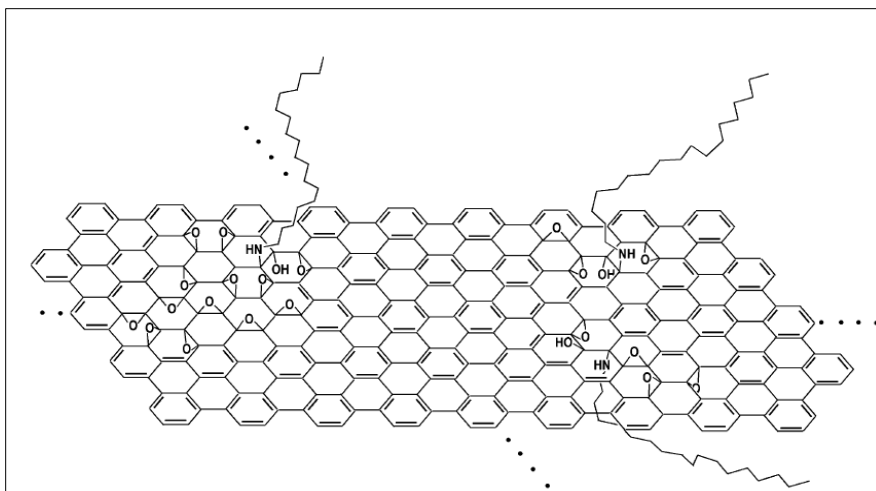


Figure 2-4. Schematic honeycomb structure of a graphene sheet (adapted from Wang et al. [85])

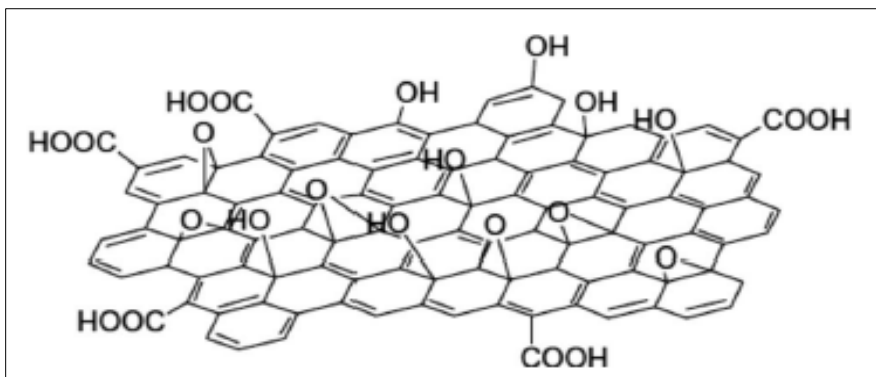


Figure 2-5. Schematic structure of graphene oxide (adapted from Nasrollahzadeh et al. [88])

Carbon nanotubes (CNTs) were discovered by Iijima [89]; they are hollow cylinders, only a few nanometers in diameter and several microns in length of aromatically bonded carbon. CNTs can exist either as single-walled carbon nanotubes (SWNT) or multi-walled nanotubes (MWNT) depending on the sheets of carbon atoms present. Figure 2-6 obtained from Choudhary and Gupta [90] illustrates the structure of SWNT and MWNTs. CNTs exhibit properties very similar to graphene and are applied extensively in various fields ranging from electrical industries to sporting goods [91, 92]. Once again, very few studies [81, 93] have looked at the possibility of using CNTs for the purpose of remediating PCBs

in the laboratory or in the field.

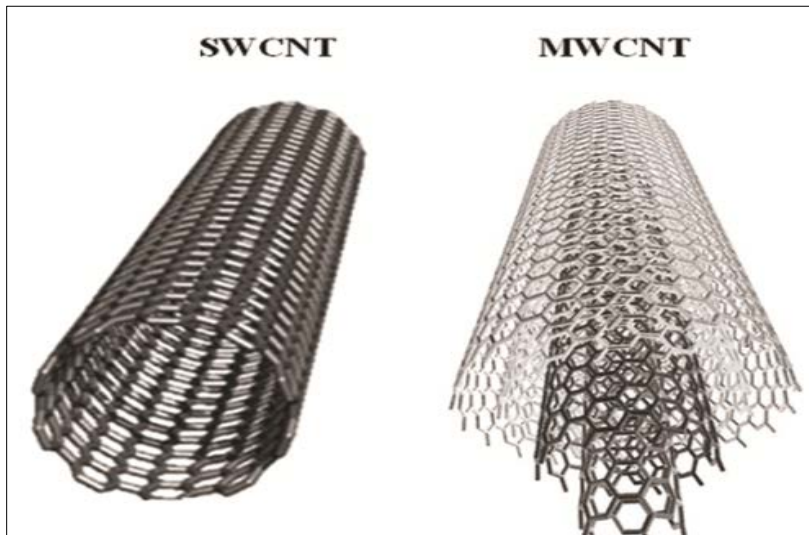


Figure 2-6. Schematic structure of single and multi-walled CNTs (adapted from Choudhary and Gupta [90])

This dissertation explores the application of all the above-mentioned carbon-based materials for remediating sediments contaminated with PCBs.

2.3 PCBs in the Houston Ship Channel and Galveston Bay System (HSC-GBS)

The current research aims to demonstrate the possibility of using carbon-based technologies for sediment remediation in natural water systems and to develop an understanding of the partitioning behavior of PCBs in the estuary. The HSC-GBS is used as a test-bed to illustrate the potential for success of carbon-based sequestration as a sediment remediation strategy via experimental studies and water quality modeling. The following section provides a brief description of the HSC-GBS and the levels and distribution of PCBs that have been measured in prior studies. This section also provides an in-depth analysis of the sources of PCBs into this coastal estuarine system, and their observed partitioning behavior over time and at various locations.

2.3.1 Description of the HSC-GBS

The Houston Ship Channel (HSC), located in the San Jacinto River (SJR) Basin in Houston, Texas, is a widened and deepened natural watercourse that was created by dredging Buffalo Bayou and Galveston Bay. The HSC is approximately 52 miles in length from the Port of Houston to the Gulf of Mexico, 13.7 meters deep, and 162 meters wide [26]. The HSC serves as the passage for transportation of cargo vessels and barges between Houston and the Gulf of Mexico.

The HSC is home to a \$15 billion petrochemical complex, the largest in the U.S., and the second largest in the world [94]. This complex contains numerous petrochemical refineries and chemical production facilities, generating over 175 billion dollars and more than one million jobs [94], and accounting for more than 40% of the chemical and petrochemical production in the U.S. [26]. The industrial activity since the mid-1900s combined with wastewater effluent discharges from the growing City of Houston adversely impacted water quality in the 1970s requiring stricter regulations and enforcement. Since then, the water quality has improved with respect to dissolved oxygen and other basic water quality parameters; however, the HSC still exhibits relatively elevated levels of PCBs, PCDD/Fs, and metals [26].

2.3.2 Occurrence and distribution of PCBs in the HSC-GBS

The HSC-GBS exhibits the presence of various pollutants including bacteria, chlordane, dieldrin, mercury, heptachlor, PCBs, and PCDD/Fs in its segments. Figure 2-7 shows the segments and bays that have been termed “impaired” by TCEQ due to elevated levels of PCBs and dioxin in edible tissue.

Other researchers have conducted extensive sampling of water, bed sediment, and

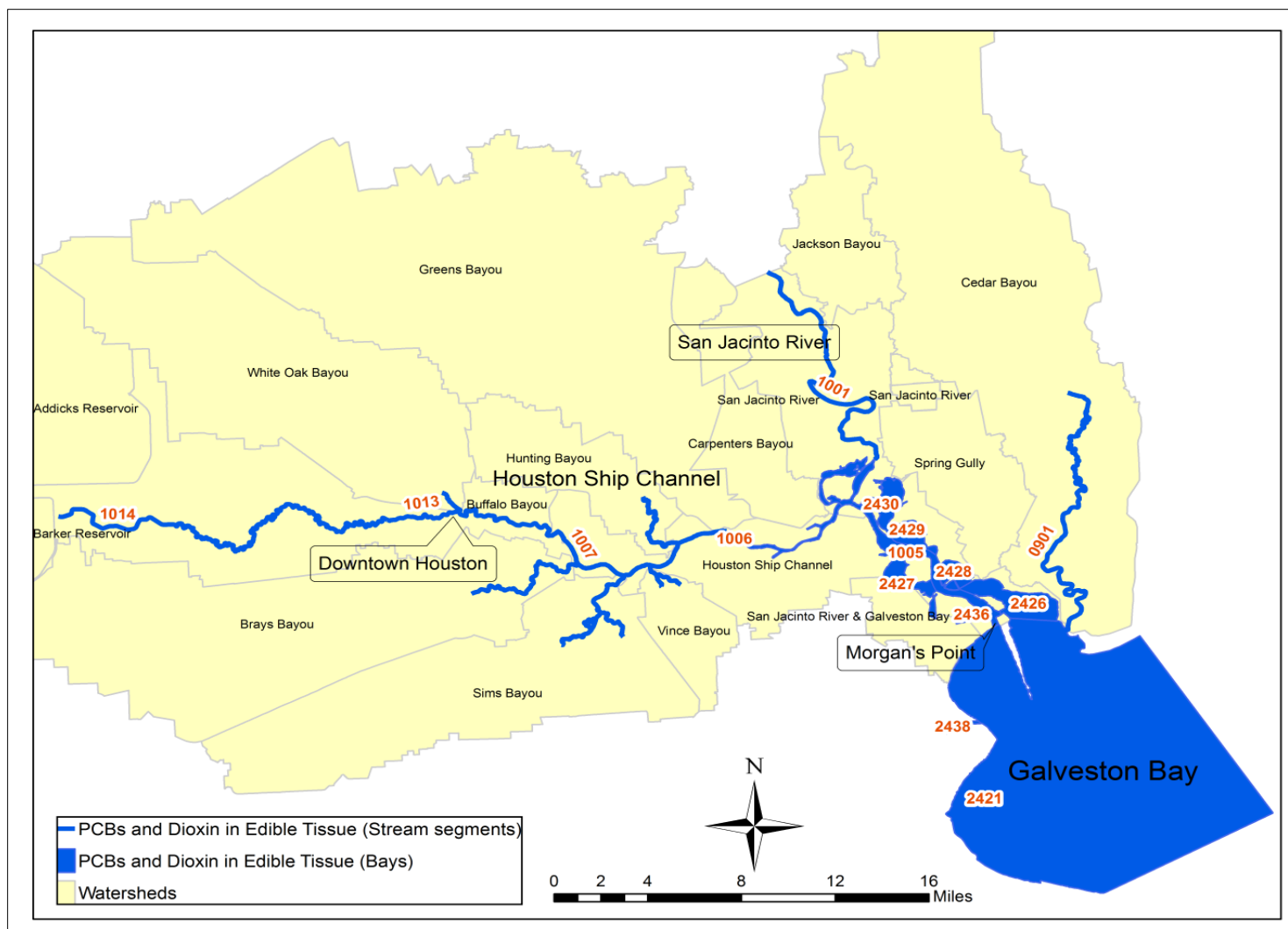


Figure 2-7. HSC-GBS segments that exhibit PCBs and dioxin in edible tissue (Source: TCEQ 2014 303(d) List)

tissue in the HSC-GBS in 2002-2003, 2008, 2009, and 2011-2012. A total of 176 locations were sampled (Figure 2-8); not all locations, however, were sampled during each campaign.

For the purposes of this dissertation, the PCB concentration in sediment is of key importance, and therefore, the total PCB ($\Sigma 209$ congeners) concentration in sediment (ng/g) is shown in Figure 2-9. Prior to 2008, total PCBs were calculated based on the 18 congeners listed as toxic by the National Oceanic and Atmospheric Administration (NOAA) [95], which was later expanded to the congeners of highest concern mentioned in McFarland and Clarke [96] in 2008-2009. In subsequent years, the list was expanded to include all 209 congeners. In order to be consistent, the total PCBs ($\Sigma 209$ congeners) was re-calculated for the sampling campaigns using the concentrations of all 209 PCB congeners, and non-detects (ND) were set to half the method detection limit (MDL), and the total PCB ($\Sigma 209$) concentrations are plotted in Figure 2-9. It is also important to note here that MDL values changed over time (this is accounted for here). As would be expected and shown in Figure 2-9, most of the observed high PCB concentrations in sediment are found in the HSC. Moreover, the hotspots of sediment contamination within the HSC are Patrick Bayou, the Turning Basin of the Port of Houston, and certain parts of Greens Bayou. The total PCBs ($\Sigma 209$) in sediment (ng/g) in Patrick Bayou, for example, increased from 4678.99ng/g in 2002-2003 to 9495.82ng/g in 2009.

Several studies [97-100] based on the collected data have informed this research and presented findings that are important for the purpose of this dissertation; these are described in more detail in section 2.3.3 below.

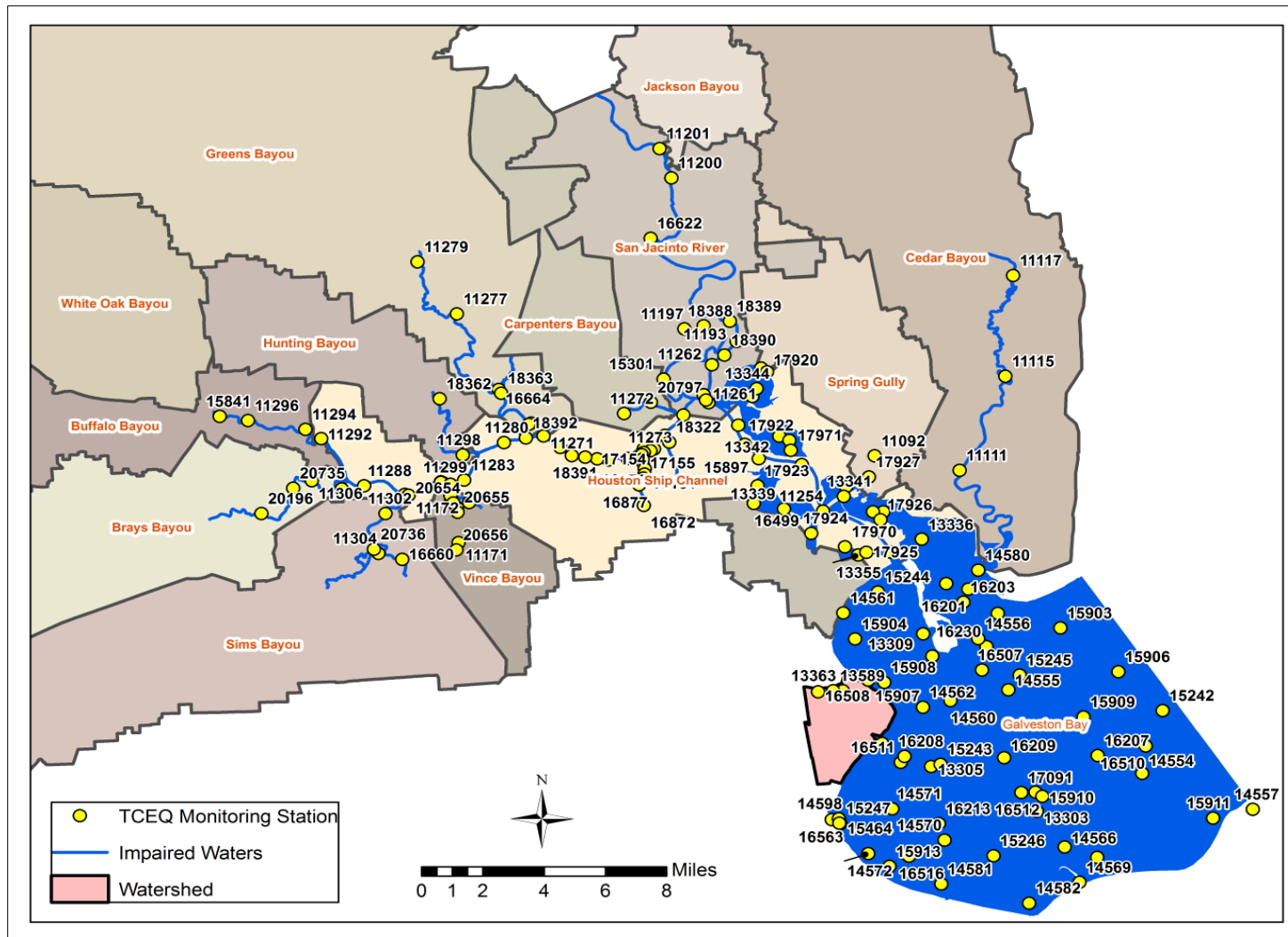


Figure 2-8. Locations sampled for PCBs in the various sampling campaigns

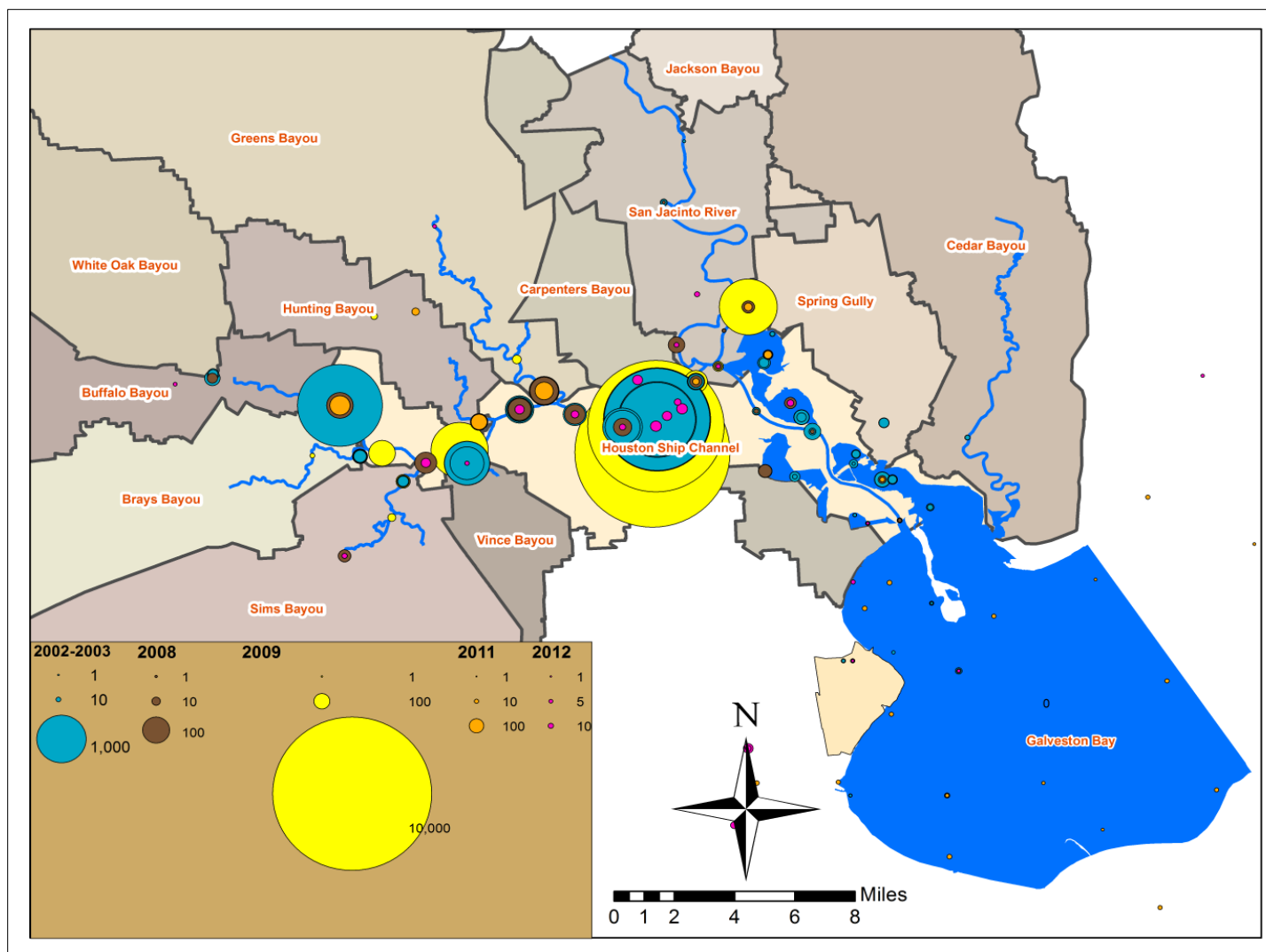


Figure 2-9. Total PCBs ($\Sigma 209$) in sediment (ng/g) over time (totals represent all 209 congeners for all the years and stations)

2.3.3 Partitioning of PCBs in the HSC-GBS

In order to understand the presence and distribution of PCBs in the environment, water and sediment samples are typically collected from waterbodies. Water samples (200-700 liters to ensure measured concentrations are above the detection limit) are collected 0.3m below the water surface using a high-volume sampler that contains one micron glass fiber filters, and a stainless-steel column packed with XAD-2 resin, to obtain the suspended (C_{susp}) and dissolved (C_{diss}) fractions of PCBs, respectively. The bulk water concentration (C_{water}) is the sum of both the dissolved and suspended fraction. Water samples are also collected for analysis of total dissolved solids (TDS), total suspended solids (TSS), and dissolved organic carbon (DOC). Sediments samples are collected from the top 5cm of sediment using a dredge to obtain the concentration of PCBs in bulk sediment (C_{sed}). Also, sediment samples are collected to quantify the total organic carbon (TOC) present in sediments. Figure 2-10 provides a schematic of the parameters that are obtained from field sampling and also the conceptual framework behind the setup of sediment and water layers in the EFDC model, which will be discussed in detail in section 3.3.

The truly dissolved concentration is the minute fraction of PCBs present in the porewater of sediments as freely dissolved molecules, and is considered to control the uptake of PCBs by micro/macro-organisms [55]. From the above discussion about sampling, it is apparent that truly dissolved concentrations were not measured in the samples collected from the field. Hence, truly dissolved concentrations are estimated using water column partitioning models which fractionate the bulk water concentration (C_{water}) against measured parameters (DOC and other organic carbon fractions). For

example, truly dissolved concentrations can be estimated from equations 2.1 and 2.2 obtained from Schwarzenbach et al. [101], which are provided below:

$$C_{water} = C_d + C_d K_{doc} C_{diss} + C_d K_{poc} C_{susp} \text{ and} \quad (2.1)$$

$$C_{water} = C_d + C_d K_{doc} C_{diss} + C_d K_{poc} C_{susp} + K_{f,bc} C_d^{n_{f,bc}} C_{susp}, \quad (2.2)$$

where C_{water} and C_d are bulk water and truly dissolved concentrations (ng/L), C_{diss} and C_{susp} are measured (sampling) water concentrations (mg/L), K_{doc} (L/kg), K_{poc} (L/kg), $K_{f,bc}$ ((μg/kg)/(μg/L)^{n_{f,bc}}) are the various organic carbon sorption fractions, and $n_{f,bc}$ is the Freundlich exponent.

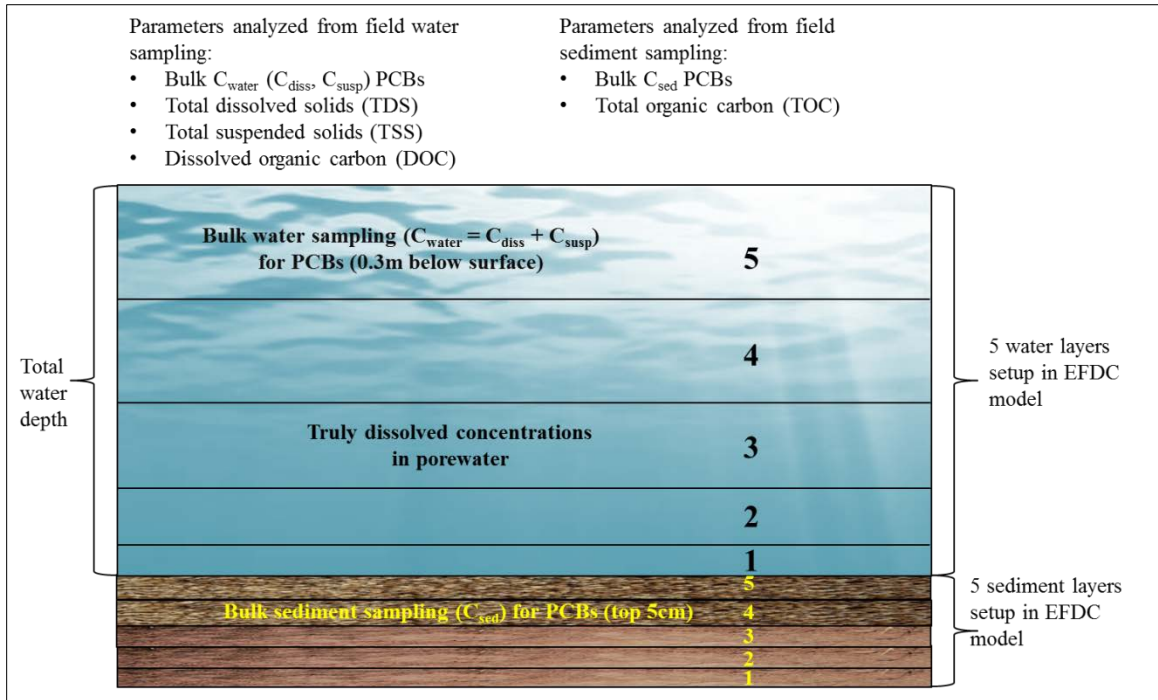


Figure 2-10. Conceptual framework of EFDC model setup and field sampling measurements

Howell [102] extensively analyzed the partitioning of PCBs in the HSC-GBS using linear free energy relationship (LFER) models that used various parameters; the important variables being: DOC, particulate organic carbon (POC), TSS, and the fraction of black carbon. Howell [102] showed that total PCB concentrations in the HSC are

generally elevated, but only the upper part of the HSC (from downtown Houston to the confluence of HSC and SJR) showed high levels of truly dissolved concentrations.

Another important finding was that higher chlorinated PCB congeners were higher in the truly dissolved phase in the water column compared to the sediment porewater, which is very different when compared to other bays and estuaries, and makes it all the more necessary to sequester them. In addition, based on the differences in total PCBs between 2002-2011 in the HSC-GBS, Howell [102] proposed that sediment has been sourcing PCBs into the water column, and that if no external loadings were coming into the HSC, PCBs would still be present in the water column due to partitioning from sediment.

In addition to the partitioning of PCBs from field sediment and water sampling, their distribution in effluent discharges and the influence of organic carbon on their partitioning behavior was studied in this dissertation [22] and will be discussed in more detail in sections 3.1 and 4.1.

2.3.4 Modeling of PCBs in bays and estuaries

Understanding the fate and transport of PCBs in natural water systems is difficult without the use of water quality models because of the variability of sources and the dynamic nature of concentration distributions and partitioning of these pollutants in such systems. Fate and transport models that have been specifically developed for PCBs are described briefly below (a more detailed listing can be found in Howell [102]). The referenced studies presented below mainly illustrate that no models have been developed to date that demonstrate the efficiency of PCB sequestration as a long-term sediment remediation technology as is done in this dissertation.

Halfon and Allan [103] used TOXFATE, a mass-balance model that was developed

to understand the fate of toxic contaminants in large lakes, and to model PCBs and Mirex in the St. Lawrence River Estuary aquatic ecosystem. Results from TOXFATE simulations indicated that PCB loadings into the River are in the dissolved phase at the beginning and partition into the particulate phase as they move downstream. Zimmerman et al. [104] used Tidal Residual Intertidal Mudflat (TRIM-3D) and Simulating Waves Nearshore (SWAN) models to predict the stability of AC amended sediments at the Hunters Point Naval Shipyard Superfund site in San Francisco Bay. Using their model, the authors concluded that the bottom shear stresses in the sediment were low enough to hold the AC in place [104]. Everaert et al. [105] used generalized additive mixing models (GAMMs) to understand how sediment PCB concentrations changed over time in the Belgian Coastal Zone, and concluded that, over the last 20 years, PCB concentrations had reduced by two to threefold in the Belgian Coastal Zone, but a significant decrease was not observed in the Western Scheldt Estuary. Bioaccumulation models have also been developed to simulate the bioaccumulation of PCBs in the Hudson River [106], and the Seine Estuary [107]; these will not be discussed here since they fall outside the scope of the dissertation.

EFDC, the water quality model that formed the basis for model development in this dissertation has been used for water quality studies in bays and estuaries [108-114], however, and as noted previously, the use of EFDC for modeling sequestration of PCBs as a sediment remediation technology using carbon-based materials is novel and has not been done before.

Chapter 3. Materials and Methods

This chapter focuses on the analyses, experimental methods, and modeling process and methodology that were used in the study. There are three different but interconnected components that are discussed: (i) effluent sampling for the purpose of understanding partitioning behavior in the HSC-GBS; (ii) experimental studies with the carbon-based materials, and (iii) EFDC model setup for the purpose of understanding the efficiency of using carbon-based materials for sequestering PCBs in natural water systems such as the HSC-GBS. The methods and materials for the three components are described in more detail in the following sections.

3.1 Effluent sampling methods and analyses

Numerous municipal and industrial facilities located within the HSC-GBS system discharge their effluent into open waters. Several of these had their effluent sampled for the purpose of quantifying PCBs as described below. This study utilized the results from the effluent sampling to understand partitioning behavior and also to assess whether continuous discharges of PCBs into the system represents a significant source of PCBs compared to partitioning from bed sediment.

3.1.1 Sample collection

The facility and the outfall within each facility discharging into the HSC to be sampled were selected based on the following criteria: proximity to the HSC, proximity to known PCB/PCDD/Fs hot spots in water, sediment, or fish; industry type; the nature of the receiving stream (tributary or main channel); the known history of upset and spill events within the facility; facility longevity; existing NPDES permits and regulations on halogenated organics; and the rate of discharge relative to the receiving waters.

The locations of the facilities that were sampled during the 2009 sampling campaign are shown in Figure 3-1. Out of the 16 effluent outfall locations shown in the Figure, six were industries (I1, I2, I3, I4, I5, and I6), six were municipal wastewater treatment plants (WWTP1, WWTP2, WWTP3, WWTP4, WWTP5, and WWTP6), two were industrial wastewater treatment plants (O3, and O4), and the remaining two were a refuse system (O1) and a special warehousing facility (O2), respectively.

The samples were taken directly from the outfalls as close to the discharge point into the receiving stream as possible. A high volume sampler was used to pump 200 liters of water for each sample through a pre-cleaned glass fiber filter (GFFs) containing a 1 μm filter then through a XAD2 resin contained in a stainless steel (SS) column. The mass that was retained on the filters was considered to be the suspended fraction, and the mass collected on the XAD2 resin was treated as the dissolved fraction. For each of the sampling events, a separate grab sample was collected and analyzed for TSS, DOC and TOC. More details on sampling and experimental methodologies and PCB concentrations in the HSC can be found in the literature [23-26].

One of the municipal wastewater treatment plants, WWTP1, was sampled in duplicate. It is noted, however, that the resulting two samples are not conventional duplicates since they were collected using two different high volume samplers; albeit the samples were collected at the same time. It is not possible to collect a conventional duplicate with high volume samplers due to the relatively large volume of water that is required which translates to very long collection times at relatively low flow rates to allow PCB to partition onto the XAD2 resin in measurable quantities. It is a well-known fact that DOC and POC cause the formation of colloids in natural waters [115] which

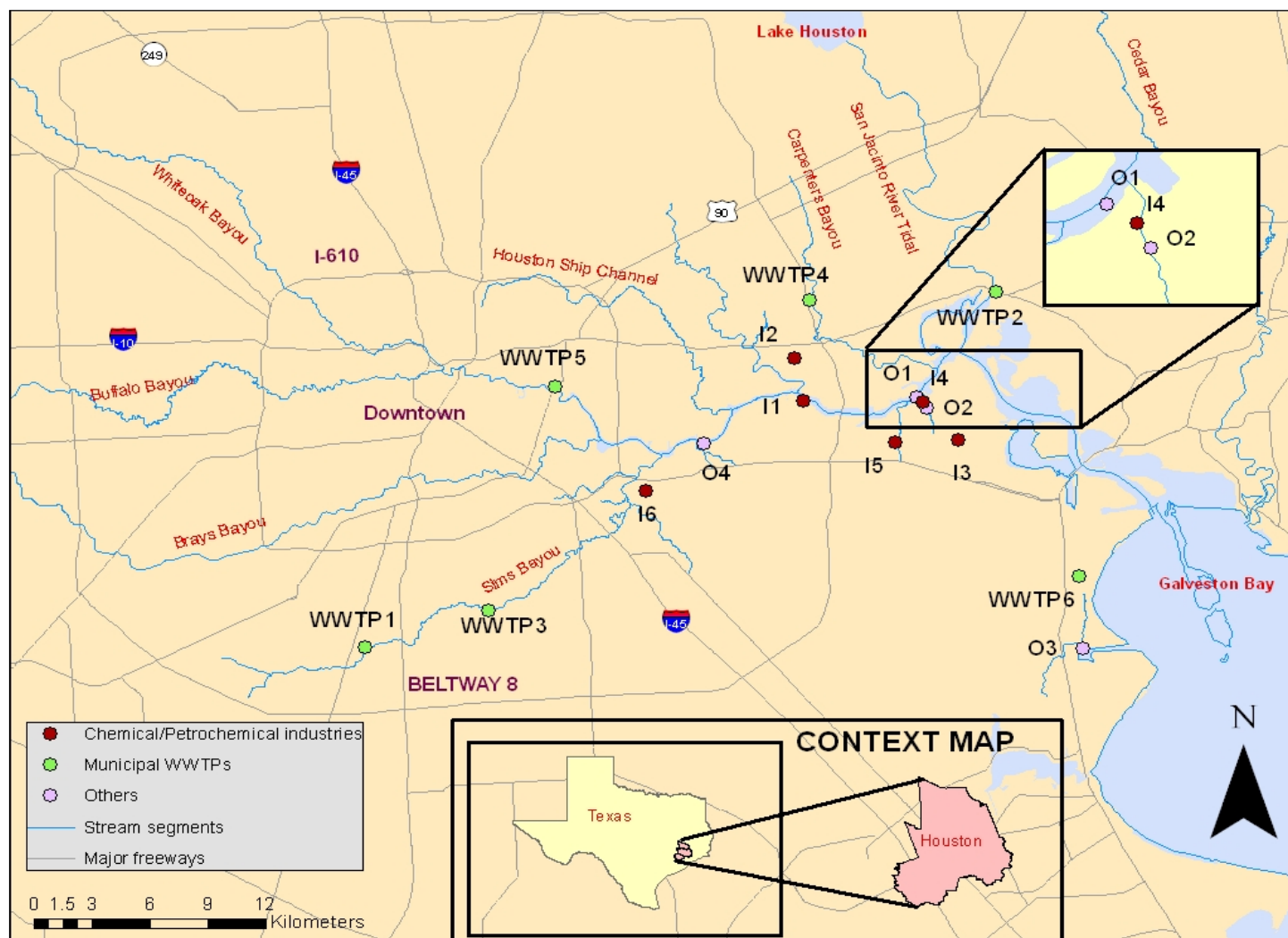


Figure 3-1. Locations of the effluent outfalls sampled for PCBs

could lead to higher suspended fractions.

3.1.2 Chemical analyses

PCB congeners in the effluent (all 209) were quantified using high resolution gas chromatography/high resolution mass spectrometry (HRGC/HRMS) using USEPA method 1668A [116]. The analyses were completed by a commercial laboratory that met the data quality objectives established for the study (see Howell et al. [23]).

Briefly, the XAD2 resin was spiked with ^{13}C -labeled PCB compounds before the sampling event occurred to measure the potential loss of PCB surrogates during the sampling event and the chemical analysis, thereafter. Also, the extract from the GFF was spiked with a mixture of ^{13}C -labeled PCB compounds and Soxhlet-extracted (after being air dried) with dichloromethane for a minimum of 16h followed by back-extraction with sulfuric acid and the resulting extract was re-concentrated using rotary evaporation. The extract was subjected to a cleanup procedure using a silica column to make the extract suitable for injection into the Gas Chromatograph (GC). The column contained alternating layers of neutral and acidic silica gel. The column was pre-eluted with hexane, the sample was applied, and then the PCBs were eluted with hexane. Finally, the sample was concentrated to a final volume of 100 μL . TSS was analyzed by SM 2540D and TOC and DOC were analyzed by SM 5310C.

The Quality Assurance/Quality Control (QA/QC) criteria of the project were met by collecting and analyzing field blanks, field duplicates, and XAD2 resin recovery samples. Field blanks were collected at a 5% frequency for all field samples. Further, a lab duplicate was run with each analytical batch typically consisting of 20 samples or less, and no failure was observed amongst all of the effluent samples. The surrogate recovery

acceptability limit was between 65% and 135% for the PCB congeners and only 1 out of 5576 analytes (0.018%) did not meet this requirement. Non-detects were assumed to be equal to half of the MDL, unless specified otherwise.

3.2 Sorbent experimental methods and materials

As mentioned previously, activated carbon (AC), black carbon (BC), graphene (GE), graphene oxide (GO), and multi-walled carbon nanotubes (CNT) were studied in laboratory experiments to determine their sorption potential in sediment. The sorption potential was quantified by determining the distribution coefficient, K_s , between the different sorbent materials and water. The sections below describe the materials/chemicals used in the experiments, the experimental setup/procedure, and the method/equations used to calculate K_s .

3.2.1 Chemicals and lab materials

The mixture of 11 PCB congeners (PCB-mix) containing the 11 PCB congeners mentioned earlier in Table 2-3 was purchased from AccuStandard, New Haven, CT, with a declared purity of >99%. The PCBs came as a solution in either hexane or acetone, sealed in amber glass ampoules. Elliott silt loam soil (taxonomic class: fine, illitic, mesic aquic arguidolls; carbon = 2.9%) was purchased from International Humic Substances Society and was used as sediment. The soil came as a dry powder packed in air-tight Ziploc[®] bags. The organic solvents used for these experiments include: acetone (ACS standards, $\geq 99.9\%$ purity; VWR, West Chester, PA), acetonitrile (HPLC grade, $\geq 99.9\%$ purity; Sigma-Aldrich, St. Louis, MO), and hexane (GC grade, $\geq 95\%$ purity; Sigma-Aldrich, St. Louis, MO). Other chemicals include: sodium azide ($\geq 99\%$ purity; Alfa Aesar, Ward Hill, MA), and anhydrous calcium chloride ($\geq 90\%$ purity, EM science,

Gibbstown, NJ).

Solid-phase microextraction (SPME) fibers were manufactured at Poly Micro Technologies, Phoenix, AZ. The fibers have a glass fiber core of 1000 μ m in diameter, a 35 μ m outer coating of polydimethylsiloxane (PDMS), thereby making the overall outer diameter of the SPME fibers 1070 μ m. Narrow-mouth Boston round amber glass bottles (240ml) with threaded septa caps containing silicone/polytetrafluoroethylene (PTFE) liner were obtained from VWR International. In addition, 2ml amber glass GC auto-sample vials used with red screw caps containing a silicone/PTFE septum was obtained from Agilent Technologies. 250 μ L glass footed inserts with polymer feet were also obtained from Agilent Technologies for use in the vials.

3.2.2 Carbon-based materials

The sorbents were selected based on the work done by Beless [53]. AquaSorb[®] BP2 AC was purchased from Jacobi Carbons Inc., Columbus, OH. The AC was in powder-form and was a bituminous coal based powder, with moisture content of $\leq 8\%$ and ash content $\leq 18\%$. The BC used in the experiments was purchased from buyactivatedcharcoal.com. Charcoal Green[®] Pure Biochar Mixed (BC) contained a mixture of hardwoods and the BC was processed using the pyrolysis method. GE, GO, and CNT were purchased from Cheap Tubes Inc., Brattleboro, VT. GE purchased from the supplier was in the form of graphene nanoplatelets (non-functionalized, research grade, grade 4), and were used as is in the experiments. The manufacturer had synthesized GE using natural graphite as the starting material by means of a split plasma process with argon gas. The graphene sheets produced by this process exhibited an average thickness of $< 4\text{nm}$, and purity of $> 99\%$ by weight.

Few layer graphene oxide (2-4L) was purchased from the supplier, and was used as provided by the supplier in the experiments. The GO was synthesized by a modified Hummer's method, and the thickness of the layers in the resulting GO ranged between 1.4nm and 4.8nm, and purity of >99% by weight.

Short multi-walled carbon nanotubes were purchased from the supplier, which were used as the CNTs in the experiments. The CNTs were synthesized by the manufacturer using a catalytic chemical vapor deposition (CCVD) process, and the resulting CNT had an outer diameter of <8nm, and purity of >95% by weight.

All of the sorbents were characterized using a 6010LA scanning electron microscope (SEM) and energy dispersive spectroscopy (EDS).

3.2.3 Experimental setup

All batch experiments were conducted in 240ml narrow-mouth Boston round amber glass bottles (batch reactors) capped with threaded caps containing a silicon/PTFE liner. This aided in preventing the loss of any PCBs due to volatilization. The glass bottles, and all other glassware used in the experiments were cleaned both before and after use by the recommended method provided in USEPA Method 8082A [117], thereby minimizing any interferences.

A total of 50g of clean, dry, soil was added into the clean batch reactors followed by the addition of 25ml of acetone containing 200 μ L of mixture of 11 PCB congeners (PCB-mix) mentioned earlier in Table 2-3 at a concentration of 250mg/L, stirred and dried under the fume hood for 12h to facilitate complete evaporation of acetone, and incorporation of the PCB congeners into the soil.

The reactor bottles were filled with 200mL of Millipore water containing 0.01M of

calcium chloride and 25mg/L of sodium azide, leaving 20mL of headspace in the bottles. Calcium chloride was added to provide a realistic ionic strength in the water, and sodium azide serves the purpose of a biocide. The Millipore water originates from a MODULAB Water System when operating at $\geq 18\text{M}\Omega\text{-cm}$. Five parent samples (one each for AC, BC, GE, GO, CNT) and five duplicate samples (one each for AC, BC, GE, GO, CNT) were prepared using the above process, and the bottles were shaken for ten days to facilitate attainment of equilibrium between sediment, the 11 PCB congeners, and water. Shaking was performed in an Innova 44r (New Brunswick Scientific Co.) incubator shaker at a temperature of 25°C and horizontal gyration of 100rpm.

After ten days of shaking, 100mg of each carbon-based sorbent was added into the respective batch reactors. The sorbents were measured using a Mettler Toledo Classic electric scale (AB304-S) to $\pm 0.1\text{mg}$ accuracy. After addition of the sorbents into the respective batch reactors, they were further shaken for 15 days in order to reach equilibrium between soil, the 11 PCB congeners, water, and sorbent. At the end of 15 days, the above-lying porewater from each of the bottles was carefully transferred to new, clean bottles. One pre-cleaned PDMS fiber of pre-determined length (5cm) was added to each of the bottles, and shaken for 21 days, to measure the equilibrium concentration. Although previous studies have mentioned allowing 28 days for equilibrium, preliminary experiments conducted by Beless [53] observed no significant difference in PCBs measured on the PDMS fibers when shaken for 21, 28, and 35 days. SPME materials measure the amount of analyte *in situ* without significantly altering the environment. The PDMS fibers were cut to the pre-determined (5cm) length and cleaned by sequential washing using hexane, acetonitrile, and Millipore water as recommended by Lu et al.

[118] before addition into the batch reactors. After this step, shaking was performed at an angle of 30° using a Glas-Col rugged rotator fitted with an Erlenmeyer flask head at a rotation rate of 40rpm, at room temperature.

In addition to the batch reactors, control samples containing only PDMS fiber in PCBs spiked sediment, and only PDMS fiber in clean sediment, were prepared in duplicate. At the end of 46 days of total shaking, the PDMS fiber from each bottle was retrieved and wiped with a damp Kimwipe to remove any sorbent material. The PDMS fibers were then placed in 250 μ L glass footed inserts containing 250 μ L of hexane placed in GC auto-sample vials. The auto-sample vials were then tightly capped and shaken at 100rpm for 24h in an Innova 44r (New Brunswick Scientific Co.) incubator at a temperature of 20°C to extract the PCBs from the PDMS fiber, after which the vials were stored (storage time <7days) at -18°C until analysis.

3.2.4 Determination of K_s

The concentrations of the PCBs extracted from the PDMS fibers were analyzed using a gas chromatography-mass spectrometer (GC-MS) (Agilent Technologies, 6890N GC with 5973 MSD). In order to ensure maximum extraction of the PCBs from the fibers, they were left in the footed insert in the auto-sample vials. A five point calibration was set up on the GC-MS, resulting in the coefficient of determination (R^2) being equal to one, which was used to quantify the samples. An Agilent HP-5 capillary column (60m length x 250 μ m inner diameter x 0.25 μ m film coating) was used with ultrahigh purity helium gas as carrier gas.

The concentration measured by extracting the PDMS fibers gave the PCB equilibrium concentrations on the PDMS (C_f). Fiber-water partitioning coefficients (K_{f-w}) were

calculated using the linear equation developed by Lu et al. [118]. The freely dissolved PCB equilibrium concentration (C_e), defined as the equilibrium concentration of sorbate in the water phase, was calculated using the relationship: $K_{f-w} = C_f/C_e$. Conservation of mass within the system was used to calculate the concentration of PCBs in the sorbent phase (q_e) ($\mu\text{g/kg}$) using the equation:

$$M_{tot} = C_{sed}(M_{sed}) + C_e(V_w) + C_f(V_f) + q_e(m_s), \quad (3.1)$$

where M_{tot} is the total mass of the PCB congener in the system (μg), C_{sed} is the concentration of PCB congener in the sediment ($\mu\text{g/L}$), M_{sed} is the mass of sediment used in the batch reactor (μg), C_e is the freely dissolved PCB equilibrium concentration ($\mu\text{g/L}$), V_w is the volume of aqueous solution (L), C_f is the PCB equilibrium concentration on the PDMS fiber ($\mu\text{g/L}$), V_f is the volume of PDMS coating on fiber (L), and m_s is the mass of sorbent added (kg).

Once the concentrations in all four phases were known (C_{sed} , C_f , q_e , C_e), the distribution coefficient between the sorbent material and water (K_s) (L/kg) were calculated for each sorbent using the equation below:

$$K_s = \frac{q_e}{C_e}. \quad (3.2)$$

The K_s values obtained from equation 3.2 were used in the model to simulate the effect of mixing the carbon-based materials into the sediment of the HSC-GBS on water column concentrations.

3.3 Model development

This section describes the setup of the EFDC water quality model for simulating the distribution of PCBs in the HSC-GBS over time and for predicting the effect of incorporating the carbon-based materials into the sediment on dissolved concentrations in

the Channel.

3.3.1 Model setup

The model setup begins with the generation of the model grid, followed by the construction of spatial and time series datasets, and configuring the *EFDC.inp* file that contains initial information and assumptions (e.g., choosing numerical methods) to manage the model runs.

Model grid. The model grid used in Howell [102] was adopted for this study; the grid contained 2649 cells and was developed using aerial photography from 2005 (see Figure 3-2). The average width and length of the grid are 40.85km and 22.41km, respectively. The model covers a total area of 57.336km². The model grid extends to downtown Houston in the east, the confluence of the SJR and Lake Houston in the north, and Galveston Bay in the south.

Model vertical discretization. Bathymetry and elevation data from Howell [102] were also adopted in this study; these data originated from the Harris County Flood Control District (HCFCD), NOAA and the U.S. Geological Survey (USGS) datasets. In addition to bathymetry and elevation data, the EFDC model was set-up to specifically enable the types of sediment remediation analyses undertaken in this dissertation. This was done by further discretization of the vertical horizon of the natural water system instead of using a single layer system. EFDC uses the sigma coordinate system [119], that allows for representation of continuous measurements such as temperature, pressure, and depth smoothly, even in the lowest layers of the model. Hence, in the EFDC model, the vertical sigma scaling approach is used to divide the depth, i.e., the model is setup to provide true dimension coordinates in the x and y direction, but a scaled z (depth)

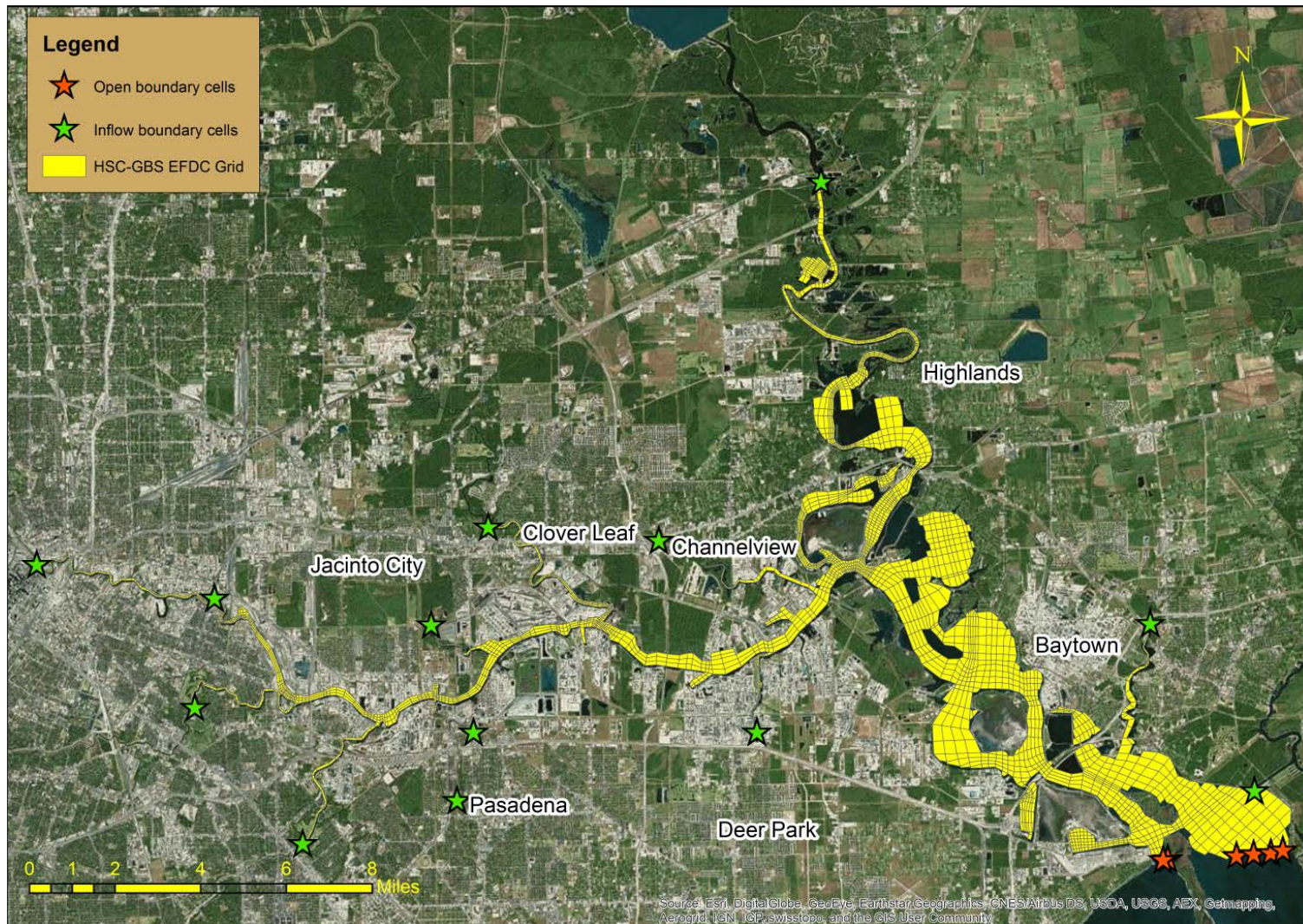


Figure 3-2. The HSC-GBS grid used in EFDC with boundary conditions

coordinate. This is especially important, as the major focus of this work lies in the partitioning of PCBs that are present in the porewater (truly-dissolved concentration) of the sediment in the bottom layer (sediment bed) of the HSC-GBS. Hence, in this model, the depth is divided into five divisions representing a percentage of the total depth for each cell as discussed below.

The five vertical fractions in the water column defined in Howell [102] were adopted in this work. They define from bottom to top the following segmentation: 0.05, 0.10, 0.20, 0.30, and 0.35 (Layers 1 through 5) of the total depth. In other words, the sediment in layer 5 is in contact with the bottom-most water layer (Layer 1). The vertical proportionality of the layers was kept very small near the bed (5% of total depth), because of the importance of the bottom layer acting as a thin film during partitioning of PCBs from the sediment, and increased to 35% of total depth in the topmost layer to represent the zone that is used for bulk sediment sampling. In addition, five sediment layers were also set up in the model by Howell [102] using sediment core data collected between 2002 and 2004, for sediment bed concentration initialization. These vertical fractionations designated by Howell [102] were maintained in this study to allow capturing sediment resuspension and deposition, and because of the critical nature of these processes towards the objective of the EFDC model development for sediment remediation. Additionally, suspended particles are present in all the layers of water and sediment using the TSS sampling data.

Model sediments. The four sediment size classes (two cohesive and two non-cohesive) that were used in Howell [102] to represent clay, silt, fine sand, and medium sand in the sediment bed were maintained in EFDC. The particle size ranges were as

follows, 1-3.90 μm , 3.90-62.5 μm , 62.50-250 μm , and 250-500 μm , for the four classes, respectively. The data were based on surface sediment samples collected between 2002 and 2004 at 48 stations. The grain sizes for clay, silt, and sand were averaged, and if gravel was present, it was removed and the data were re-normalized. Figure 3-3 provides the fraction of clay, silt, and sand at the 48 stations. Clay fractions were higher in the SJR, Greens Bayou, and the side bays, whereas most of the HSC main channel was silty/sandy. These values were input into the Sediments module present in EFDC to model sediment transport.

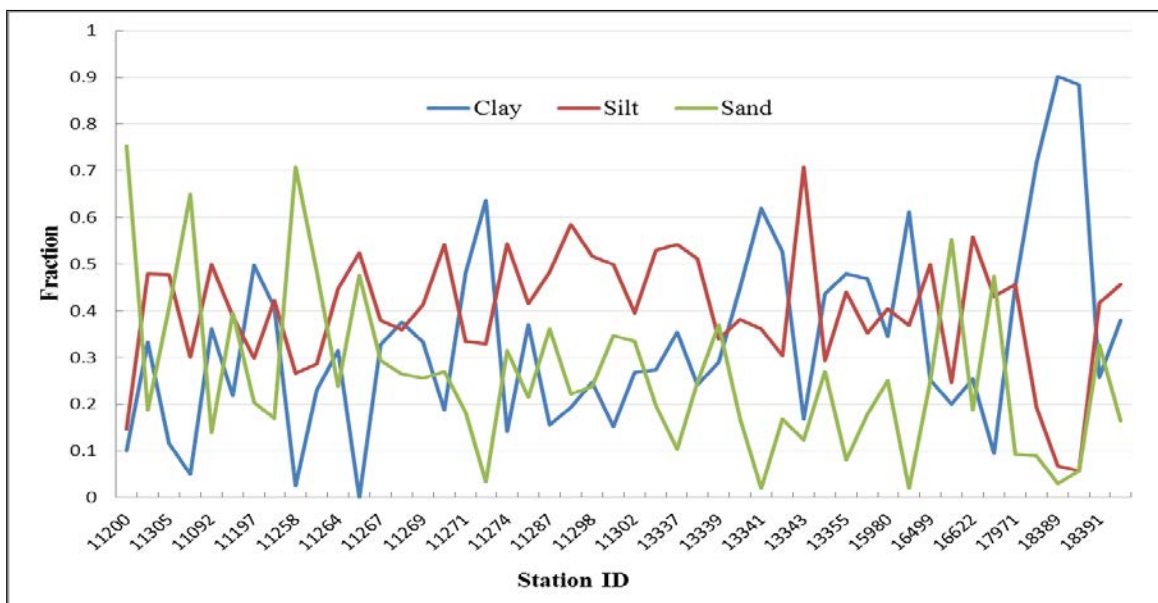


Figure 3-3. Fraction of clay, silt and sand in the sediment bed measured in the HSC-GBS

Model time. Extensive PCB sampling was conducted in the HSC-GBS by University of Houston in 2002-2003, 2008-2009, 2011, and 2012. The model was calibrated for PCBs in the HSC-GBS between 02/25/2003-06/20/2003 (115 days – time period of calibration run), and the effect of remediation using carbon-based materials was also evaluated within this time period. The data used to setup the initial conditions for the model were data collected between August 2002 and December 2002. This time period

was chosen because PCB data were available as discussed in detail in the next section, and there were no extreme hydrological events during this period such as hurricanes or severe storms. Sensitivity analyses were completed for a shorter time, 02/25/2003-03/27/2003 (1 month) as discussed in section 3.3.2.

Flow boundary conditions. Flows were obtained from USGS gages in the study area between 2002-2009 to derive the flow boundary conditions for the model [102]. Figure 3-4 shows the EFDC grid developed for the HSC-GBS with the boundary conditions and the USGS gages of bayous/tributaries coming into the HSC. Open boundary cells (Galveston Bay) represent the cells where there is both inflow and outflow of water into the grid, and inflow boundary cells (bayous/tributaries connecting to the HSC) represent the cells in which there are only inflows of water into the grid.

Most of the flow data were readily available through the USGS, with the exception of 69th Street wastewater treatment plant (WWTP) in East Houston; these were obtained from Howell [102] as estimated flows, using monthly self-reported flows from EPA databases. Inflow into the upstream boundary of the SJR was obtained from a rating curve that was developed by the Texas Water Development Board for estimating flows directly out of Lake Houston. Tidal stage (NOAA gage 8770613) was used at Morgan's Point to obtain water surface elevations (WSE) at the mouth of the HSC at Tabbs Bay for the open boundary. The model grid has three tidal boundaries (Tabbs Bay south, Tabbs Bay west, and Morgan's Point south).

Lastly, within the modeling period, the highest flows for the tributaries in the system were seen from the SJR (maximum of $440\text{m}^3/\text{s}$), followed by Brays Bayou (maximum of $100\text{m}^3/\text{s}$), and Greens Bayou (maximum of $60\text{m}^3/\text{s}$). The tributaries represent sources of

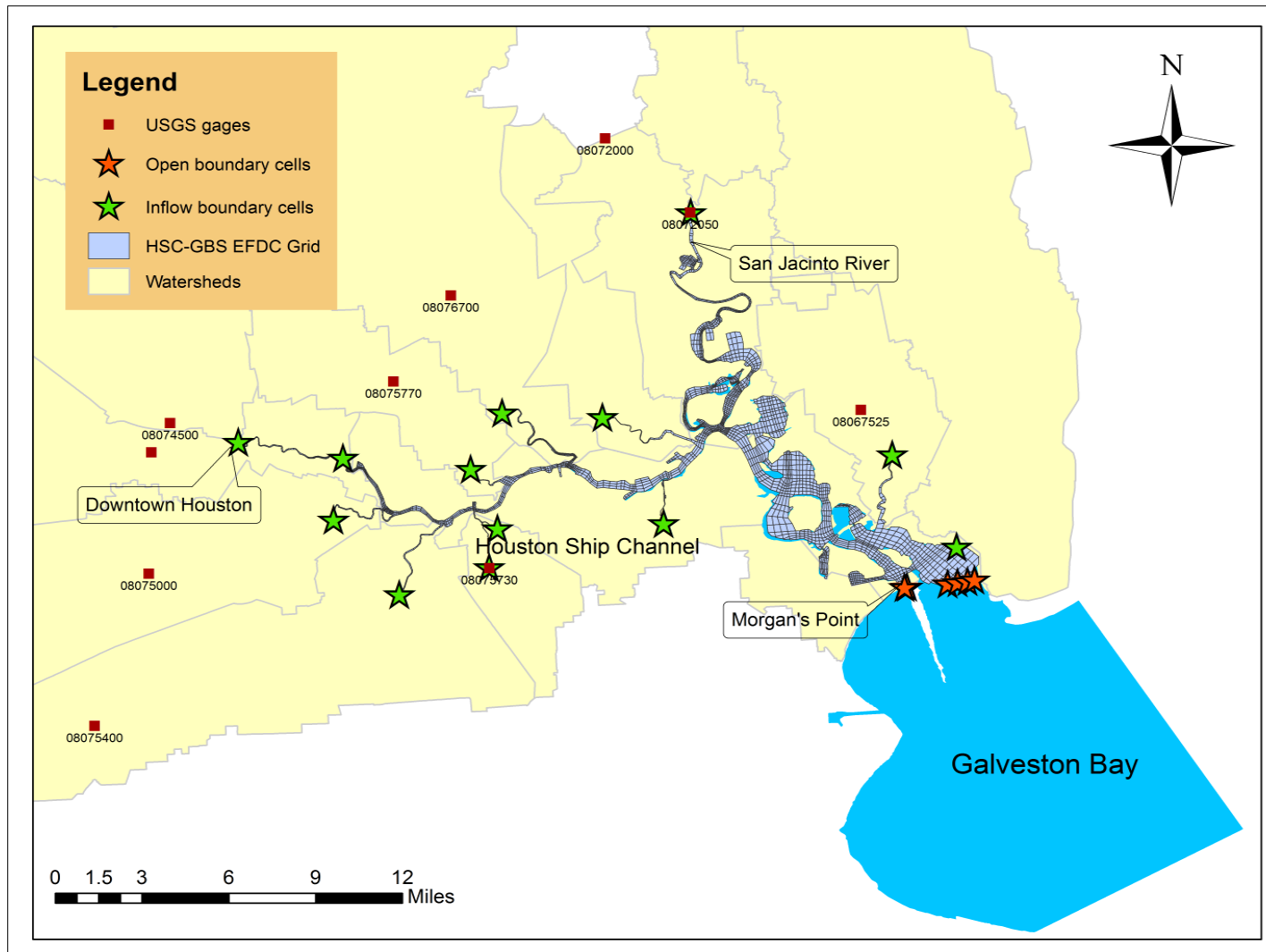


Figure 3-4. Locations of USGS gages that were used to obtain flows for the model

PCBs in the model and that is the main reason their flows were included in the model. It is noted, however, that on a relative basis, the flows from the tributaries is much smaller than the flow in the HSC towards Galveston Bay.

PCB initial and boundary conditions. To model the fate and transport of PCBs in the sediment, the Toxics module in EFDC was activated. The EFDC Toxics module uses an integrated model of hydrodynamics, sediment transport, and toxic chemical fate and transport [120] (see Figure 3-5). Equilibrium partitioning is used in the model to simulate the total contaminant concentration in the water column and sediment bed. The 3D transport equation solved in the model to obtain the total toxic concentration C (dissolved, C_d in mg/L, plus suspended, C_p in mg/L) is given by equation 3.3 obtained from Ji [120]:

$$\begin{aligned} \partial_t(HC) + \partial_x(HuC) + \partial_y(HvC) + \partial_z(wC) - \partial_z(w_s f_p C) \\ = \partial_x(HK_H \partial_x C) + \partial_y(HK_H \partial_y C) + \partial_z\left(\frac{K_v}{H} \partial_z C\right) + R + Q_c, \end{aligned} \quad (3.3)$$

where H = total depth (m), u = water speed (m/s), v = velocity in y direction (m/s), w = vertical velocity (m/s), K_H = hydrolysis coefficient (day^{-1}), K_v = volatilization coefficient (day^{-1}), w_s = sediment settling velocity (m/s), R = reactivity of chemical and biological processes, Q_c = external toxic sources and sinks, x and y = Cartesian coordinates in the horizontal directions and z = sigma coordinate in the vertical direction. The particulate fraction of the toxic (f_p) and the dissolved fraction of the toxic (f_d) are given by equations 3.4, and 3.5 below, which were also obtained from Ji [120]:

$$f_p = \frac{C_p}{C} = \frac{PS}{\theta + PS} \text{ and} \quad (3.4)$$

$$f_d = \frac{C_d}{C} = \frac{\theta}{\theta + PS}, \quad (3.5)$$

where θ = porosity (~ 1 for the water column), and PS = dimensionless parameter representing the product of partition coefficient (P) and sediment concentration (S).

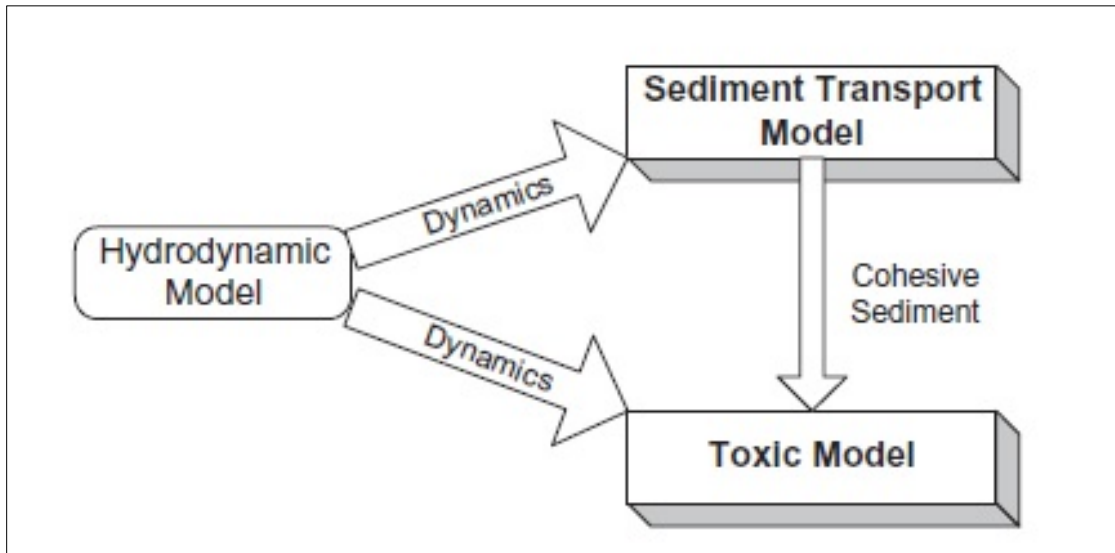


Figure 3-5. Structure of toxic module (adapted from Ji [120])

In addition, EFDC includes deposition and associated surface water entrapment, resuspension and associated porewater entrapment, porewater expulsion, and diffusion between surface water and porewater phases while modeling water column-sediment bed exchange [120]. Hence, for example, the model is capable of generating time series data for the sediment thickness, which can be used to identify the areas in the HSC-GBS with low or high erosion. The model also takes into account the sorption-desorption interaction between dissolved and particulate toxics, fate and transport of toxics in the system, and external loadings of toxics into the system.

A total of five PCB congeners (PCB-1, PCB-3, PCB-11, PCB-17, and PCB-25) were used in the model simulations. Table 3-1 provides the physical properties of the five congeners. In addition, Table 3-1 also provides the organic carbon partitioning coefficients in the sediment bed, K_{doc} and K_{poc} values used in the model (see section 4.1.7 for equations used to estimate these variables). The aforementioned congeners were

selected because they had the most detailed datasets and the least number of non-detects in the sampling data available for PCBs between 2002 and 2012. In addition, they also represent the lower chlorinated, more soluble PCBs that were studied and would therefore, be a better indicator of achievable reductions of dissolved PCB concentrations in the HSC-GBS.

Table 3-1. Physical properties of PCB congeners used in the EFDC model

PCB Congener	IUPCA Name	# of Chlorine Substitutions	Ortho-Positions	Log (K_{ow})	K_{poc} (L/mg)	K_{dpc} (L/mg)
PCB-1	2-Chlorobiphenyl	1	mono	4.46	0.0151	0.00504
PCB-3	4-Chlorobiphenyl	1	non	4.69	0.0134	0.00457
PCB-11	3,3'-Dichlorobiphenyl	2	non	5.28	0.039	0.011
PCB-17	2,2',4-Trichlorobiphenyl	3	non	5.25	0.215	0.0451
PCB-25	2,3',4-Trichlorobiphenyl	3	mono	5.67	0.178	0.0386

Figure 3-6 shows the locations where PCB sediment and water samples were collected in the HSC-GBS in 2002-2003. Sediment samples were collected at 45 locations and water samples were collected at 32 locations. Out of the sampled locations, data from four locations were not used in any calculations as they were outside of the HSC-GBS EFDC model grid. The EFDC model has a limitation associated with the initial PCB spatial sediment concentrations; a constant value is required for the entire grid. Hence, average initial PCB concentrations in sediment for each of the five PCB congeners were calculated by using the concentrations obtained at the stations on the main channel, and the model was initiated with these concentrations. The boundary conditions at Galveston Bay were set by averaging the concentrations obtained at the five sampling stations in Galveston Bay, for each of the five congeners.

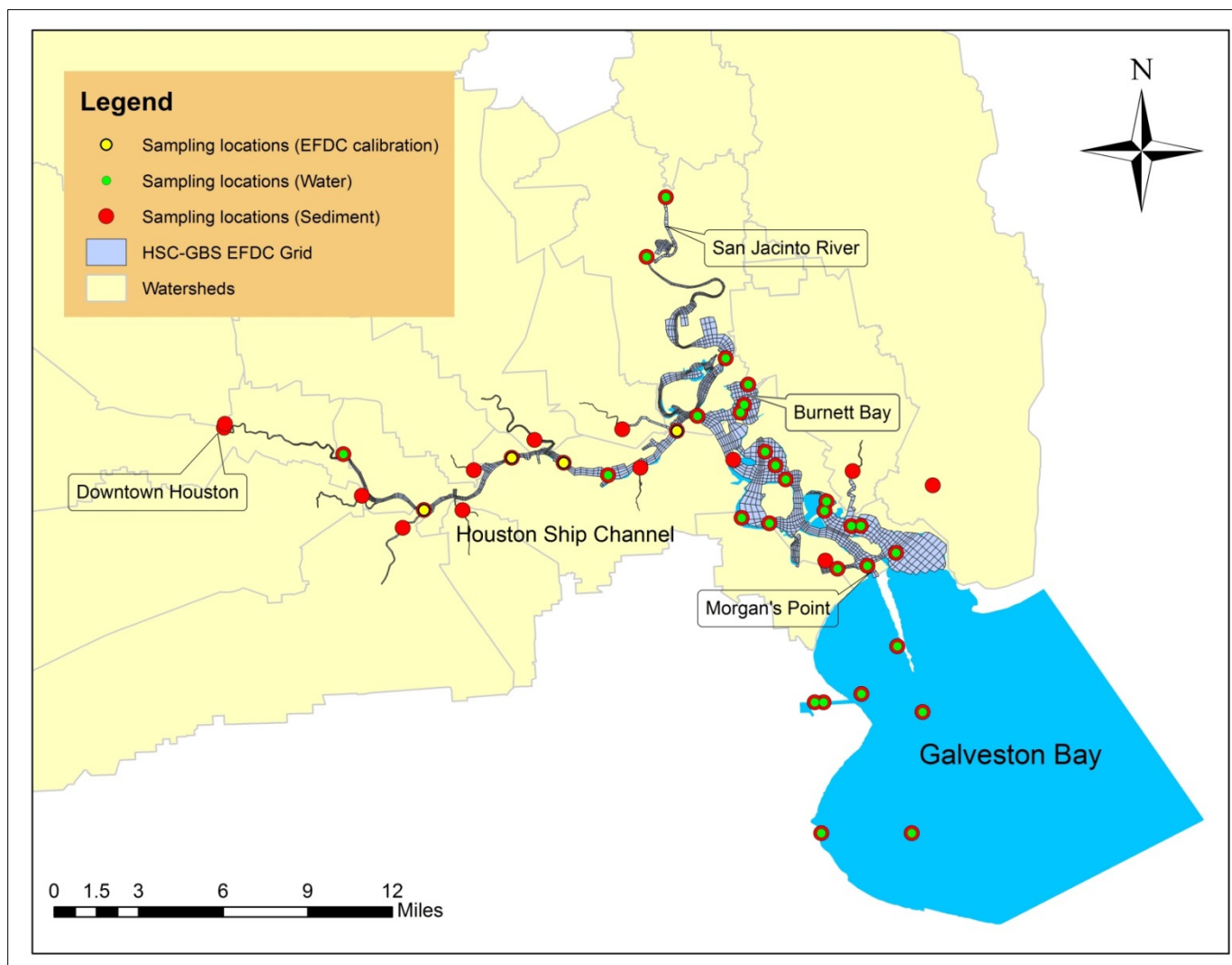


Figure 3-6. PCB water and sediment sampling locations in 2002-2003

Input files (*fpocb.inp*, *fpocw.inp*, *toxw.inp*, and *toxb.inp*) were created to provide model input such as the fraction of organic carbon in bed and water, and the initial PCB concentrations in water and bed sediment, respectively. The *toxb.inp* file was built using the sampling data from 2002-2003 as noted before. The initial concentrations for the five congeners in sediment: PCB-1, PCB-3, PCB-11, PCB-17, and PCB-25 were 0.00038mg/kg, 0.00023mg/kg, 0.00022mg/kg, 0.00074mg/kg, and 0.00020mg/kg, respectively. The *toxw.inp* file was initiated with concentrations of zero “0” for the five PCBs in water so that the model could capture the partitioning of PCBs from the sediment and the loadings from the bayous/tributaries.

Time step size and spin-up time. The spin-up time of a model is defined as the time required for a hydrological model to internally adjust to the provided initial and boundary conditions (e.g., tide, input flows) [121]. Howell [102] demonstrated in their model that 60 days was an appropriate spin-up time. A spin-up simulation confirmed the appropriateness of this value to allow the model hydrodynamics to stabilize. The model was then run for 40 days to simulate the real conditions in the HSC-GBS. The model was hot-started at day 100 (02/10/2003), with the Toxics module activated (a hot-start means the initial conditions for the run is derived from the simulated conditions of the spin-up run). Based on initial testing of the model, a sharp increase followed by a sharp decline in PCB concentrations was observed within the first 15 days (100-115 days) (see Figure 3-7). Further investigation revealed that the concentration of PCBs in the sediment decreased very quickly within the same time period. This decrease was mainly due to partitioning of the PCB from the sediment into the water column. With the passage of time, the washing out by the ebb tide to Galveston Bay caused a decline in the PCBs

available in the sediment. This fluctuation in concentrations continued to the point until both the sediment and water column reached equilibrium (approximately within 15 days). Hence, to overcome this, higher concentrations (approximately 292 times higher) were used in the *tox.b* input file, and a new spin-up time (15 days) was used for the EFDC model when the Toxics module was activated after the 100 days mentioned previously. This enabled the use of model results when the sediment concentrations in the model were equal to the aforementioned sampling values, and when the concentrations in the water column were stable. In other words, the model results were analyzed starting at day 115 (02/25/2003).

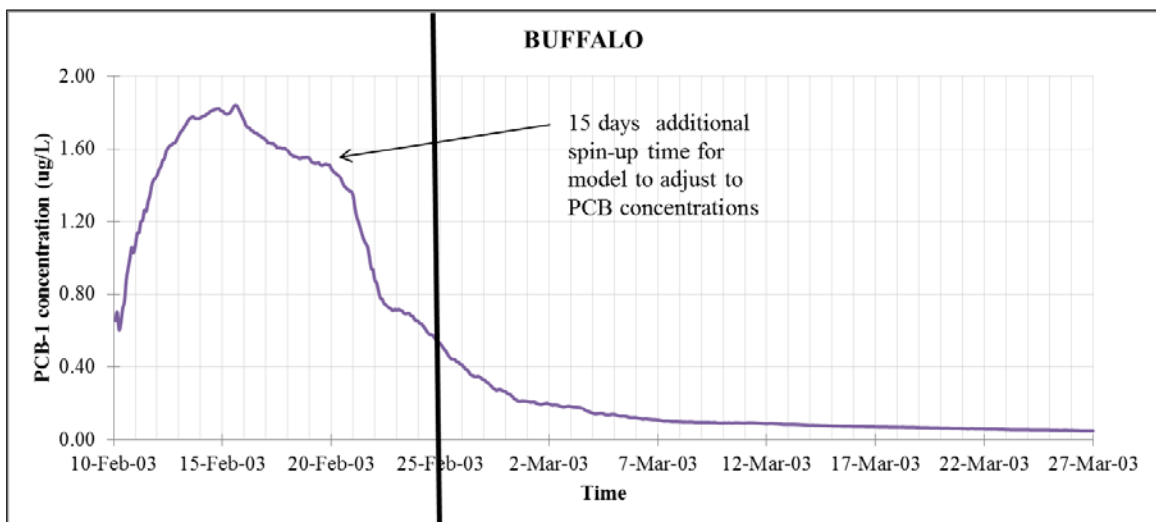


Figure 3-7. Evaluation of spin-up time for the model

The model was “hot-started” for all subsequent runs using the simulated conditions at the end of the spin-up of 115 days, and the results presented in section 4.3 are starting from day 115. The time step used in the model varied based on the length of the run. For shorter runs (1 month), a time step of 1 second was used; whereas a smaller time step was required for longer runtimes to ensure convergence of model results. Hence, a time step of 0.5 seconds was used for the longer 115 day runs (calibration run).

3.3.2 Model calibration

The model was previously calibrated by Howell [102] for water surface elevations, salinity, and TSS. Hence, in this dissertation, the hydrodynamic parameters were not changed and only the parameters in the model (including organic carbon fractions, and partitioning coefficients) that affect toxics (PCBs) were evaluated in terms of their effect on model predictions as will be seen in the remainder of the section.

The model was calibrated for the total water concentrations of each of the five PCB congeners obtained from the sampling data collected in 2003 during the time period of the model run after spin-up (02/25/2003-06/20/2003 = 115 days). Within this 115 days period, only four stations (11264, 11270, 11280, and 11287) in the HSC-GBS were sampled for PCBs (see Figure 3-6), and the concentrations are provided in Table 3-2. The lowest concentrations for all the PCBs except PCB-11 were recorded at station 11280. PCB loadings from tributaries were used as input sources into the model. The model was not validated since the goal of the model was to evaluate the potential for remediating existing contamination.

Sensitivity analyses. In order to develop a better understanding of the variables that affect predicted water concentrations in the model, sensitivity analyses were undertaken. Three different types of sensitivity analyses as shown in Table 3-3 were completed: (i) the organic carbon (OC) in sediment bed was both increased and decreased, (ii) the organic carbon partitioning coefficients were changed, and (iii) the loadings from tributaries were omitted. To perform the run without any loading from the tributaries, it was assumed that none of the tributaries input PCBs into the HSC, i.e., the flows from the tributaries were kept but the PCB concentrations in the tributaries were set to zero.

The values for the partitioning coefficients in the sediment bed in the sensitivity analyses (runs 5 – 8) were chosen based on the range of K_{poc} and K_{doc} values of the 209 PCB congeners as described in section 4.1.7.

Table 3-2. PCB concentrations at stations sampled in 2003 within the time period of EFDC calibration run

Station ID	Sample Date	Station Name	PCB-1 (µg/L)	PCB-3 (µg/L)	PCB-11 (µg/L)	PCB-17 (µg/L)	PCB-25 (µg/L)
11264	6/2/03	HSC @ SJR Park	0.0021	0.01505	0.00448	0.00741	0.0065
11280	6/11/03	HSC @ ARMCO	0.00175	0.00137	0.00480	0.00301	0.00074
11287	6/17/03	HSC @ Sims Bayou	0.00336	0.00286	0.00840	0.00948	0.00235
11270	6/18/03	HSC @ Beltway 8	0.00460	0.00402	0.00840	0.0078	0.00237

Table 3-3. Description of sensitivity analysis runs

Sensitivity Run Number	Variables of Interest	Calibration Run Values	Factor of Change/ New Values
Run 1	Organic carbon (OC) in sediment bed	5g/m ³	1g/m ³
Run 2			2g/m ³
Run 3			10g/m ³
Run 4			20g/m ³
Run 5	Partitioning coefficients (K_{poc} and K_{doc}) in sediment bed (both dissolved and particulate)	See Table 3-1	Increase by 90%
Run 6			Decrease by 90%
Run 7			Increase by 50%
Run 8			Decrease by 50%
Run 9	Loadings from tributaries	Flows from USGS and PCB sampling data	PCB concentrations in tributaries set to 0

3.3.3 Model output

The EFDC model provides results for various variables (salinity, TSS, toxics, etc.), but for the purpose of this dissertation, only toxics (PCB) data in the sediment and water column were analyzed. The PCB results were extracted from the model for the various runs as described below:

Calibration run. As mentioned before, the calibration run was run for a time period of 115 days (02/25/2003-06/20/2003) after spin-up. The concentration of PCBs in the water column over the entire HSC-GBS grid was extracted and setup in Microsoft Excel along with the latitude and longitude of the grid cells. The Excel file was then imported into ArcGIS to create maps that provide a spatial representation of the PCB concentrations in the water column in the HSC-GBS.

Time series data were also extracted and exported to Excel for plotting at five different locations: Buffalo Bayou before Vince Bayou (Buffalo Bayou), the confluence of the HSC and the San Jacinto River (HSC-SJR Confluence), the San Jacinto River (SJR), Tabbs Bay (Tabbs Bay), and Morgan's Point (Morgan's Point). The five locations were considered to be representative of change in modeled concentrations for the various runs that were simulated.

The results from the 115 days run (02/25/2003-06/20/2003) were compared to the measured data presented in Table 3-2. The grid cell in which each monitoring station was located was identified in ArcGIS, and the time series data were extracted at each of the monitoring stations for all five PCB (PCB-1, PCB-3, PCB-11, PCB-17, and PCB-25) congeners for comparison to the measured data.

Sensitivity analysis runs. Time series data were extracted from the EFDC model for

a 30-day period (02/25/2003-03/27/2003) at the five different locations noted above. The percent difference (% change) between each sensitivity run (runs 1 – 8) when compared to the calibration run was calculated for each location and illustrated graphically for ease of visualization of the effect of a specific variable on model results. For run 9, the time series was obtained at the five locations between 02/25/2003 and 06/03/2003, and compared with the calibration run both spatially and temporally.

In addition, the mass balance tool in the model was used to obtain the time series data for the PCB loadings that were discharged from the Channel into Galveston Bay. The mass loadings from the south (Tabbs Bay) and the west (Tabbs Bay and Morgan's Point) open boundaries in the model were summed to obtain the total mass loading. The mass loading was further cumulatively summed to obtain the cumulative loading from the grid into Galveston Bay, and the percent change between sensitivity runs and calibration run were plotted.

3.3.4 Model predictions

To simulate the effect of sediment remediation with the carbon-based materials, the K_{poc} and K_{doc} values were back-calculated using the K_s obtained in the laboratory experiments for the 11 PCB congeners (see Table 3-4). While only one congener (PCB-1) was simulated in the remediation runs, it is expected that the results overall will be similar in context for the other congeners since they are less soluble and will be expected to exhibit even lower concentrations remaining in the water column once the carbon materials are added into the sediment. The values used for PCB-1 in the calibration run were 0.00504L/mg (K_{doc}) and 0.0151L/mg (K_{poc}).

The concentration of PCBs in the water column over the entire HSC-GBS grid was

extracted at the end of one month of remediation and processed for visualization as described above. Additionally, the time series data were extracted at one of the areas exhibiting higher contamination (Burnett Bay, see Figure 3-6 for location) and the percent change was illustrated graphically.

Table 3-4. Partitioning coefficients used in the model for the carbon-based materials

	AC	BC	GE	GO	AC	BC	GE	GO	CNT
PCB congener	Log K _s (L/kg)				K _{doc} and K _{poc} used in EFDC (L/mg)				
PCB-1	7.86	6.89	6.26	6.37	2475.94	266.25	62.79	80.77	1787.89
PCB-2	8.21	7.69	6.92	7.16	5619.52	1691.40	285.17	494.96	6256.73
PCB-4	8.14	6.82	6.47	6.47	4743.93	227.01	101.42	101.00	2105.38
PCB-8	8.52	7.69	6.79	6.98	11384.91	1699.75	212.83	331.17	20424.62
PCB-15	8.77	8.53	8.44	8.25	20354.95	11786.11	9438.19	6069.67	39780.13
PCB-52	8.76	7.90	7.42	7.64	19752.20	2738.31	899.91	1492.36	64573.36
PCB-72	9.22	8.48	8.15	8.20	57232.98	10434.58	4848.06	5499.33	251082.80
PCB-77	9.56	9.19	9.94	9.77	126032.13	53347.76	301139.88	201036.96	398954.29
PCB-138	9.31	9.01	9.16	9.22	70511.58	35138.11	49333.61	57115.94	1175131.72
PCB-156	10.33	9.58	10.03	9.97	740031.75	129927.44	369335.06	322895.66	4015652.02
PCB-169	10.76	10.01	11.28	10.99	1997183.62	351401.16	6594227.44	3380754.36	7620086.76

Chapter 4. Results and Discussion

This section presents the results from the sampling of effluent in the HSC-GBS, experiments that were conducted with the carbon-based materials, and the results from the EFDC simulations that were completed as part of the dissertation.

4.1 PCBs in industrial and municipal effluents in the HSC-GBS

4.1.1 PCB congener patterns

Table 4-1 provides the number of detects obtained in both the dissolved and the suspended phases in the various effluents. Table 4-1 also provides information about the congeners that exhibited maximum concentrations at each of the effluent outfalls along with their TSS and TOC concentrations. It was observed from Table 4-1 that 12 out of the 17 (WWTP1-DUP included) sampling locations had greater than 50% detection in the dissolved matrix whereas only 7 out of the 17 (WWTP1-DUP included) sampling locations had greater than 50% detection in the suspended matrix, indicating that a low enough detection limit was achieved in the dissolved phase. The dissolved matrix, as can be seen in Table 4-1, furthermore exhibited a greater variety of quantified PCB congeners compared to the suspended matrix. TSS concentrations ranged from 4mg/L to 137mg/L with a median value of 14mg/L across all the effluent outfalls and the detection limit was 4mg/L, which is relatively low (Bolzonella et al. [122]). TOC concentrations ranged from 1.51mg/L to 54.80mg/L with a median value of 11.4mg/L across all the effluent outfalls and the detection limit was 1mg/L. At the industrial outfalls, TSS concentrations were in between 14mg/L and 45mg/L whereas at the municipal wastewater treatment plant outfalls, the TSS concentrations were in between 4mg/L and 10mg/L. The TOC concentrations at the industrial outfalls ranged between 1.51mg/L and 34.54mg/L

Table 4-1. Number of detects and the three congeners which show maximum concentrations in the dissolved and suspended phases for all effluents

Facility	TSS (mg/L)	TOC (mg/L)	Number of Detects		%Detects		Three Highest Concentration PCB Analytes	
			Dissolved Phase	Suspended Phase (>1um)	Dissolved Phase	Suspended Phase (>1um)	Dissolved Phase	Suspended Phase (>1um)
I1	30	11.60	116	102	71	62	110/115, 52, 95	110/115, 129/138/163, 90/101/113
I2	34.50	1.51	74	23	45	14	8, 4, 1	15, 209, 8
I3	21	10.69	77	83	47	51	11, 8, 44/47/65	129/138/163, 110/115, 118
I4	14	21.80	87	108	53	66	1, 8, 3	129/138/163, 153/168, 180/193
I5	45	34.54	99	84	60	51	4, 8, 11	44/47/65, 61/70/74/76, 52
I6	20	14.91	87	97	53	59	8, 4, 15	129/138/163, 110/115, 153/168
WWTP1	10	14	88	28	54	17	11, 4, 8	129/138/163, 153/168, 90/101/113
WWTP1 -DUP	4	13.80	85	29	52	18	8, 4, 11	129/138/163, 90/101/113, 110/115
WWTP2	0	6.80	64	2	39	1	4, 8, 1	209 (all other non-detects)
WWTP3	7	6.81	103	72	63	44	11, 52, 20/28	129/138/163, 11, 110/115
WWTP4	4.50	7.40	61	40	37	24	11, 20/28, 31	11, 129/138/163, 153/168
WWTP5	9.60	9.50	106	66	65	40	11, 8, 18/30	129/138/163, 153/168, 147/149
WWTP6	8	11.40	83	47	51	29	8, 4, 11	153/168, 129/138/163, 147/149
O1	74	6.44	107	100	65	61	8, 4, 18/30	129/138/163, 153/168, 180/193
O2	11	7.47	114	101	70	62	8, 4, 18/30	129/138/163, 61/70/74/76, 153/168
O3	137	54.80	73	29	45	18	8, 4, 1	129/138/163, 90/101/113, 209
O4	24	37.40	89	62	54	38	4, 8, 11	129/138/163, 147/149, 153/168

whereas at the municipal wastewater treatment plant outfalls, the TOC concentrations ranged between 6.8mg/L and 14mg/L.

In general, it was observed that the congeners that exhibited maximum concentrations in the dissolved and suspended phases were different. PCB-8 was among the highest three congeners in 14 out of the 17 dissolved effluent samples followed by PCB-4 in 12 out of the 17 dissolved phase samples. PCB-129/138/163, in comparison, was among the highest three congeners measured in the suspended phase in 14 out of the 17 samples as shown in Table 4-1.

Out of the 209 congeners, 36 of them were always detected in all the effluent samples in the dissolved phase. It was also noteworthy that only 5 of the PCB congeners in the chlorination range of 6-10: PCB-129/138/163, PCB-135/151, PCB-147/149, PCB-153/168, and PCB-180/193, were detected in the dissolved phase at all the effluent sites. Though it was observed that greater than 50% detection was achieved at 12 of the 17 sampling locations, only one PCB congener: PCB-90/101/113, was detected in the suspended phase in all the effluent samples. These findings confirmed the hypothesis that lower detection limits could be achieved in the dissolved phase whereas it was not possible in the suspended phase, to measure the low concentrations that may be present.

The MDL of the PCB congeners in the dissolved phase ranged between 0.0024ng/L and 4ng/L whereas it ranged between 0.004ng/L and 3.5ng/L in the suspended medium. The volume collected per sample was 200 liters and the detection percentage could have been increased if more water was pumped. On the other hand, it should also be noted that if certain congeners were not detected, there exists the possibility that they might not have been present in the first place.

Measured individual concentrations of the 209 PCB congeners at the various outfalls in both the dissolved and suspended phase were summed to determine total PCBs for the effluent samples; the results are presented below.

4.1.2 Total PCB (Σ 209) concentrations

Figure 4-1 and Figure 4-2 show the total concentration of the 209 PCB congeners in the suspended and dissolved media, respectively. The concentration range in the dissolved medium was between 1.01ng/L and 8.12ng/L with a median value of 2.29ng/L. The lowest concentration of 1.01ng/L was observed in the effluent obtained from WWTP3 and the highest concentration of 8.12ng/L was observed in the effluent obtained from O2. It was noted that the dissolved concentrations were relatively constant in industrial effluents but exhibited wider variability for municipal facilities and the facilities in the “other” category.

In the case of the suspended medium, the concentrations ranged from 2.03ng/L to 31.19ng/L with a median value of 3.58ng/L. The lowest concentration of 2.03ng/L was observed in the effluent obtained from WWTP4 and the highest concentration of 31.19ng/L was observed in the effluent obtained from industrial wastewater treatment plant O4. Similarly, suspended concentrations from industrial effluents exhibited less variability than those measured for municipal and “other” effluents. Additionally, average concentrations in the dissolved and suspended media at each of the outfalls were also calculated using only the detected congeners at each of the outfalls, and it was noted that O2 and O4 still had the highest concentrations in the dissolved and suspended media, respectively.

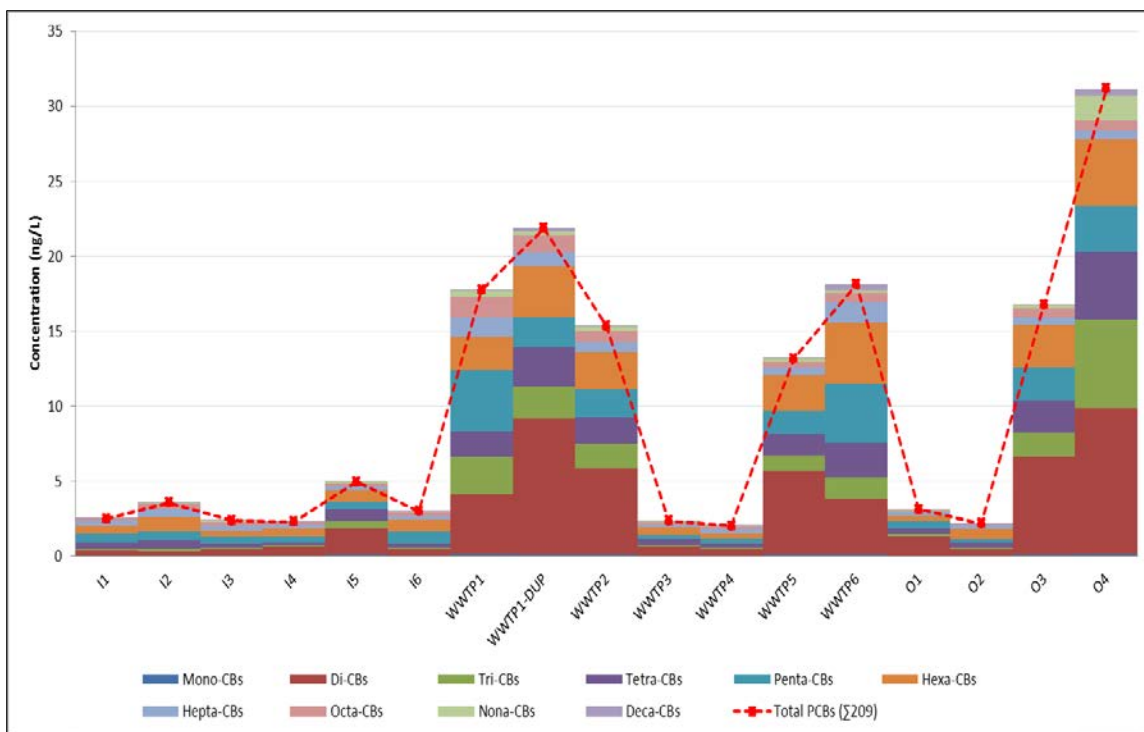


Figure 4-1. Total PCBs ($\Sigma 209$) and distribution of PCB homolog concentration at each of the effluent outfalls in the suspended phase. Non-detects = $\frac{1}{2}$ MDL

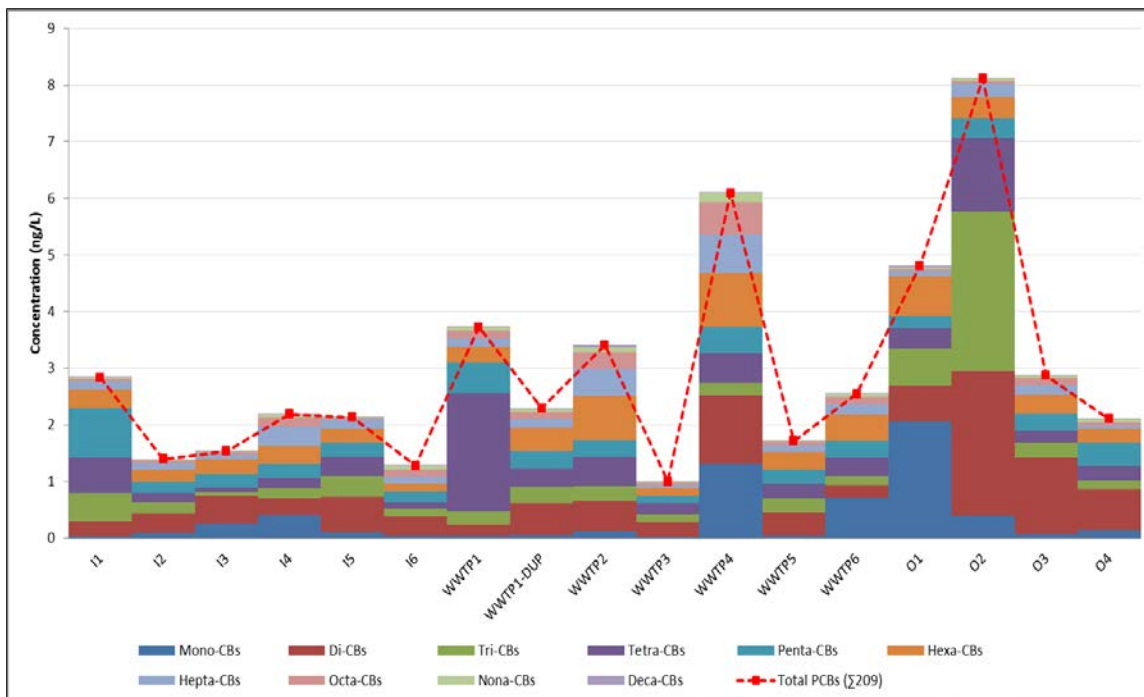


Figure 4-2. Total PCBs ($\Sigma 209$) and distribution of PCB homolog concentrations at each of the effluent outfalls in the dissolved phase. Non-detects = $\frac{1}{2}$ MDL

In general, the total PCBs ($\Sigma 209$) concentration in the suspended medium was much higher (mean $C_{\text{suspended}}/C_{\text{dissolved}} = 4.03$) than that observed in the dissolved medium. Additionally, there was a significant difference in the total PCBs ($\Sigma 209$) concentration between the parent and the duplicate sample obtained at WWTP1. Out of the 77 PCB analytes that were detected in both the parent and the duplicate sample in the dissolved medium, 10 had a relative percentage difference greater than 50% whereas none of the 19 PCB analytes that were detected in both the parent and the duplicate sample in the suspended medium had a relative percentage difference greater than 50%.

The number of different PCB congeners/coelutes required to reach 85% of the total PCBs in both the dissolved and suspended phases, at the various effluent outfalls was calculated. 85% was chosen arbitrarily rather than choosing 90% or 80% or 75%. The data showed that at each effluent outfall, the number of congeners required to make 85% of the total concentration was different. It was observed that at all the wastewater treatment plants, more congeners were required to make 85% of the total concentration in the dissolved phase than the suspended phase. The same trend was also observed at industrial wastewater treatment plants, O3 and O4. The trend is reversed for the chemical/petrochemical industries, i.e., significantly more congeners were required to make 85% of the total concentration in the suspended phase than the dissolved phase. Both PCB-8 and PCB-4 contributed significantly towards 85% of the total concentration at all the effluent outfalls in the dissolved phase whereas PCB-129/138/163 was the major contributor towards 85% of the total concentration at all the effluent outfalls except those obtained from I5 and I2 in the suspended phase. This further confirmed that different PCB congeners were detected at higher levels between the dissolved and

suspended phases.

4.1.3 Suspended mass concentrations

In order to completely understand the distribution of PCBs in each of the effluent outfall locations irrespective of the suspended solids concentration, mass basis concentrations (mass PCB/mass solids) were calculated using TSS measurements ($C_{\text{susp}}[\text{TSS}]^{-1}$) (Figure 4-3).

Overall, it was observed that the effluent from the wastewater treatment plants had statistically significant higher total mass concentrations than the effluents from other types of industries. Also, when normalized by TSS, O4 was not the maximum contributor towards PCBs contamination; in this case WWTP1-DUP exhibited the maximum concentration of 1227.50pg/g dry. This indicated that at O4, a large quantity of low mass basis concentration suspended particles generated a large suspended phase water concentration and that the high PCB concentration was not due to inherently high concentration particulates.

WWTP5 exhibited the highest average detected mass concentration of PCBs closely followed by WWTP1-DUP and the sample obtained at O4. It should be noted that this was due to significant PCB contamination in both those areas and not due to background concentrations as the TSS measurements at both these locations were pretty low (9.60mg/L and 4mg/L).

4.1.4 PCB homolog concentrations in dissolved and suspended phases

Figure 4-1 shows the homolog concentrations at each of the effluent outfall locations in the suspended medium. The data in the Figure shows that at some plants, which include I1, WWTP4, WWTP3, and I3, no dominant homologs were found whereas for

others, which include all the remaining wastewater treatment plants, I5, and O1, specific and relatively few homologs dominated the total PCB concentration. Another observation was that relatively high concentrations were exhibited by homologs one through six and much less contribution was made by the other homologs. Amongst these homologs that exhibited high concentrations, dichlorobiphenyls had the highest concentration at most of the effluent outfall locations.

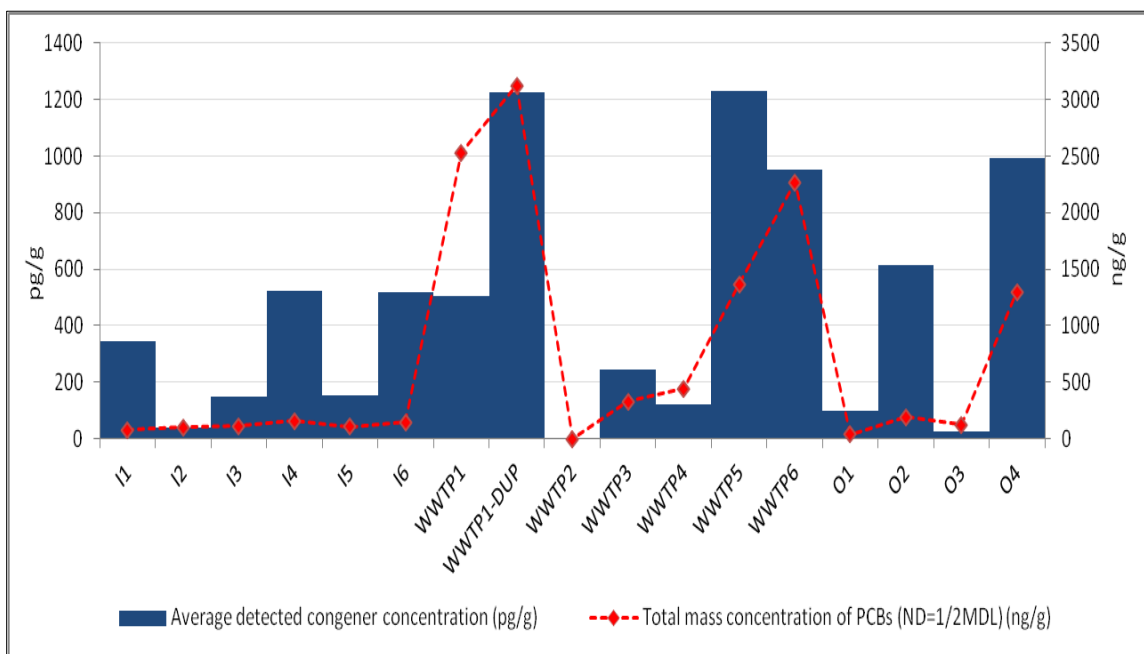


Figure 4-3. Total mass concentration of the PCBs and the average detected congener concentration of the PCBs in the suspended phase at each of the outfalls

The high concentration of dichlorobiphenyls at the various municipal and industrial wastewater treatment plants (WWTP1, WWTP1-DUP, WWTP2, WWTP3, WWTP4, WWTP5, WWTP6, O3, and O4) was due to the unique nature of the effluents from these facilities. Another reason for the accumulation of dichlorobiphenyls could be because of the dechlorination of higher chlorinated PCBs.

Yet another interesting point was that though the highest homolog concentration was not observed consistently in all the wastewater treatment plants, most of the high

concentrations were measured at wastewater treatment plants. Even though dichlorobiphenyls still had the highest concentration at plant O4, it was observed from analyzing the data that nonachlorobiphenyls peaked up higher than octachlorobiphenyls and decachlorobiphenyls. This differed from what was observed in Guo et al. [123] which reported that decachlorobiphenyls had high absolute concentrations in wastewater treatment plants which was attributed to the inputs of industrial effluent being deposited into the sewage sludge during the wastewater treatment process. Hence, the difference observed in the HSC-GBS effluents could be attributed to the fact that maybe the source and transport of PCBs into this wastewater treatment plant was different from the rest of them and those observed previously.

As interesting observations were made in the effluents in the suspended phase, they were also analyzed in the dissolved phase. Figure 4-2 shows the PCBs homolog concentration distribution in the dissolved medium at the various effluent outfall locations. In general, it was observed from the Figure that the lower homologs exhibited much higher concentrations than the higher homologs, which was similar to the data shown in Figure 4-1.

4.1.5 Distribution of PCBs between dissolved and suspended media

Fractional analysis of PCBs between the dissolved and suspended media was studied to analyze the differences in the partitioning of PCBs between the industrial and municipal wastewater treatment plants. Figure 4-4 shows plots of the suspended congener concentration against the corresponding dissolved congener concentration for the eight wastewater treatment facilities. The plots in Figure 4-4 contain only detected concentrations to minimize the bias in the plots and subsequent analyses. Also, the

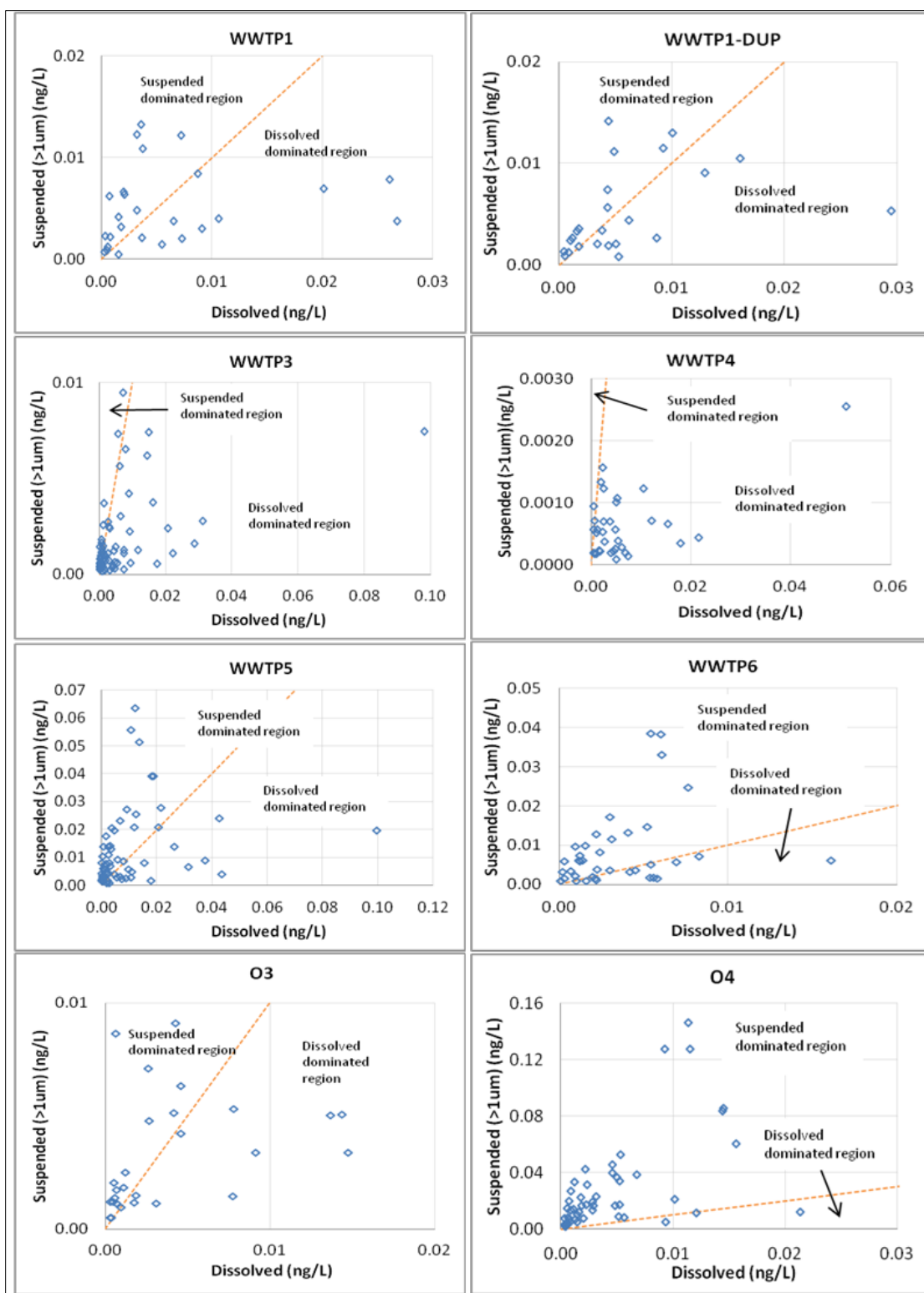


Figure 4-4. Distribution of all detected PCB congener concentrations between the dissolved and suspended phases at the sampled wastewater treatment plants (except for WWTP2 that had a very low detection rate)

particle phase concentration is expressed in ng/L to allow assessment of the effect of pollutant load on the water body on a volume of water basis. In general, there was no obvious correlation between dissolved and suspended concentrations at the eight plants. However, some observations could be made from the plots and they are discussed below.

Both the parent and the duplicate sample obtained from the WWTP1 effluent outfall, for example, and the sample from O3 had a similar pattern. Their dissolved and suspended congeners were distributed almost equally with concentrations in the range of 0.29-30pg/L in both matrices. Though WWTP5 also had equal distribution of the PCB congeners between the dissolved and suspended phases, the concentrations were much higher and ranged from 0.26-100pg/L. At both WWTP3 and WWTP4, the congeners were found predominantly in the dissolved phase and the concentrations were in the range of 0.08-100pg/L. On the other hand, at O4 and WWTP6, the congeners were concentrated in the suspended phase. Though at both the aforementioned wastewater treatment plants the congeners were found extensively in the suspended phase, at O4, the concentration ranged from 0.26-160pg/L whereas at WWTP6, the concentration ranged from 0.15-40pg/L. Also at WWTP3 and WWTP5, PCB-11 exhibited a much higher concentration of 0.1ng/L in the dissolved medium, when compared to the other wastewater treatment plants.

4.1.6 Suspended fraction as a function of $\log(K_{ow})$

The data in Figures 4-5, 4-6, and 4-7 show the suspended fraction against $\log K_{ow}$ for only the detected concentrations in both the dissolved and suspended phases at the municipal wastewater treatment plants, chemical/petrochemical industries, and other types of facilities, respectively. The suspended fraction of each congener was calculated

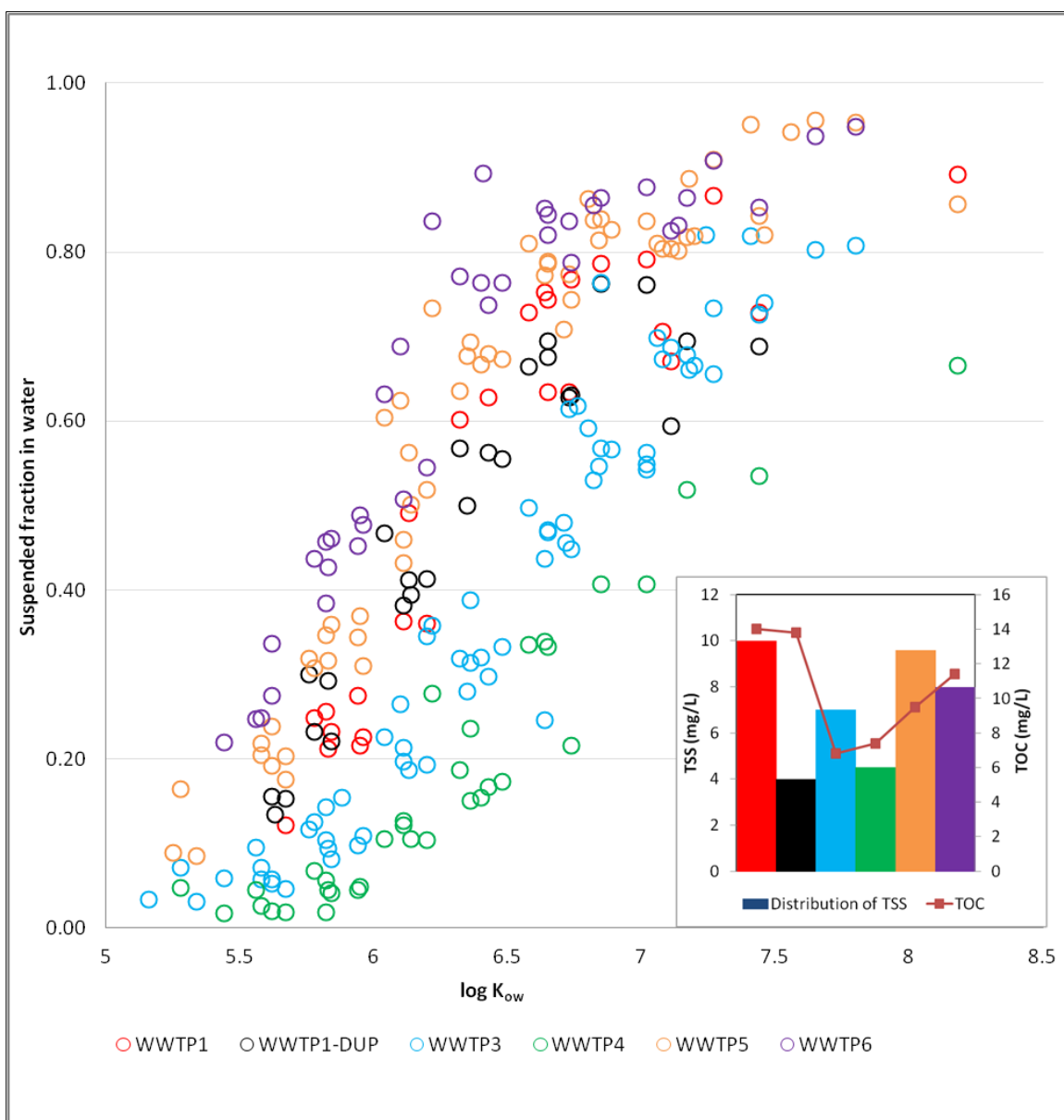


Figure 4-5. Suspended fraction of PCBs in water at each of the municipal wastewater treatment plant outfall locations plotted against the $\log K_{ow}$ for the detected concentrations in the suspended and dissolved phases

by dividing the suspended concentration by the sum of dissolved and suspended concentration of the same congener, and the values of $\log K_{ow}$ were obtained from Hawker and Connell [49]. The suspended fraction of the PCBs ranged in between 0.0011 and 0.979 across the various effluents. As expected, the suspended fraction for a congener was a function of $\log K_{ow}$, i.e., the higher the $\log K_{ow}$, the higher the suspended

PCB fraction.

Interestingly enough, the suspended fractions for the same congener varied widely depending on the TSS and TOC concentrations at the outfalls, as seen in Figures 4-5, 4-6, and 4-7. For the same $\log K_{ow}$, the facility that had almost equal or similar TSS and TOC concentrations had the highest operationally suspended fraction of PCBs when compared with the other industries. At the municipal wastewater treatment plants shown in Figure 4-5, for instance, the high-suspended fractions observed at WWTP6, WWTP1, and WWTP5 could be attributed to the high concentration of TSS at these facilities. The high-suspended fractions exhibited by the sample obtained at WWTP1-DUP, though it had very low TSS concentration, maybe because of the high TOC concentration observed in the sample. This observation confirmed that TOC played an important role in determining the suspended fraction of PCBs at the facilities.

Similarly, for the petrochemical industries shown in Figure 4-6, the operationally suspended fraction distribution at the same $\log K_{ow}$ depended heavily on the similarity between the TOC and the TSS concentrations. Thus, if an industry had similar TSS and TOC concentration, and the TOC value was slightly lower than the TSS value, the effluent had a higher operationally suspended fraction at lower values of $\log K_{ow}$ (less than 6.25). Another possible explanation for this could be that at low $\log K_{ow}$, DOC was able to be more competitive with POC on a mass basis. The effluent from I4 was an outlier amongst these industries as it had a relatively high suspended fraction even though it did not have comparable TSS and TOC concentrations; this may be due to the specialty chemicals manufactured at I4 that include methyl methacrylate, amines, acrylic acid, and the like [124].

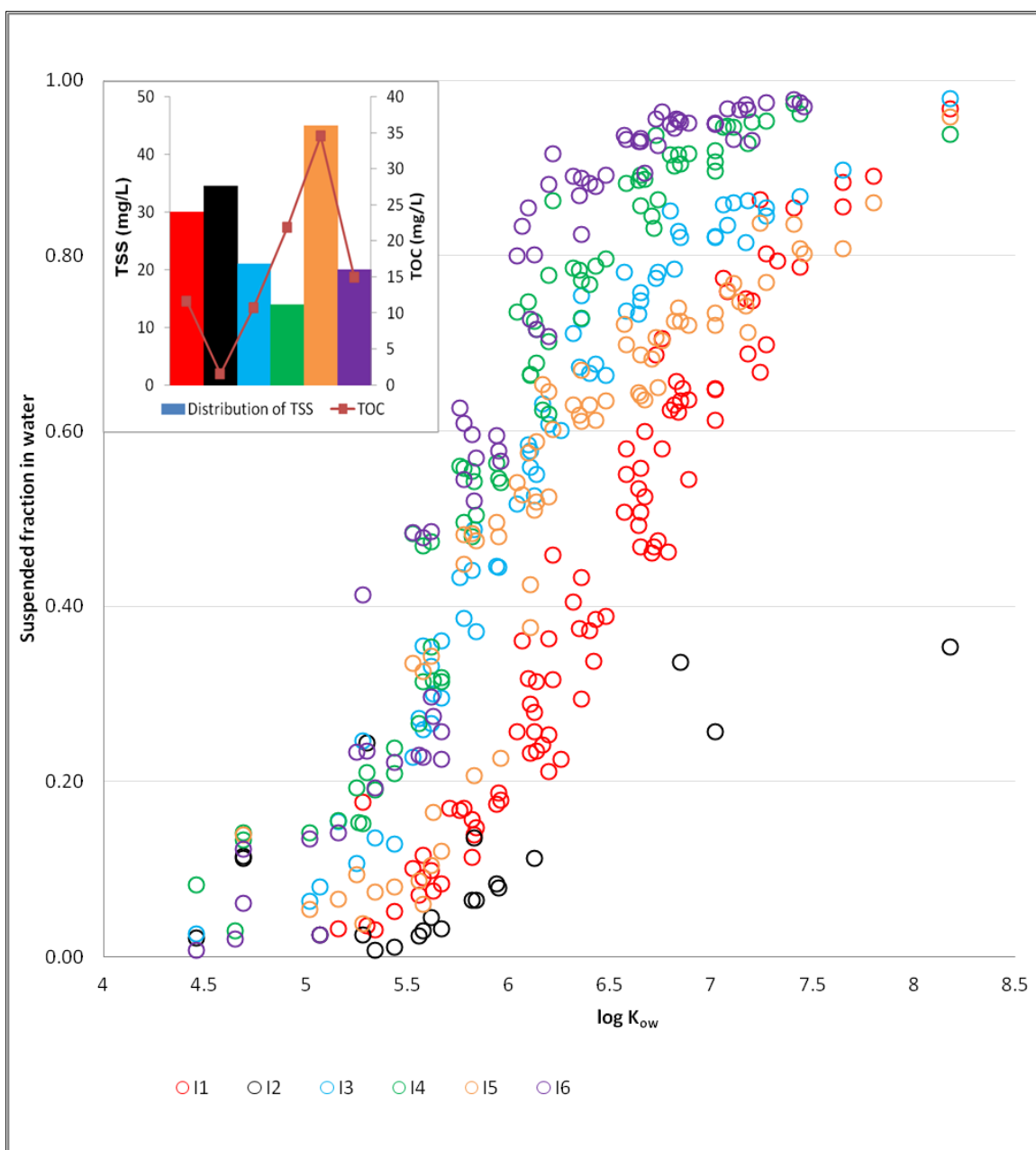


Figure 4-6. Suspended fraction in water at each of the industrial effluent outfall locations plotted against the log K_{ow} for the detected concentrations in the suspended and dissolved phases

The distributions of the suspended fractions of PCBs at the four remaining facilities are shown in Figure 4-7. O3 and O4 are industrial wastewater treatment plants and hence, they had much higher TSS concentrations than those observed at the municipal wastewater treatment plants. Between these two wastewater treatment plants, O4 had a

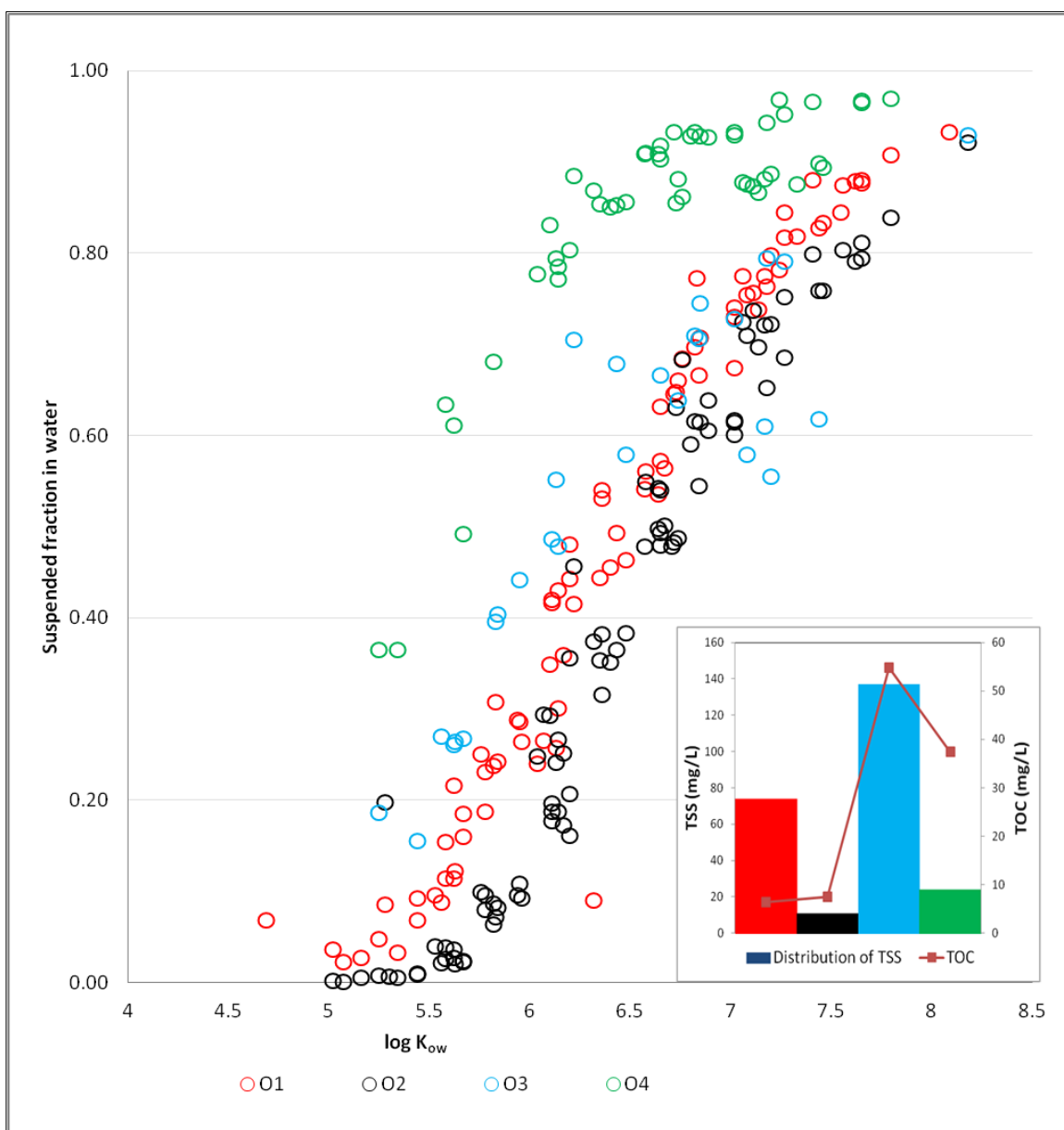


Figure 4-7. Suspended fraction in water at the two industrial wastewater treatment plants (O3 and O4), refuse system (O1), and special warehousing and storage facility (O2) plotted against the log K_{ow}

higher suspended fraction for the same log K_{ow}. The reason for this observation was not clear as O4 had both TSS and TOC concentrations lower than those observed at O3. On the other hand, between O1 and O2, which are both industries handling very little manufacturing and chemical processes, TSS played a major factor in the observed

suspended fractions. For the same $\log K_{ow}$, O1 that had a TSS concentration of 74mg/L exhibited higher suspended fractions than O2 which had lower suspended fractions with a TSS concentration of only 11mg/L.

The major conclusion that was derived from the analysis of the suspended fraction against $\log K_{ow}$ was that though $\log K_{ow}$ was a good indicator of the partitioning of PCBs, it did not provide the complete picture. The $\log K_{ow}$ value alone was not sufficient to understand partitioning of PCBs since it did not give any indication of the level of TOC and/or TSS or the type of effluent stream (industrial, municipal, or other) that determined the extent to which specific congeners were present predominantly in the dissolved or suspended phase. Also the effect caused by POC and DOC at lower values of $\log K_{ow}$ (less than 6.25) was much different when one moves to higher values of $\log K_{ow}$ as higher POC caused higher suspended fractions but, higher DOC did not result in lower suspended fractions. Hence, this showed that the need to understand the role played by TSS and the various fractions of carbon in effluent outfalls to control the contamination of PCBs in natural water systems was extremely important.

4.1.7 Estimating organic carbon partitioning coefficients in effluents

The suspended fraction (suspended concentration/sum of dissolved and suspended concentration) for a congener was observed to be a function of $\log (K_{ow})$, but varied widely depending on the TSS and TOC concentrations. While TOC played an important role in determining the suspended fraction of PCBs for municipal wastewater treatment plants (WWTP), a higher operationally suspended fraction at lower values of $\log (K_{ow})$ (less than 6.25) was observed in industrial effluents when the TOC value was slightly lower than the corresponding TSS value. Hence, $\log (K_{ow})$ alone was not sufficient to

understand partitioning of PCBs, and this is further observed in the results presented in section 4.2.

The partitioning of PCBs between dissolved and suspended media was analyzed by normalizing the congener concentration of each PCB by both POC and TOC concentrations. Additionally, the total dissolved concentrations were adjusted for the DOC contribution using the PCB-specific K_{doc} (L/kg) LFER of Burkhard [125] provided in equation 4.1 below:

$$K_{doc} = 0.85 \log(K_{ow}) - 0.25. \quad (4.1)$$

Lastly, the $\log K_{poc}$ and $\log K_{toc}$ at each of the effluent outfalls and the average $\log K_{poc}$ and $\log K_{toc}$ values were calculated. The distribution of $\log K_{poc}$ and $\log K_{toc}$ against $\log (K_{ow})$ obtained from Hawker and Connell [49] showed that the adjusted $\log K_{poc}$ and $\log K_{toc}$ values corresponded better to a generally accepted increasing trend of partitioning coefficient increase with increase in $\log (K_{ow})$. It was also noted that the $\log K_{poc, total}$ and $\log K_{poc, adj}$ were not that different when $\log (K_{ow})$ was less than 6. The same trend was observed between $\log K_{toc, total}$ and $\log K_{toc, adj}$ as well. This was because this region is only moderately hydrophobic and the K_{doc} did not have any impact on the trend, i.e., most of the total dissolved concentration should be truly dissolved at these surface water DOC concentrations. When $\log (K_{ow})$ was greater than 6, the truly dissolved concentrations were overestimated when the DOC-associated PCB fraction was included in the calculation.

Adjusted $\log K_{poc}$ and $\log K_{toc}$ provided a more reasonable trend of partitioning with changes in hydrophobicity. Thus, only those values were used to compare the partitioning behavior between different types of effluents. The difference observed between the

industrial and wastewater treatment plants were because the model described by Burkhard [125] accurately described the industrial DOC total dissolved fraction whereas it overestimated it for wastewater treatment plants. Another reason could also be that the differences are due to POC quality. This suggested that POC was a better sorbent for PCBs in the industrial effluents compared to wastewater treatment plants.

Next, the average $\log K_{toc}$ (L/kg) values were compared against those that were obtained using the model described by Seth et al. [126] provided in the equation below:

$$\log(K_{toc}) = 1.03 \log(K_{ow}) - 0.61. \quad (4.2)$$

Figure 4-8 shows the comparison of average $\log K_{toc}$ for industrial and wastewater treatment plants against the Seth et al. [126] model and Hansen et al. [127] data, separately. It was observed from the Figure that the HSC-GBS data did not have a slope of unity as was observed in the study conducted by Seth et al. [126]. For $\log (K_{ow})$ values between 5.5 and 7.5, the HSC-GBS data were seen to be within the upper limit and lower limit of $\log K_{oc}$ described by Seth et al. [126], thereby showing that the data closely followed the model for these $\log (K_{ow})$ values. The values of $\log K_{toc}$ that fell outside the bounds of the Seth et al. [126] model at the industries were mostly dichlorobiphenyls (includes PCB-11 modeled in EFDC) and those that fell outside the bounds at the wastewater treatment plants were dominated by dichlorobiphenyls (PCB-4, PCB-8, and PCB-15 used in experiments) and trichlorobiphenyls (PCB-25 modeled in EFDC). This depicted that these congeners were harder to measure accurately perhaps due to volatility or to not being captured as well by the XAD2 resin during sampling.

The data were also compared with the $\log K_{oc}$ values obtained from Hansen et al. [127] and it was observed that the HSC-GBS data were consistent with their findings

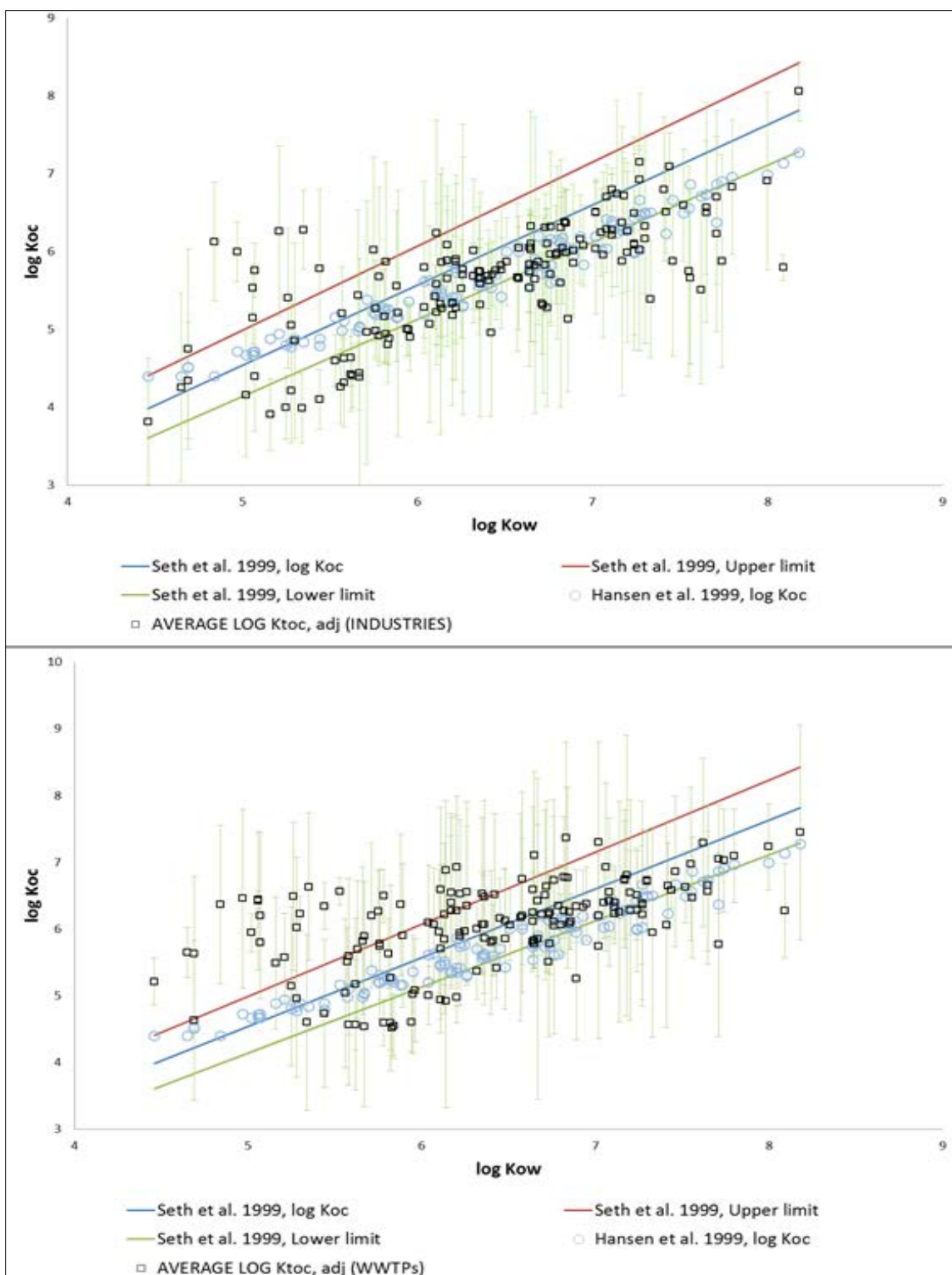


Figure 4-8. Comparison of HSC-GBS $\log K_{toc,adj}$ values of industries and wastewater treatment plants with data obtained from Seth et al. [126] model and Hansen et al. [127]. Error bars represent standard deviation

between $\log(K_{ow})$ values of 6 and 8. The comparison suggested that there was a possibility that the partitioning of industrial, wastewater treatment plant, and other type of effluents to particles was different and this could be due to differences in POC, DOC, or maybe both. It should also be noted here that the lab measurements obtained by Hansen et al. [127] exhibited variation which is greater than a simple standard multiple of $\log(K_{ow})$, and hence it was not that surprising that the same behavior was exhibited by the HSC-GBS data. It can also be observed from Figure 4-8 that the partitioning behaviors in effluents are often weaker than what was predicted in Seth et al. [126], especially at higher hydrophobicity because the slope of $\log K_{toc}$ Vs $\log(K_{ow})$ was smaller for effluents. The above partitioning analyses aided in understanding the specific parameters (organic carbon fractions and sorption constants) to analyze while performing sensitivity analyses with the EFDC model.

4.1.8 Discussion

Total PCB ($\Sigma 209$) concentrations in the suspended medium, was on an average, four times higher than the total PCB ($\Sigma 209$) concentrations obtained in the dissolved medium. While municipal wastewater treatment plants did not have the highest concentration of total PCBs, they are the largest contributors to natural water systems because of the relatively larger volume of effluents discharged on a daily basis. The fact that the observed dissolved and suspended concentrations were not similarly correlated at the various plants, while confirming earlier studies regarding variable treatment efficiencies among treatment plants, points to differences in levels of treatment for dissolved and suspended media. This difference in the level of treatment administered could be attributed to the variable sourcing of PCBs in the influent or the actual treatment

processes within the plants or the chemical make-up of the effluent (organic carbon fractions, TSS).

Homolog concentrations of PCBs obtained at the effluent outfall locations were seen to be dominated by lower chlorinated congeners (monochlorobiphenyls through hexachlorobiphenyls) with dichlorobiphenyls exhibiting the highest concentration at most of the outfalls. This was an interesting observation that had not been noted in prior studies. The observed accumulation of dichlorobiphenyls could be attributed to the nature of the influent being treated at the sampled locations but could also be due to the treatment processes that are likely causing the dechlorination of heavier PCBs into lighter PCBs.

Suspended fractions of PCBs, for the same congener, varied widely amongst the different effluent outfalls. While the suspended fraction of a congener was a function of $\log K_{ow}$, as would be expected, it was observed that $\log K_{ow}$ alone was not the deciding factor for the suspended fraction and that other parameters such as TSS, TOC, DOC, and POC played an important role in the partitioning of the PCBs. Consequently, it was observed that controlling total PCBs from a water quality standpoint might not be sufficient since partitioning within the water column affects the truly dissolved concentration or the concentration that is bioavailable for biota within the natural water system. It was also seen from the $\log K_{oc}$ values determined that for many congeners, the bioavailable fraction (truly dissolved) of the total water concentration was under predicted by Seth et al. [126] model, suggesting that effluent PCB loads might have more risk and impact than what the standard models would generally predict.

As a more rigorous approach that includes understanding of the chemical makeup of

effluent waters and their organic carbon content and speciation has to be undertaken to reduce the environmental impact of PCBs on biota in natural water systems, these factors were kept in mind during the setup of experiments with the carbon-based materials and the setup of EFDC model to manage the truly dissolved concentration of PCBs in the HSC-GBS.

4.2 Experimental results

4.2.1 Sorbent characteristics

Before the sorbents were used in the experiments, SEM was used to obtain the images of the five carbon-based materials: AC, BC, GE, GO, and CNT, with magnifications ranging between x450 and x4000 (see Figure 4-9). The resulting images were similar to those obtained by Beless [53].

The AC particles were seen to possess heterogeneous characteristics and a defined surface porosity. The surface porosity is an important factor as it is responsible for the large surface area of the AC particles that is available for the sorption of PCBs on the surface. The BC particles exhibited a more ‘shard’ like structure with higher homogeneity on the surface. The GE was aggregated, and a more ‘scale-like’ structure was observed on the larger aggregates. In contrast, the GO, while also aggregated, was not as clearly distinguished as the GE particles. The fibers of CNT were aggregated together and exhibited a ‘coral-like’ structure, thereby making it difficult to differentiate between the aggregates.

Table 4-2 provides the atomic mass fractions of the sorbents obtained from the EDS elemental analysis. Evidently, carbon accounted for the majority of the atomic makeup of all five sorbent materials. GO exhibited the lowest carbon content and the highest oxygen

content, confirming the presence of oxygen functional groups. The amount of oxygen present in AC was slightly higher than what was reported in Beless [53] which could likely be due to moisture effects, even though the AC was stored in clear glass vials with septum caps in a cool, dry place at room temperature. The observed slightly higher oxygen content, however, was not expected to affect the sorption effectiveness of the AC particles. BC exhibited a carbon content of 82.95% and an oxygen content of 17.05%.

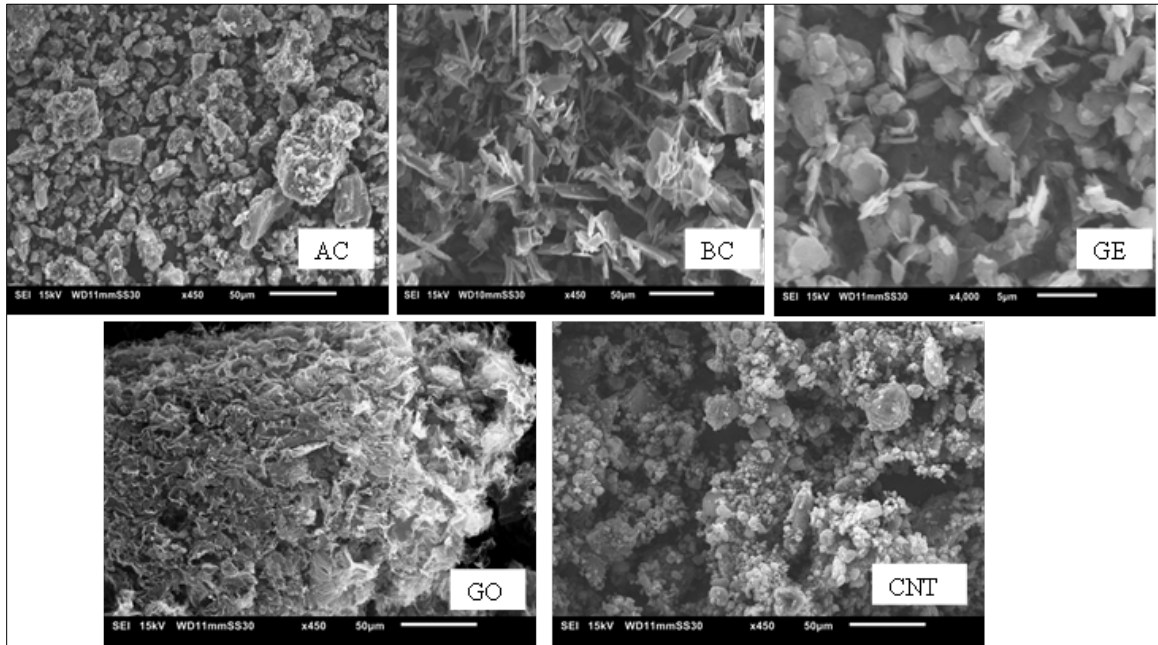


Figure 4-9. SEM images of activated carbon, black carbon, zoomed in image of graphene, graphene oxide particles, and non-functionalized carbon nanotubes

Table 4-2. Atomic mass fractions determined using EDS elemental analysis

Nanomaterial	Mass %	
	C	O
AC	71.62	28.38
BC	82.95	17.05
GE	87.41	12.59
GO	61.07	38.93
CNT	100	-

The GE material was predominantly carbon (87.41%), and the rest was oxygen, which could be due to the small amounts of oxygen functional groups formed during the production of the graphene sheets and due to moisture effects. Finally, CNT showed 100% carbon content confirming the fact that they contain no oxygen functional groups.

4.2.2 Quality assurance (QA)/Quality control (QC)

To ensure the quality of the data obtained from the experiments, numerous measurements were taken. Two types of experimental controls: PDMS fiber in PCB-mix spiked sediment and only PDMS fiber in clean sediment were analyzed in duplicate along with the other samples. The purpose of having these controls was to determine if any contamination was introduced into the samples unintentionally by: (i) improperly cleaned glassware that may have retained the PCBs, (ii) improperly cleaned PDMS fibers that may have retained the PCBs, or (iii) any other contamination that could have been introduced during creating, handling, and processing of the samples [53]. The results from the control samples did not result in any PCB detection, and this proved that the systems were clean, and that no detectable contamination was introduced during the sample preparation processes.

Samples were prepared in duplicate in accordance to standard laboratory procedures in order to account for any inconsistencies or human error. The coefficient of variation ($CV = \text{standard deviation}/\text{mean}$) between the parent and duplicate samples were calculated to gauge the precision of the samples. A large CV ($CV > 0.5$) indicates a high variation between the sample and the duplicate. The median value of all CV values was 0.224, with 80% of all duplicates having CV values less than 0.5. These results indicate that the measured duplicates, as a whole, had a low variation.

4.2.3 Appropriate use of PDMS fibers

The simplest design for batch experiments is the use of only the aqueous phase, and sorbent phase, and measuring the analyte concentrations in both the phases. This won't work for the current experiment setup due to two main reasons. First, in the traditional two phase design, complete separation of the aqueous and sorbent phases are required to measure the analyte, and this is difficult in this case due to the nanosized sorbent materials. Secondly, higher concentrations are required to achieve detection on the GC-MS, thereby requiring the need for larger volumes of both phases [53]. Hence, there was a need for the addition of a third phase (PDMS fiber). Although this complicated the experiment setup, it allowed for analyte detection at lower concentrations when at equilibrium. There is always the possibility that the PDMS fibers might remove too much of the PCBs, thereby creating a risk of altering the partitioning of the PCBs between the various phases; caution was taken so that not more than 5% of total analyte by mass was removed by the fiber.

As in these experiments only the PCBs that partition to the PDMS fibers were measured, it was important to understand how these fractions were generated in the various phases. Firstly, the equation developed by Lu et al. [118] was used to calculate the PDMS fiber-water partitioning coefficients (K_{f-w} as L_{water}/L_{PDMS}) using the octanol-water partitioning coefficient (K_{ow} as L/kg) of the 11 PCB congeners obtained from the literature [49]. The equation derived by Lu et al. [118] is given below:

$$\log(K_{f-w}) = 1.06(\pm 0.058)\log(K_{ow}) - 1.16(\pm 0.35). \quad (4.3)$$

Once the K_{f-w} was calculated using the above equation, which represents the ratio between the concentrations of PCBs on the PDMS fiber to the concentration of PCBs in

the aqueous phase, the equilibrium concentration of PCBs in the aqueous phase (C_e as $\mu\text{g}_{\text{PCB}}/\text{L}_{\text{water}}$) was determined by the following equation:

$$K_{f-w} = \frac{C_f}{C_e}. \quad (4.4)$$

Upon completion of the experiment, the concentration of PCBs on the PDMS fiber (C_f as $\mu\text{g}_{\text{PCB}}/\text{L}_{\text{PDMS}}$) is known for each of the samples. As the volume of PDMS coating on the PDMS fiber is known, the mass of PCBs on the fiber was calculated. Hence, in order to make sure that the PDMS fiber did not remove too much PCBs from the system, the percent mass of PCBs on the fiber with respect to total PCBs were calculated and they were all below the 5% level. This process confirmed that the PDMS fibers were used appropriately and they did not alter the partitioning of the PCBs between the various phases.

4.2.4 Distribution coefficients (K_s) and comparison between sorbents

Log (K_s) values were calculated for the parent and duplicate samples of each of the five sorbents, and for the control samples using equation 3.2 presented above. Average log (K_s) was calculated for each of the sorbents and is presented in Table 4-3. Average log (K_s) values ranged between 7.86 ± 0.07 and 10.76 ± 0.21 for AC, 6.89 ± 0.005 and 10.01 ± 0.01 for BC, 6.26 ± 0.02 and 11.28 ± 0.07 for GE, 6.37 ± 0.17 and 10.99 ± 0.24 for GO, and 7.71 ± 0.14 and 11.34 ± 0.01 for CNT. Figure 4-10 graphically illustrates the log (K_s) values presented in Table 4-3. It should be noted that the error bars were an order of magnitude lower for CNT and BC than for most congeners, and are hence, sometimes not visible on the graph. It can also be observed from Figure 4-10 that CNT had larger K_s values compared to the other four sorbents with all the 11 PCB congeners except PCB-1 and PCB-4. The dominance was greater for the more chlorinated PCB congeners and

Table 4-3. Average log (K_s) values calculated for each sorbent with each of the 11 PCB congeners used in the experiment. The \pm values indicate the standard deviation from the average

PCB Congener	Log (K_s) ($L_{\text{water}}/kg_{\text{sorbent}}$)				
	AC	BC	GE	GO	CNT
PCB-1	7.86 ± 0.07	6.89 ± 0.005	6.26 ± 0.02	6.37 ± 0.17	7.71 ± 0.14
PCB-2	8.21 ± 0.07	7.69 ± 0.02	6.92 ± 0.07	7.16 ± 0.40	8.26 ± 0.003
PCB-4	8.14 ± 0.13	6.82 ± 0.03	6.47 ± 0.003	6.47 ± 0.25	7.79 ± 0.22
PCB-8	8.52 ± 0.12	7.69 ± 0.09	6.79 ± 0.03	6.98 ± 0.25	8.77 ± 0.07
PCB-15	8.77 ± 0.01	8.53 ± 0.04	8.44 ± 0.36	8.25 ± 0.53	9.06 ± 0.01
PCB-52	8.76 ± 0.25	7.90 ± 0.15	7.42 ± 0.11	7.64 ± 0.07	9.27 ± 0.01
PCB-72	9.22 ± 0.26	8.48 ± 0.13	8.15 ± 0.005	8.20 ± 0.02	9.86 ± 0.001
PCB-77	9.56 ± 0.33	9.19 ± 0.02	9.94 ± 0.12	9.77 ± 0.11	10.06 ± 0.00
PCB-138	9.31 ± 0.54	9.01 ± 0.07	9.16 ± 0.11	9.22 ± 0.11	10.53 ± 0.01
PCB-156	10.33 ± 0.20	9.58 ± 0.04	10.03 ± 0.24	9.97 ± 0.13	11.07 ± 0.01
PCB-169	10.76 ± 0.21	10.01 ± 0.01	11.28 ± 0.07	10.99 ± 0.24	11.34 ± 0.01

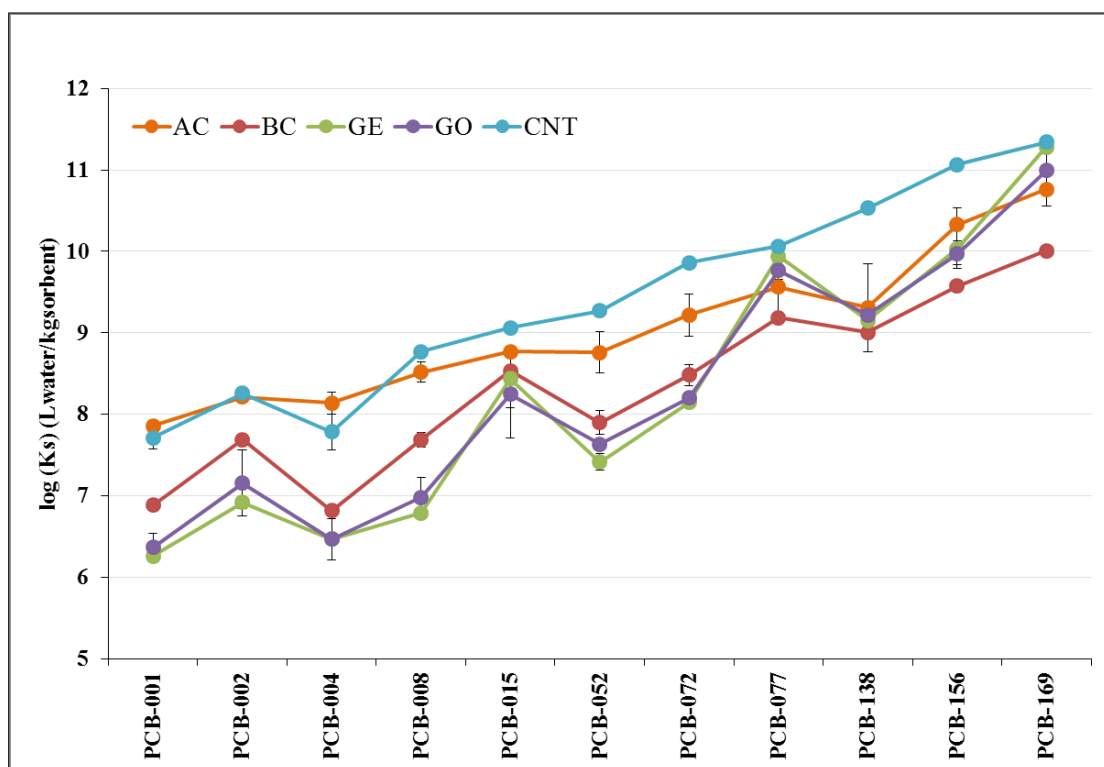


Figure 4-10. Line graph of log (K_s) values for each of the 11 PCB congeners and five sorbent materials. Each point represents the average measured log (K_s) value for that congener-sorbent combination

decreased with decreasing chlorination. The AC sorbent exhibited the second highest K_s values. Amongst BC, GE, and GO, BC exhibited higher K_s values for smaller PCBs and GE and GO exhibited higher K_s values with increasing congener chlorination.

Numerically, the average of differences in $\log(K_s)$ values among the sorbents for each of the 11 congeners shows that $\log(K_s)$ for CNT is 1.16, 1.15, 1.13, and 1.04 log units greater than GE, GO, BC, and AC, respectively. Table 4-4 provides the rankings based on $\log(K_s)$ values for the five sorbents illustrating that CNT had the strongest sorption for nine (9) out of the 11 PCB congeners. The sorbents AC and BC among the lower chlorinated congeners followed the sorbent CNT, whereas in the higher chlorinated congeners, GE and GO performed better than BC.

Table 4-4. Rankings of the five sorbent materials based on their K_s values

PCB Congener	Sorbent K_s Rank							
	1		2		3		4	5
PCB-1	AC	>	CNT	>	BC	>	GO	> GE
PCB-2	CNT	>	AC	>	BC	>	GO	> GE
PCB-4	AC	>	CNT	>	BC	>	GE	= GO
PCB-8	CNT	>	AC	>	BC	>	GO	> GE
PCB-15	CNT	>	AC	>	BC	>	GE	> GO
PCB-52	CNT	>	AC	>	BC	>	GO	> GE
PCB-72	CNT	>	AC	>	BC	>	GO	> GE
PCB-77	CNT	>	GE	>	GO	>	AC	> BC
PCB-138	CNT	>	AC	>	GO	>	GE	> BC
PCB-156	CNT	>	AC	>	GE	>	GO	> BC
PCB-169	CNT	>	GE	>	GO	>	AC	> BC

As shown earlier in Table 2-3, the $\log(K_{ow})$ values of the 11 PCB congeners increase linearly with chlorination. However, when comparing $\log(K_{ow})$ and the calculated $\log(K_s)$ values in this study, a linear relationship was not found indicating a possible effect due to planarity of the studied congeners. Planar congeners have maximum contact with planar sorbents, and this affects the sorption of PCBs by the sorbents. Similar to results

from Beless [53], the $\log(K_s)$ values for PCBs 4, 52, and 138 were smaller than the less hydrophobic congeners present immediately before them, likely due to the positioning of two chlorine atoms in the ortho positions for the three congeners (see Figure 4-11 for example where $\log(K_s)$ values are smaller for PCB-4 when compared to PCB-2 for the five sorbents). Hence, this suggests that the sorbents need to be selected based on the planarity of the PCB congeners that need to be sorbed, and not purely by K_s alone. Due to this, AC need not always be the best choice, and in addition AC could be mixed with nanomaterials, which could enhance the effect of remediation. While AC was less sensitive to planarity except for the higher chlorinated PCBs (PCB-138 in this case), CNT was less sensitive to planarity except for the lower chlorinated PCBs (PCB 4 in this case). The remaining nanomaterials were highly sensitive to planarity for all chlorination levels. This might be expected when looking at the SEM images shown in Figure 4-9 showing the surface structure for the five sorbents.

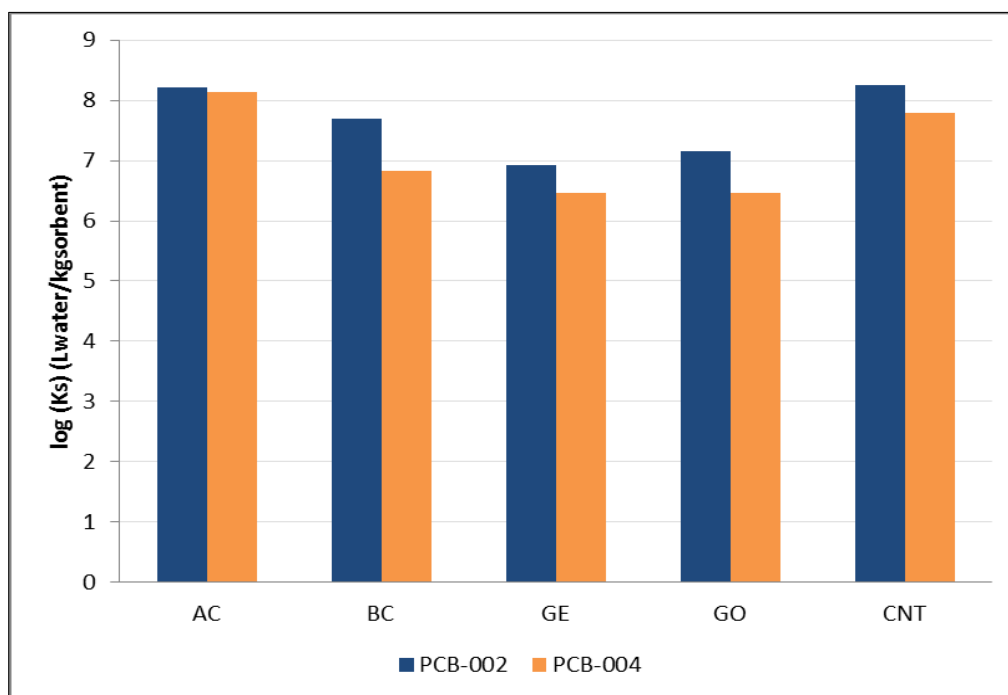


Figure 4-11. Comparison of $\log(K_s)$ values of PCB-4 and PCB-2

4.2.5 Discussion

The mechanism of sorption focuses on sequestering PCBs from the sediment, thereby reducing their partitioning into the water column and in turn their bioavailability to biota. Here, the effectiveness of five carbon-based materials to sorb PCBs from sediment was examined by conducting experiments with a mixture of 11 PCB congeners (mono-hexachlorinated). CNT performed the best overall followed by AC, BC, GO, and GE. With respect to individual congeners, CNTs exhibited the strongest sorption towards nine of the 11 congeners. Overall, it was interesting to observe, however, that CNTs outperformed AC for all chlorination levels except (PCB 4) and that the difference in sorption capacity between the two (CNT and AC) increased with chlorination level and was independent of planarity of the studied congeners. In addition, it was also striking to observe that the other nanomaterials were susceptible to planarity and had lower K_s values for PCBs 4, 52, and 138.

4.3 Modeling results

4.3.1 Calibration run

Figure 4-12 shows the spatial distribution of the total water concentration ($C_{\text{diss}} + C_{\text{susp}}$) for PCB-1 in the water column at the end of one month of the run. As it was not possible to extract values smaller than $0.001\mu\text{g/L}$ from the EFDC model, the data are shown as $<0.001\mu\text{g/L}$. It can be seen from the Figure that higher concentrations are observed in the main channel and Burnett Bay.

Figure 4-13 shows the spatial distribution of the total water concentration of the remaining four PCB congeners: PCB-3, PCB-11, PCB-17, and PCB-25 in the water column, one month after the start of the model, i.e. on 03/27/2003 (i.e., $115 + 30 = 145^{\text{th}}$

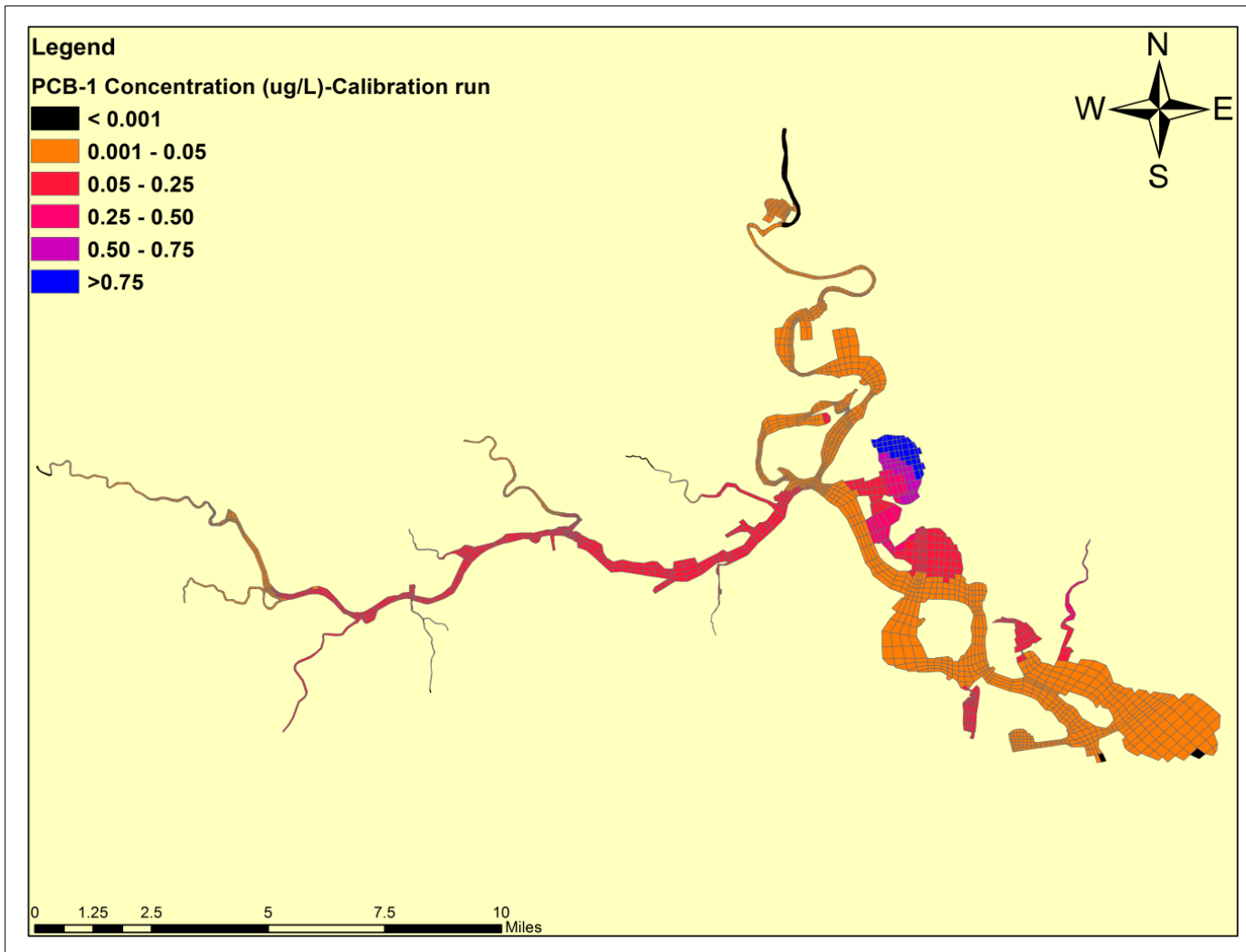


Figure 4-12. Spatial distribution of PCB-1 in the water column after 30 days of simulation time

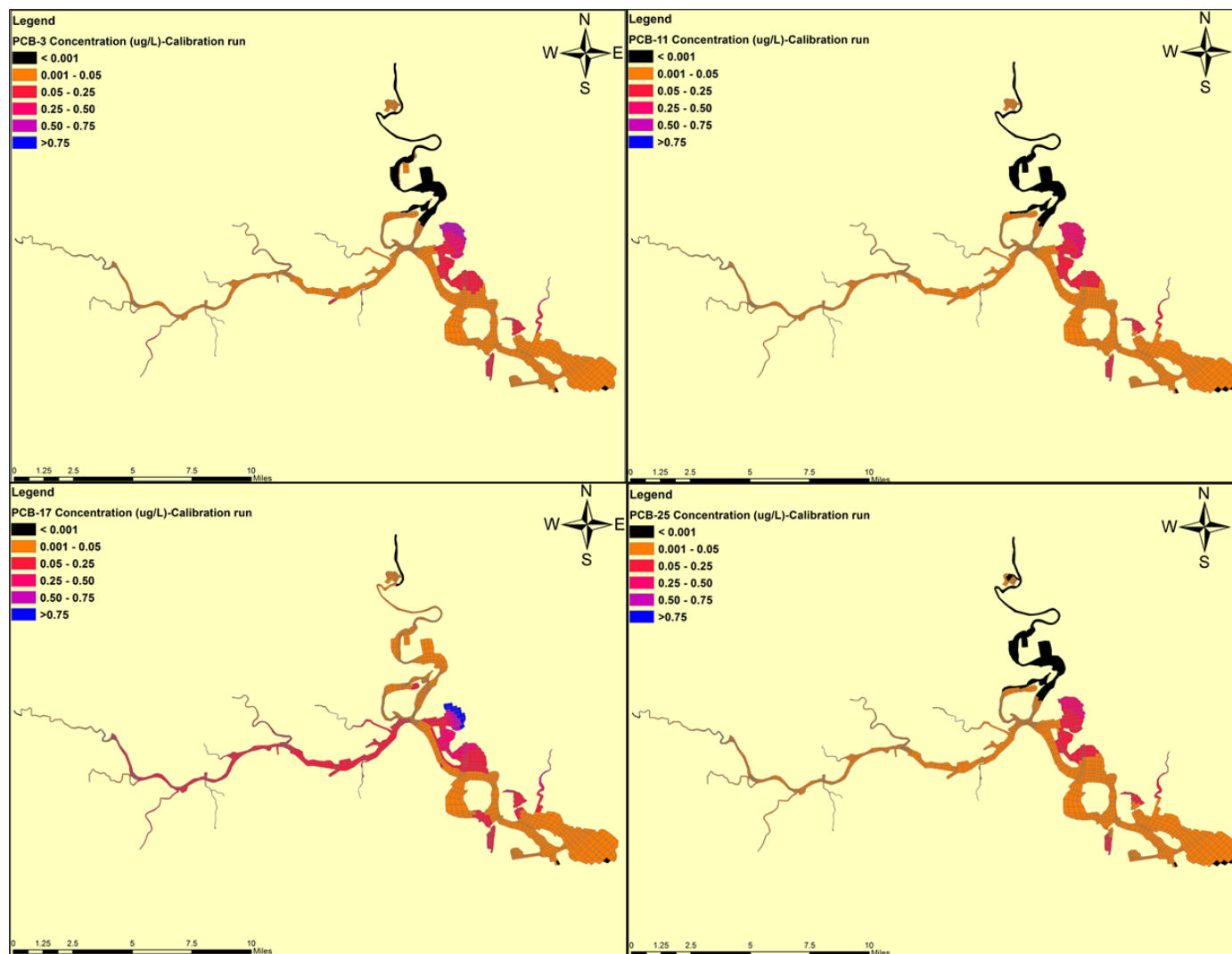


Figure 4-13. Spatial distribution of PCB-3, PCB-11, PCB-17, and PCB-25 in the water column after 30 days

day in the model) as well. It is apparent from both the figures that Burnett Bay exhibits higher contamination of PCBs. The reason for this could be due to the longer residence time of PCBs in Burnett Bay because of the low flow in the area. Three monitoring stations in Burnett Bay: 13343, 13344, and 16496 were sampled in 2002-2003 for PCBs, and they exhibited relatively high levels of PCB-1 in the water column.

Also, it was observed that the concentration distribution for PCB-17 was different compared to the other four congeners, and this is because the initial concentration for PCB-17 was twice as high as PCB-1. The remainder of the figures will focus on PCB-1 since there was not a significant difference between the simulated concentrations of the five congeners.

The time series for PCB-1 at the five locations that were chosen for graphical illustrations is shown in Figure 4-14.

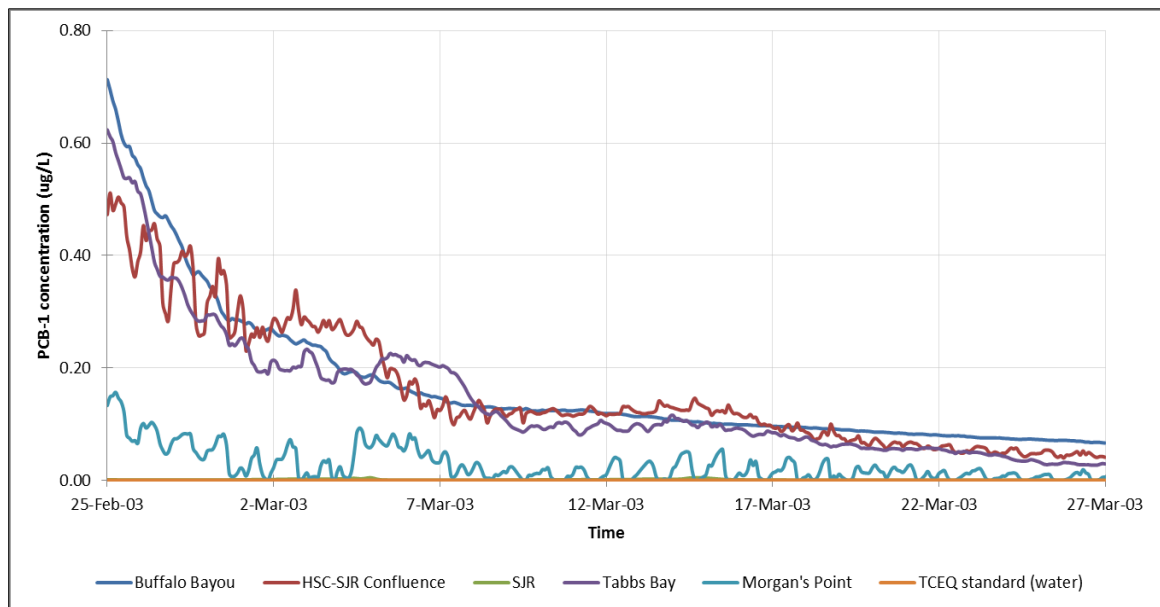


Figure 4-14. Temporal distribution of PCB-1 in the water column at five different locations in the HSC-GBS

For reference, the TCEQ water quality standard for PCBs (0.64ng/L) was also plotted

to illustrate that PCB concentrations are of concern system-wide. The concentration of PCB-1 at monitoring stations sampled in 2002-2003 at the abovementioned five locations were 3.36ng/L, 4.8ng/L, 22.2ng/L, 2.17ng/L, and 2.95ng/L, which were all higher than the TCEQ water quality standard as well.

4.3.2 Model calibration/validation

Table 4-5 shows the total water concentration for PCBs obtained from the model along with the concentration obtained for the corresponding congeners from field sampling. It can be seen that the simulated concentrations were of the same order of magnitude as their measured counterparts indicating that the model was representative of the conditions in the Channel.

Table 4-5. Total water concentrations obtained from the EFDC model compared to the sampling data

Station ID	Value Type	PCB-1 (µg/L)	PCB-3 (µg/L)	PCB-11 (µg/L)	PCB-17 (µg/L)	PCB-25 (µg/L)
11264	Sampling	0.0021	0.0151	0.0045	0.0074	0.0065
	EFDC	0.0042	0.0027	0.0020	0.0055	0.0015
11280	Sampling	0.0018	0.0014	0.0048	0.0030	0.0007
	EFDC	0.0036	0.0023	0.0017	0.0048	0.0013
11287	Sampling	0.0034	0.0029	0.0084	0.0095	0.0024
	EFDC	0.0022	0.0014	0.0010	0.0029	0.0008
11270	Sampling	0.0046	0.0040	0.0084	0.0078	0.0024
	EFDC	0.0024	0.0015	0.0011	0.0032	0.0009

4.3.3 Sensitivity analyses

OC. Figure 4-15 illustrates the percent change that resulted in the HSC-GBS from varying OC in EFDC. Overall, the behavior obtained from the model coincided with the theoretical expectation that higher concentrations would be observed in the water column when the OC in the sediment bed is lowered. While decreasing the OC had a significant

effect, increasing it did not produce a similar level of change. From the results it was observed that the model responded very effectively to a decrease in OC, but it was not that effective for an increase in OC. For example, at Buffalo Bayou, it was observed from the Figure that when OC was decreased by 20% ($OC=1\text{g/m}^3$), and by 40% ($OC=2\text{g/m}^3$) from the base value ($OC=5\text{g/m}^3$), the average percent change in the PCB concentrations in the water column were 138%, and 52%, respectively, but when it was increased by 200% ($OC=10\text{g/m}^3$), and by 400% ($OC=20\text{g/m}^3$), the average percent change was only -17%, and -26%, respectively.

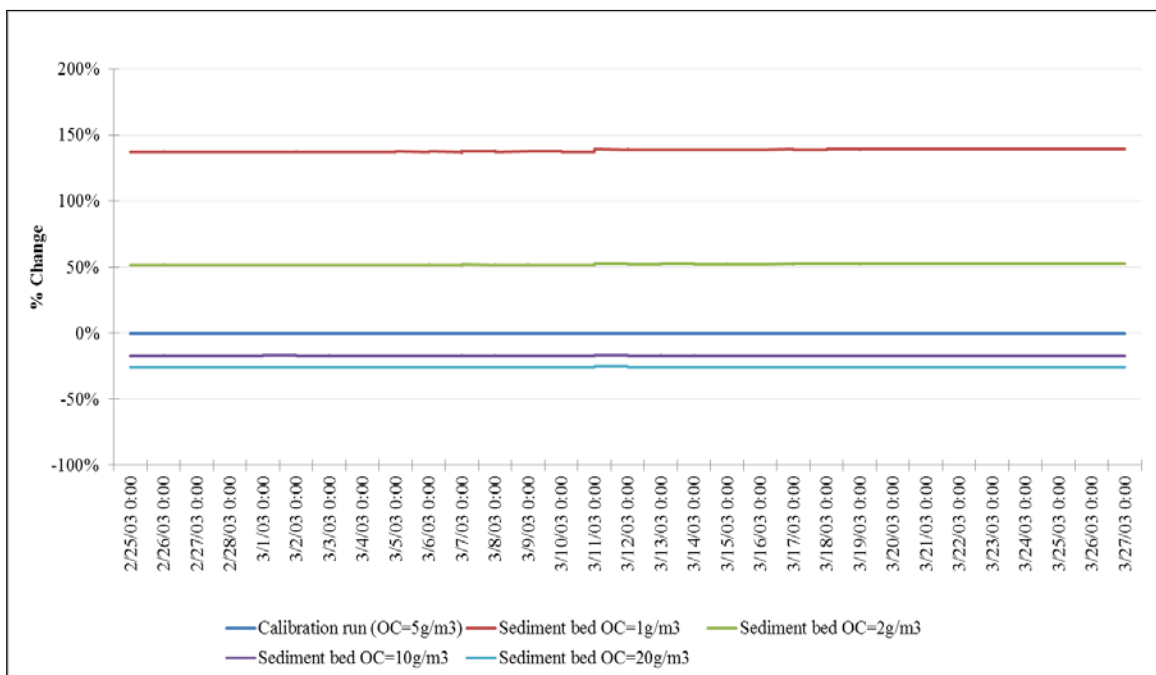


Figure 4-15. Results of sensitivity analysis for OC for PCB-1 at Buffalo Bayou

K_{poc} and K_{doc} . Similar to what was observed in the sensitivity analysis runs with OC, and as shown in Figure 4-16, the modeled results corresponded well with the theoretical understanding of higher PCB concentrations in the water column when the partitioning coefficients in the sediment bed are reduced. For example, at the HSC-SJR confluence, it was observed that when the K_{poc} and K_{doc} were decreased by 90% and by 50% from the

base values (see Table 3-1), the average percent change in the PCB concentrations in the water column were 317%, and 35%, respectively. On the other hand, when the K_{poc} and K_{doc} were increased by 90% and by 50%, the average percent change was only -16%, and -11%, respectively. It should be noted here that the K_{poc} and K_{doc} values entered in the model for the 90% increase and 50% increase sensitivity runs were higher than the values PCB-1 would exhibit in reality, but the analysis was performed so that an understanding could be garnered about how the addition of carbon-based materials (which have extremely high K_{poc} and K_{doc}) would affect the partitioning of PCBs from sediment bed to water column.

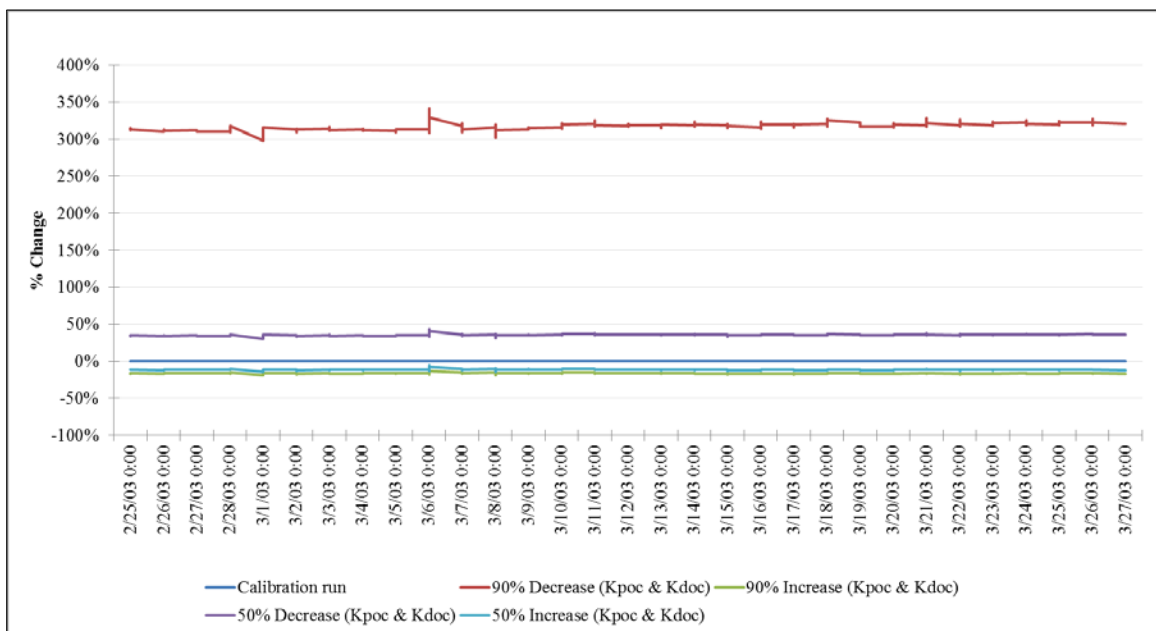


Figure 4-16. Results of sensitivity analysis of K_{poc} and K_{doc} for PCB-1 at the HSC-SJR confluence

Temporal mass loading of PCBs into Galveston Bay. Another important result obtained from the model was the concentration of PCBs (as represented by the sum of the five modeled congeners) that would be discharged into Galveston Bay. The percent change between runs 1 – 8 (see Table 3-3) compared to the calibration run is plotted in

Figure 4-17.

When K_{poc} and K_{doc} were decreased by 90%, the average percent change in the loading to Galveston Bay was the highest (187%) over the 30-day modeled period, and the lowest (-7%) was observed when K_{poc} and K_{doc} were increased by 50%. These results coincided with the behavior that would be expected thereby allowing for a quantification of the mass that would be sequestered via sediment remediation.

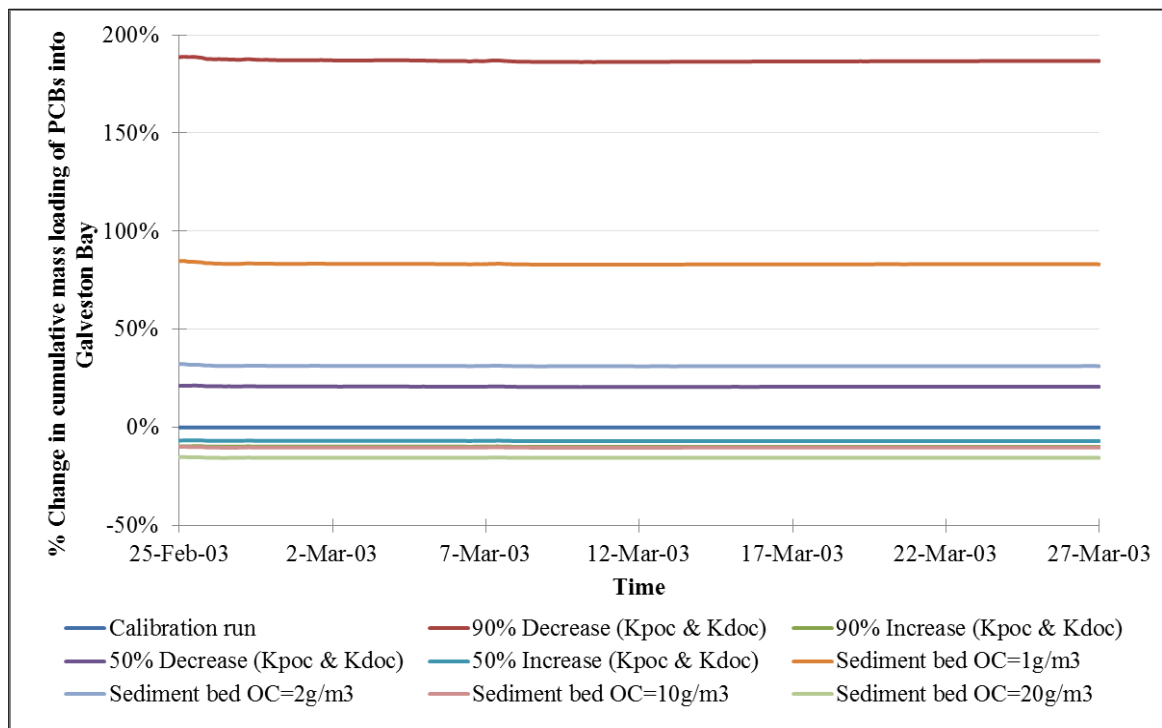


Figure 4-17. Percent change in the cumulative mass loading of PCBs into Galveston Bay

It was observed for the sensitivity analyses runs that a decrease in the concentration of PCBs in the sediment caused an increase in the loading into Galveston Bay. This observation from the model results indicated that sediments in the HSC-GBS are a major source of PCBs.

Effect of PCB loading from tributaries. Figure 4-18 shows the distribution of PCB-1 concentration in the water column between the calibration run and the run without

loading from tributaries (run 9 in Table 3-3) at two of the aforementioned five locations. It can be observed from the Figure that the tributaries have a minor effect on the loading of PCBs in the main Channel. This behavior can be attributed to the fact that the tributaries have relatively smaller overall flows relative to the flow in the HSC.

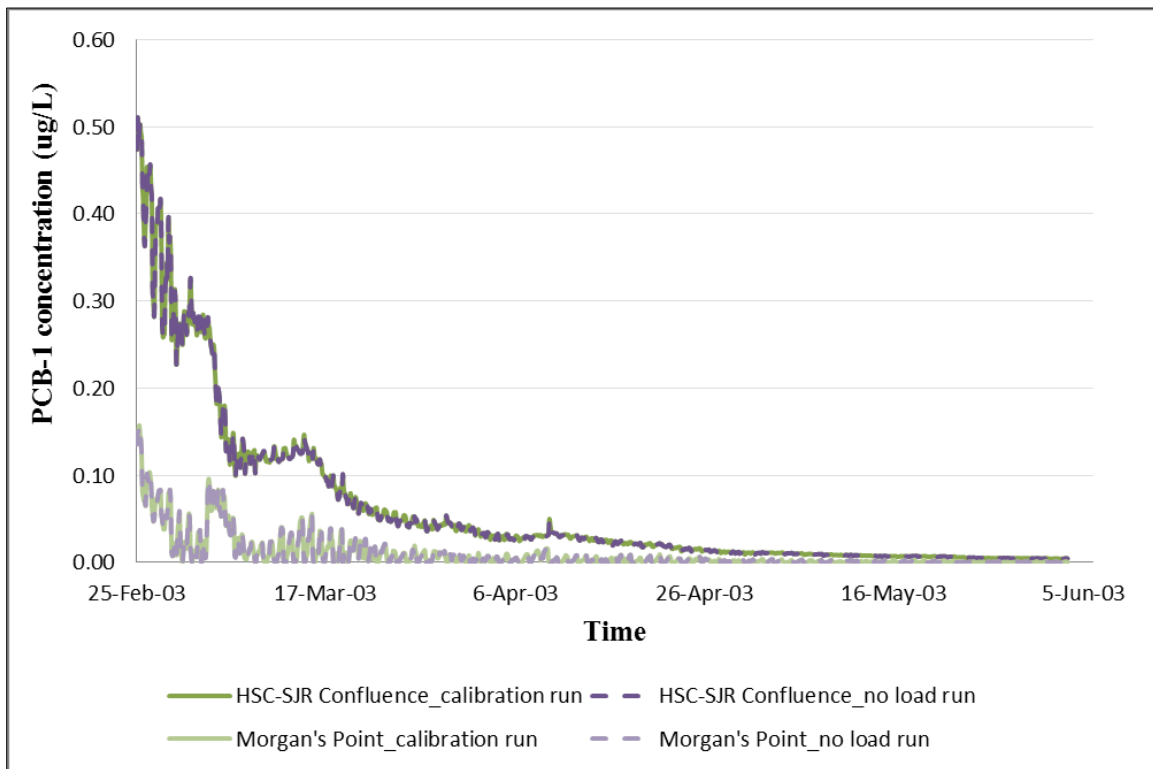


Figure 4-18. Temporal distribution of PCB-1 in the HSC-GBS between run 9 and calibration run

Additionally, the % difference in PCB-1 concentration at the end of 90 days of model simulation (02/25/2003-05/26/2003) between run 9 and calibration run was calculated spatially (see Figure 4-19). Overall, the loadings from the tributaries did not have a major effect as seen before, but the loadings had minor effects in the side bays (Burnett Bay, and some parts of Scott Bay).

4.3.4 Sediment remediation using carbon-based materials

The spatial distribution between the calibration run and carbon run after one month of

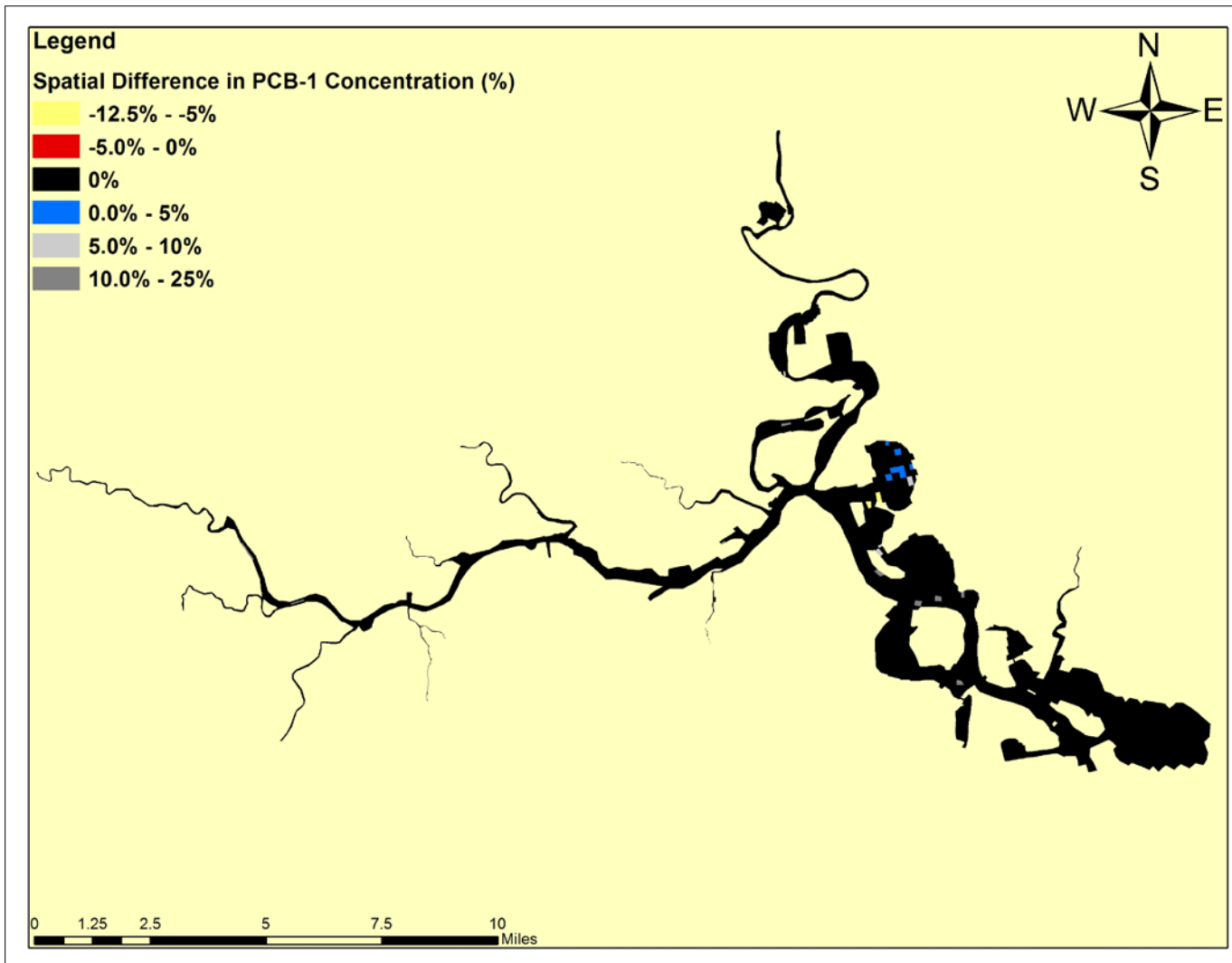


Figure 4-19. Spatial difference in PCB-1 concentration in the water column between run 9 and the calibration run

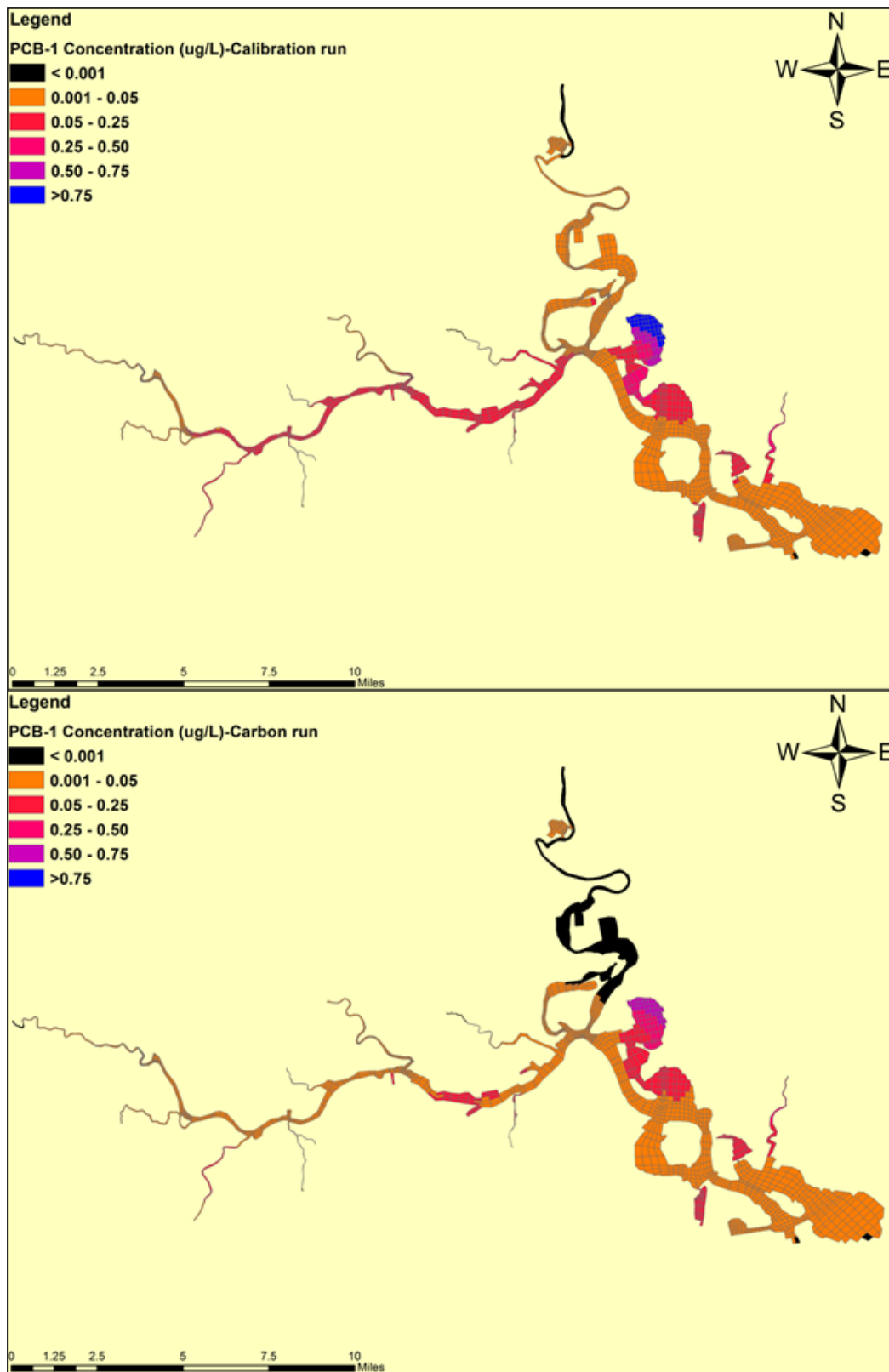


Figure 4-20. Spatial distribution of PCB-1 concentration in the water column between the calibration run and the carbon run

model simulation time (on 03/27/2003) are presented in Figure 4-20. From the Figure it can be observed that addition of the carbon-based materials lowered the PCB-1 concentration in the water column system-wide, and a reduction of approximately 30% - 35% was observed in most parts of the Channel.

Additionally, the time series from an area exhibiting higher contamination as mentioned before (Burnett Bay) was extracted, and the results were compared with the calibration run (see Figure 4-21). There was a significant change in the concentrations observed between the carbon runs and the calibration run (average difference of 35%). This showed that the carbon-based materials were aiding in the significant reduction of PCB concentrations in the water column.

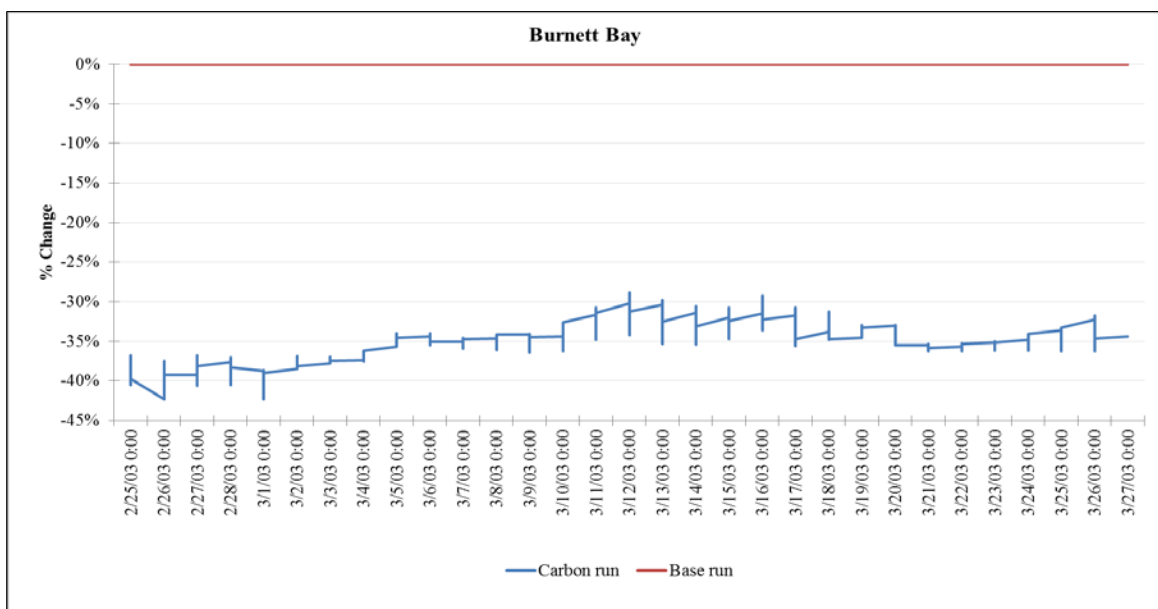


Figure 4-21. Time series comparison at area of higher contamination (Burnett Bay) for PCB-1

4.3.5 Discussion

The model was calibrated to the total concentration of PCBs (for each of the five congeners) observed in the water column in the HSC-GBS. The model was highly

sensitive to the decrease of K_{poc} and K_{doc} in sediment bed, and to the decrease of OC in sediment bed; and moderately sensitive to an increase in the aforementioned parameters. A very important conclusion obtained from the EFDC model runs was that sediment in the HSC-GBS acted as the major source of PCBs into the water column. The hydrodynamics of the HSC is mainly attributed to the flows from the tributaries and the tidal flows. Under normal conditions (no severe storm events or hurricanes), the amount of water that comes into the HSC from the tributaries and tidal flows is relatively insignificant. Hence, the HSC tends to behave like a stagnant reactor in which the diffusion from the sediment controls the concentration of PCBs in the system. Additionally, the model results indicated areas of higher contamination (Burnett Bay) in the HSC-GBS, and that the concentration of PCBs in the water column was highly sensitive to the various partitioning coefficients in the sediment bed over PCB loadings.

Chapter 5. Summary and Conclusions

The removal of PCBs from natural water systems poses an enormous challenge because these compounds accumulate in the sediment, continuously pollute the overlying water and are taken up by biota. While the suspended fraction of a congener was a function of $\log K_{ow}$, as was determined in the analysis of the effluent sampling data in this dissertation, it was observed that $\log K_{ow}$ alone was not the deciding factor for the suspended fraction and that other parameters such as TSS, TOC, DOC, and POC played an important role in the partitioning of PCBs.

From the sorption experiments, it was observed that CNT performed the best overall followed by AC, BC, GO, and GE. Average $\log (K_s)$ values obtained indicated that CNT was 1.16, 1.15, 1.13, and 1.04 log units greater than GE, GO, BC, and AC, respectively. As expected, a linear relationship was not observed between $\log (K_{ow})$ and $\log (K_s)$, which could be attributed to the planarity of the PCB congener. This observation suggested that a certain carbon-based material might not always be the best choice, and the choice of a sorbent may depend on the PCB being targeted for sequestration.

Although it might be expected for CNTs to perform better due to their greater surface area, it is also acknowledged that this needs to be explored in more detail because of the potential toxicity of CNTs to biota in sediment and their observed capacities under a variety of environmental conditions and different types of sediment. Also, the role of carbon content in soil and other naturally occurring carbons in water and sediments as well as the various types in natural water systems on the behavior of the five sorbents needs to be further elucidated.

Model simulations using EFDC illustrated the variables that affect water column

concentrations. The most influential variables were the organic carbon partitioning coefficients in the sediment bed, and carbon content in the sediment bed. The least influential variables were the PCB concentrations entering the Channel via discharges from the tributaries and the long-term effects need to be further demonstrated. This behavior (model being more sensitive to partitioning coefficients in the sediment bed over loadings) also led to the conclusion that sediments were the major source of PCBs in the HSC-GBS.

Results from the EFDC model illustrated the presence of areas of higher contamination in the HSC-GBS (Burnett Bay, parts of Scott Bay) that experienced an average decrease of 35% in PCB concentrations in the water column when carbon-based materials were added to the sediments, thereby controlling the bioavailability of the PCBs.

References

- [1] Rauner, B. "Polychlorinated Biphenyls (PCBs)." 2009; Available from: <http://www.idph.state.il.us/envhealth/factsheets/polychlorinatedbiphenyls.htm>.
- [2] USEPA. "Polychlorinated Biphenyls (PCBs)." 2013b 10/10/2015]; Available from: <http://www3.epa.gov/epawaste/hazard/tsd/pcbs/about.htm>.
- [3] Bremle, G. and P. Larsson, "PCB concentration in fish in a river system after remediation of contaminated sediment," *Environmental Science and Technology*, 1998. 32(22): p. 3491-3495.
- [4] Brown, M.P., M.B. Werner, R.J. Sloan, and K.W. Simpson, "Polychlorinated biphenyls in the Hudson River," *Environmental Science and Technology*, 1985. 19(8): p. 656-661.
- [5] Carrer, S. and R. Leardi, "Characterizing the pollution produced by an industrial area. Chemometric methods applied to the Lagoon of Venice," *Science of the Total Environment*, 2006. 370(1): p. 99-116.
- [6] Domingo, J.L. and A. Bocio, "Levels of PCDD/PCDFs and PCBs in edible marine species and human intake: A literature review," *Environment International*, 2007. 33(3): p. 397-405.
- [7] Engwall, M., C. Näf, D. Broman, and B. Brunström, "Biological and chemical determination of contaminant levels in settling particulate matter and sediments: A Swedish river system before, during, and after dredging of PCB-contaminated lake sediments," *Ambio*, 1998. 27(5): p. 403-410.
- [8] Franz, T.P., S.J. Eisenreich, and T.M. Holsen, "Dry deposition of particulate polychlorinated biphenyls and polycyclic aromatic hydrocarbons to Lake

- Michigan," *Environmental Science and Technology*, 1998. 32(23): p. 3681-3688.
- [9] Green, M.L., J.V. Depinto, C. Sweet, and K.C. Hornbuckle, "Regional spatial and temporal interpolation of atmospheric PCBs: Interpretation of Lake Michigan Mass Balance data," *Environmental Science and Technology*, 2000. 34(9): p. 1833-1841.
- [10] Guerzoni, S., P. Rossini, A. Sarretta, S. Raccanelli, G. Ferrari, and E. Molinaroli, "POPs in the Lagoon of Venice: budgets and pathways," *Chemosphere*, 2007. 67(9): p. 1776-1785.
- [11] Hileman, B., "The Great Lakes Cleanup Effort," *Chemical & Engineering News Archive*, 1988. 66(6): p. 22-39.
- [12] HRNRT. "PCB Contamination of the Hudson River Ecosystem: Compilation of Contamination Data through 2008." 2013; Available from: <https://www.fws.gov/northeast/ecologicalservices/HudsonRiver/docs/Hudson%20River%20Status%20Report%20Update%20January%202013.pdf>.
- [13] Manodori, L., A. Gambaro, I. Moret, G. Capodaglio, and P. Cescon, "Air-sea gaseous exchange of PCB at the Venice lagoon (Italy)," *Marine Pollution Bulletin*, 2007. 54(10): p. 1634-1644.
- [14] Peré-Trepat, E., L. Olivella, A. Ginebreda, J. Caixach, and R. Tauler, "Chemometrics modelling of organic contaminants in fish and sediment river samples," *Science of the Total Environment*, 2006. 371(1-3): p. 223-237.
- [15] Pojana, G., A. Critto, C. Micheletti, C. Carlon, F. Buseti, and A. Marcomini, "Analytical and environmental chemistry in the framework of risk assessment and management: The lagoon of Venice as a case study," *Chimia*, 2003. 57(9): p. 542-

549.

- [16] Risebrough, R.W., P. Rieche, D.B. Peakall, S.G. Herman, and M.N. Kirven, "Polychlorinated biphenyls in the global ecosystem," *Nature*, 1968. 220(5172): p. 1098-1102.
- [17] Srogi, K., "Levels and congener distributions of PCDDs, PCDFs and dioxin-like PCBs in environmental and human samples: A review," *Environmental Chemistry Letters*, 2008. 6(1): p. 1-28.
- [18] Urbaniak, M., "Polychlorinated biphenyls: Sources, distribution and transformation in the environment - A literature review," *Acta Toxicologica*, 2007. 15(2): p. 83-93.
- [19] Wolska, L., A. Mechlińska, J. Rogowska, and J. Namieśnik, "Polychlorinated biphenyls (PCBs) in bottom sediments: Identification of sources," *Chemosphere*, 2014. 111: p. 151-156.
- [20] USEPA. "CERCLIS Public Access Database." 2015 10/12/2015]; Available from:
<http://cumulis.epa.gov/supercpad/Cursites/srchrslt.cfm?start=1&CFID=15927925&CFTOKEN=41543247>.
- [21] TCEQ. "2014 Texas Integrated Report - Texas 303(d) List (Category 5)." 2014a 11/07/2015]; Available from:
https://www.tceq.texas.gov/assets/public/waterquality/swqm/assess/14txir/2014_303d.pdf.
- [22] Balasubramani, A., N.L. Howell, and H.S. Rifai, "Polychlorinated biphenyls (PCBs) in industrial and municipal effluents: Concentrations, congener profiles,

- and partitioning onto particulates and organic carbon," *Science of the Total Environment*, 2014. 473-474: p. 702-713.
- [23] Howell, N.L., D. Lakshmanan, H.S. Rifai, and L. Koenig, "PCB dry and wet weather concentration and load comparisons in Houston-area urban channels," *Science of The Total Environment*, 2011b. 409(10): p. 1867-1888.
- [24] Howell, N.L., H.S. Rifai, and L. Koenig, "Comparative distribution, sourcing, and chemical behavior of PCDD/Fs and PCBs in an estuary environment," *Chemosphere*, 2011a. 83(6): p. 873-881.
- [25] Howell, N.L., M.P. Suarez, H.S. Rifai, and L. Koenig, "Concentrations of polychlorinated biphenyls (PCBs) in water, sediment, and aquatic biota in the Houston Ship Channel, Texas," *Chemosphere*, 2008. 70(4): p. 593-606.
- [26] Lakshmanan, D., N.L. Howell, H.S. Rifai, and L. Koenig, "Spatial and temporal variation of polychlorinated biphenyls in the Houston Ship Channel," *Chemosphere*, 2010. 80(2): p. 100-112.
- [27] HRTC. "Hudson River Natural Resource Damage Assessment Plan." 2002; Available from:
<http://www.fws.gov/northeast/EcologicalServices/HudsonRiver/docs/HudsonRiverNRDASep2002.pdf>.
- [28] Kelly, S.M., K.M. Eisenreich, J.E. Baker, and C.L. Rowe, "Accumulation and maternal transfer of polychlorinated biphenyls in snapping turtles of the Upper Hudson River, New York, USA," *Environmental Toxicology and Chemistry*, 2008. 27(12): p. 2565-2574.
- [29] USEPA. "Just the Facts: Cleaning Up Hudson River PCBs." 2010b; Available

- from: http://www3.epa.gov/ HUDSON/just_facts_08_04.pdf.
- [30] Mahan, L.M. "Are PCBs Still a Problem in the Great Lakes?" *Geology* 201: The Dynamic Earth 2012 10/10/2015]; Available from: <http://archive.is/29w5>.
- [31] Ogura, I., "Half-life of each dioxin and PCB congener in the human body," in *Organohalogen Compounds*. 2004.
- [32] TCEQ, "Chapter 307 - Texas Surface Water Quality Standards," 2014b, *Texas Commission on Environmental Quality (TCEQ)*. p. 217.
- [33] USEPA. "Aroclor and Other PCB Mixtures." 2013a 02/17/2016]; Available from: <http://www3.epa.gov/epawaste/hazard/tsd/pcbs/pubs/aroclor.htm>.
- [34] ATSDR. "Toxicological profile for polychlorinated biphenyls (PCBs)." 2000 02/17/2016]; Available from: <http://www.atsdr.cdc.gov/toxprofiles/tp17.pdf>.
- [35] Safe, S., "Toxicology, Structure-Function Relationship, and Human and Environmental Health Impacts of Polychlorinated Biphenyls: Progress and Problems," *Environmental Health Perspectives*, 1993. 100: p. 259-268.
- [36] De Bruijn, J. and J. Hermens, "Relationships between octanol/water partition coefficients and total molecular surface area and total molecular volume of hydrophobic organic chemicals," *Quantitative Structure-Activity Relationships*, 1990. 9(1): p. 11-21.
- [37] Van Noort, P.C.M., M.T.O. Jonker, and A.A. Koelmans, "Modeling maximum adsorption capacities of soot and soot-like materials for PAHs and PCBs," *Environmental Science and Technology*, 2004. 38(12): p. 3305-3309.
- [38] van den Berg, M., L.S. Birnbaum, M. Denison, M. De Vito, W. Farland, M. Feeley, H. Fiedler, H. Hakansson, A. Hanberg, L. Haws, M. Rose, S. Safe, D.

- Schrenk, C. Tohyama, A. Tritscher, J. Tuomisto, M. Tysklind, N. Walker, and R.E. Peterson, "The 2005 World Health Organization Re-evaluation of Human and Mammalian Toxic Equivalency Factors for Dioxins and Dioxin-like Compounds," *Toxicological sciences : an official journal of the Society of Toxicology*, 2006. 93(2): p. 223-241.
- [39] Lauby-Secretan, B., D. Loomis, Y. Grosse, F.E. Ghissassi, V. Bouvard, L. Benbrahim-Tallaa, N. Guha, R. Baan, H. Mattock, and K. Straif, "Carcinogenicity of polychlorinated biphenyls and polybrominated biphenyls," *The Lancet Oncology*, 2013. 14(4): p. 287-288.
- [40] USEPA. "Health Effects of PCBs." 2013c 11/07/2015]; Available from: <http://www3.epa.gov/epawaste/hazard/tsd/pcbs/pubs/effects.htm>.
- [41] TCEQ, "Future Revisions to Fish Tissue-Based Criteria in the 2013 Texas Water Quality Standards (TSWQS)," 2012, *Texas Commission on Environmental Quality (TCEQ)*. p. 2.
- [42] Breivik, K., A. Sweetman, J.M. Pacyna, and K.C. Jones, "Towards a global historical emission inventory for selected PCB congeners - A mass balance approach. 3. An update," *Science of the Total Environment*, 2007. 377(2-3): p. 296-307.
- [43] Rossberg, M., W. Lendle, G. Pfeleiderer, A. Tögel, T.R. Torkelson, and K.K. Beutel, "Chloromethanes," in Ullmann's Encyclopedia of Industrial Chemistry. 2000, Wiley-VCH Verlag GmbH & Co. KGaA.
- [44] Ashworth, W., "The Late, Great Lakes." 1987: *Wayne State University Press*.
- [45] Harbor, N.B. "New Bedford Harbor Superfund Site, Bristol County,

- Massachusetts." 2015 10/10/2015]; Available from: <http://www2.epa.gov/new-bedford-harbor/harbor-cleanup#Why>.
- [46] USEPA. "Hudson River PCBs." 2010a 10/10/2015]; Available from: <http://www3.epa.gov/hudson/background.htm>.
- [47] Brenner, R.C., V.S. Magar, J.A. Ickes, E.A. Foote, J.E. Abbott, L.S. Bingler, and E.A. Creclius, "Long-Term Recovery of PCB-Contaminated Surface Sediments at the Sangamo-Weston/Twelvemile Creek/Lake Hartwell Superfund Site," *Environmental Science and Technology*, 2004. 38(8): p. 2328-2337.
- [48] Borja, J., D.M. Taleon, J. Auresenia, and S. Gallardo, "Polychlorinated biphenyls and their biodegradation," *Process Biochemistry*, 2005. 40(6): p. 1999-2013.
- [49] Hawker, D.W. and D.W. Connell, "Octanol water partition-coefficients of polychlorinated biphenyl congeners," *Environmental Science & Technology*, 1988. 22(4): p. 382-387.
- [50] Mackay, D., W.Y. Shiu, and K.C. Ma, "Illustrated Handbook of Physical-Chemical Properties and Environmental Fate for Organic Chemicals." 1992, Chelsea: *Lewis Publishers, Inc.*
- [51] Brodsky, J. and K. Ballschmiter, "Reversed phase liquid chromatography of PCBs as a basis for the calculation of water solubility and log Kow for polychlorobiphenyls," *Fresenius' Zeitschrift für analytische Chemie*, 1988. 331(3): p. 295-301.
- [52] Sinkkonen, S. and J. Paasivirta, "Degradation half-life times of PCDDs, PCDFs and PCBs for environmental fate modeling," *Chemosphere*, 2000. 40(9–11): p. 943-949.

- [53] Beless, B.D., "Natural and anthropogenic carbonaceous materials for the remediation of polychlorinated biphenyls from aqueous solution," in Civil and Environmental Engineering 2013, *University of Houston*. p. 113.
- [54] Moermond, C.T.A., J.J.G. Zwolsman, and A.A. Koelmans, "Black carbon and ecological factors affect in situ biota to sediment accumulation factors for hydrophobic organic compounds in flood plain lakes," *Environmental Science and Technology*, 2005. 39(9): p. 3101-3109.
- [55] Mayer, P., W.H.J. Vaes, F. Wijnker, K.C.H.M. Legierse, R. Kraaij, J. Tolls, and J.L.M. Hermens, "Sensing dissolved sediment porewater concentrations of persistent and bioaccumulative pollutants using disposable solid-phase microextraction fibers," *Environmental Science and Technology*, 2000. 34(24): p. 5177-5183.
- [56] De Boer, J., F. Van Der Valk, M.A.T. Kerkhoff, P. Hagel, and U.A.T. Brinkman, "8-year study on the elimination of PCBs and other organochlorine compounds from eel (*Anguilla anguilla*) under natural conditions," *Environmental Science & Technology*, 1994. 28(13): p. 2242-2248.
- [57] Army Corps of Engineers, U.S., "Evaluating Environmental Effects of Dredged Material Management Alternatives-A Technical Framework," D.o.t. Army, 2004, *USEPA*. p. 95.
- [58] Bergen, B.J., W.G. Nelson, J. Mackay, D. Dickerson, and S. Jayaraman, "Environmental monitoring of remedial dredging at the New Bedford Harbor, MA, superfund site," *Environmental Monitoring and Assessment*, 2005. 111(1-3): p. 257-275.

- [59] Madenjian, C.P., D.J. Jude, R.R. Rediske, J.P. O'Keefe, and G.E. Noguchi, "Gender difference in walleye PCB concentrations persists following remedial dredging," *Journal of Great Lakes Research*, 2009. 35(3): p. 347-352.
- [60] Su, S.H., L.C. Pearlman, J.A. Rothrock, T.J. Iannuzzi, and B.L. Finley, "Potential long-term ecological impacts caused by disturbance of contaminated sediments: A case study," *Environmental Management*, 2002. 29(2): p. 234-249.
- [61] Voie, O.A., A. Johnsen, and H. Kristin Rossland, "Why biota still accumulate high levels of PCB after removal of PCB contaminated sediments in a Norwegian fjord," *Chemosphere*, 2002. 46(9-10): p. 1367-1372.
- [62] Mikszewski, A., "Emerging Technologies for the In Situ Remediation of PCB-Contaminated Soils and Sediments: Bioremediation and Nanoscale Zero-Valent Iron," N.N.f.E.M.S. Fellow, 2004, *USEPA*. p. 30.
- [63] Förstner, U. and S.E. Apitz, "Sediment remediation: U.S. Focus on Capping and Monitored Natural Recovery. Fourth International Battelle Conference on Remediation of Contaminated Sediments," *Journal of Soils and Sediments*, 2007. 7(6): p. 351-358.
- [64] Vita, C., P. Johanson, and D. Leisle. "Marine Sediment Monitoring and Natural Recovery at the Bremonton Naval Complex," in *Battelle Sediment Conference Proceedings*. 2011. Columbus.
- [65] Carbonnenu, K. and C.H. Floess. "Thin Layer Capping and Long-Term Environmental Monitoring: A Design Plan, Marathon Environmental Remediation, Marathon, Ontario," in *Battelle Sediment Conference Proceedings*. 2011.

- [66] Merritt, K., J. Conder, and V. Magar, "Enhanced Monitored Natural Recovery Case Studies Review," 2009. p. 55.
- [67] Sumari, A. "Dredged Materials is of a Spoil-A Status on the Use of Dredged Material in Puget Sound to Isolate Contaminated Sediments," in *14th World Dredging Congress*. 1995. Amsterdam, The Netherlands.
- [68] Cornelissen, G., K. Amstaetter, A. Hauge, M. Schaanning, B. Beylich, J.S. Gunnarsson, G.D. Breedveld, A.M.P. Oen, and E. Eek, "Large-scale field study on thin-layer capping of marine PCDD/F-contaminated sediments in grelandfjords, Norway: Physicochemical effects," *Environmental Science and Technology*, 2012. 46(21): p. 12030-12037.
- [69] Ghosh, U., R.G. Luthy, G. Cornelissen, D. Werner, and C.A. Menzie, "In-situ sorbent amendments: A new direction in contaminated sediment management," *Environmental Science and Technology*, 2011. 45(4): p. 1163-1168.
- [70] McDonough, K.M., P. Murphy, J. Olsta, Y. Zhu, D. Reible, and G.V. Lowry, "Development and placement of a sorbent-amended thin layer sediment cap in the Anacostia River," *Soil and Sediment Contamination*, 2007. 16(3): p. 313-322.
- [71] Cho, Y.M., U. Ghosh, A.J. Kennedy, A. Grossman, G. Ray, J.E. Tomaszewski, D.W. Smithenry, T.S. Bridges, and R.G. Luthy, "Field application of activated carbon amendment for in-situ stabilization of polychlorinated biphenyls in marine sediment," *Environmental Science and Technology*, 2009. 43(10): p. 3815-3823.
- [72] Cho, Y.M., D.W. Smithenry, U. Ghosh, A.J. Kennedy, R.N. Millward, T.S. Bridges, and R.G. Luthy, "Field methods for amending marine sediment with activated carbon and assessing treatment effectiveness," *Marine Environmental*

- Research*, 2007. 64(5): p. 541-555.
- [73] Choi, H., S. Agarwal, and S.R. Al-Abed, "Adsorption and Simultaneous Dechlorination of PCBs on GAC/Fe/Pd: Mechanistic Aspects and Reactive Capping Barrier Concept," *Environmental Science and Technology*, 2009a. 43(2): p. 488-493.
- [74] Cornelissen, G., M. Elmquist Kruså, G.D. Breedveld, E. Eek, A.M.P. Oen, H.P.H. Arp, C. Raymond, G. Samuelsson, J.E. Hedman, O. Stokland, and J.S. Gunnarsson, "Remediation of contaminated marine sediment using thin-layer capping with activated carbon-A field experiment in Trondheim harbor, Norway," *Environmental Science and Technology*, 2011. 45(14): p. 6110-6116.
- [75] Kalinovich, I., A. Rutter, J.S. Poland, G. Cairns, and R.K. Rowe, "Remediation of PCB contaminated soils in the Canadian Arctic: Excavation and surface PRB technology," *Science of the Total Environment*, 2008. 407(1): p. 53-66.
- [76] Tomaszewski, J.E., D. Werner, and R.G. Luthy, "Activated carbon amendment as a treatment for residual DDT in sediment from a superfund site in San Francisco Bay, Richmond, California, USA," *Environmental Toxicology and Chemistry*, 2007. 26(10): p. 2143-2150.
- [77] Jonker, M.T.O., A.M. Hoenderboom, and A.A. Koelmans, "Effects of sedimentary sootlike materials on bioaccumulation and sorption of polychlorinated biphenyls," *Environmental Toxicology and Chemistry*, 2004. 23(11): p. 2563-2570.
- [78] Jonker, M.T.O. and A.A. Koelmans, "Sorption of polycyclic aromatic hydrocarbons and polychlorinated biphenyls to soot and soot-like materials in the

- aqueous environment: Mechanistic considerations," *Environmental Science and Technology*, 2002. 36(17): p. 3725-3734.
- [79] Nollet, H., M. Roels, P. Lutgen, P. Van Der Meeren, and W. Verstraete, "Removal of PCBs from wastewater using fly ash," *Chemosphere*, 2003. 53(6): p. 655-665.
- [80] Shaheen, S.M., P.S. Hooda, and C.D. Tsadilas, "Opportunities and challenges in the use of coal fly ash for soil improvements – A review," *Journal of Environmental Management*, 2014. 145: p. 249-267.
- [81] Beless, B., H.S. Rifai, and D.F. Rodrigues, "Efficacy of carbonaceous materials for sorbing polychlorinated biphenyls from aqueous solution," *Environmental Science and Technology*, 2014. 48(17): p. 10372-10379.
- [82] Lin, S.C., N. Gan, J.B. Zhang, X.D. Chen, Y.T. Cao, and T.H. Li, "A novel reductive graphene oxide-based magnetic molecularly imprinted poly (ethylene-co-vinyl alcohol) polymers for the enrichment and determination of polychlorinated biphenyls in fish samples," *Journal of Molecular Recognition*, 2015. 28(6): p. 359-368.
- [83] Ndunda, E.N. and B. Mizaikoff, "Multi-walled carbon nanotubes: innovative sorbents for pre-concentration of polychlorinated biphenyls in aqueous environments," *Analytical Methods*, 2015. 7(19): p. 8034-8040.
- [84] Parks, A.N., G.T. Chandler, L.M. Portis, J.C. Sullivan, M.M. Perron, M.G. Cantwell, R.M. Burgess, K.T. Ho, and P.L. Ferguson, "Effects of single-walled carbon nanotubes on the bioavailability of PCBs in field-contaminated sediments," *Nanotoxicology*, 2014. 8: p. 111-117.

- [85] Wang, S., P.J. Chia, L.L. Chua, L.H. Zhao, R.Q. Png, S. Sivaramakrishnan, M. Zhou, R.G.S. Goh, R.H. Friend, A.T.S. Wee, and P.K.H. Ho, "Band-like transport in surface-functionalized highly solution-processable graphene nanosheets," *Advanced Materials*, 2008. 20(18): p. 3440-3446.
- [86] Allen, M.J., V.C. Tung, and R.B. Kaner, "Honeycomb carbon: A review of graphene," *Chemical Reviews*, 2010. 110(1): p. 132-145.
- [87] Novoselov, K.S., A.K. Geim, S.V. Morozov, D. Jiang, Y. Zhang, S.V. Dubonos, I.V. Grigorieva, and A.A. Firsov, "Electric field in atomically thin carbon films," *Science*, 2004. 306(5696): p. 666-669.
- [88] Nasrollahzadeh, M., F. Babaei, P. Fakhri, and B. Jaleh, "Synthesis, characterization, structural, optical properties and catalytic activity of reduced graphene oxide/copper nanocomposites," *RSC Advances*, 2015. 5(14): p. 10782-10789.
- [89] Iijima, S., "Helical microtubules of graphitic carbon," *Nature*, 1991. 354(6348): p. 56-58.
- [90] Choudhary, V. and A. Gupta, "Polymer/Carbon Nanotube Nanocomposites." Carbon Nanotubes - Polymer Nanocomposites. 2011.
- [91] De Volder, M.F.L., S.H. Tawfick, R.H. Baughman, and A.J. Hart, "Carbon nanotubes: Present and future commercial applications," *Science*, 2013. 339(6119): p. 535-539.
- [92] Spitalsky, Z., D. Tasis, K. Papagelis, and C. Galiotis, "Carbon nanotube-polymer composites: Chemistry, processing, mechanical and electrical properties," *Progress in Polymer Science (Oxford)*, 2010. 35(3): p. 357-401.

- [93] Long, R.Q. and R.T. Yang, "Carbon nanotubes as superior sorbent for dioxin removal [1]," *Journal of the American Chemical Society*, 2001. 123(9): p. 2058-2059.
- [94] Port of Houston Authority, U.S. "About the Port." The Port Delivers 2015 10/10/2015]; Available from: <http://www.portofhouston.com/about-us/overview/>.
- [95] MacLeod Jr., W.D., D.W. Brown, A.J. Friedman, D.G. Burrows, O. Maynes, R.W. Pearce, C.A. Wigren, and R.C. Bogar. "Standard Analytical Procedures of the NOAA National Analytical Facility." Extractable Toxic Organic Compounds, Second Edition 1985 02/20/2016]; Available from: <http://www.st.nmfs.noaa.gov/tm/nwc/nwc092.pdf>.
- [96] McFarland, V.A. and J.U. Clarke, "Environmental Occurrence, Abundance, and Potential Toxicity of Polychlorinated Biphenyl Congeners: Considerations for a Congener-Specific Analysis," *Environmental Health Perspectives*, 1989. 81: p. 225-239.
- [97] Balasubramani, A. and H.S. Rifai, "Occurrence and distribution of polychlorinated dibenzo-p-dioxins and polychlorinated dibenzofurans (PCDD/Fs) in industrial and domestic sewage sludge," *Environmental Science and Pollution Research*, 2015. 22(19): p. 14801-14808.
- [98] Howell, N.L. and H.S. Rifai, "Longitudinal estimates of sediment-water diffusive flux of PCB congeners in the Houston Ship Channel," *Estuarine, Coastal and Shelf Science*, 2015a. 164: p. 19-27.
- [99] Howell, N.L. and H.S. Rifai, "PCDD/F and PCB water column partitioning examination using natural organic matter and black carbon partition coefficient

- models," *Environmental Science and Pollution Research*, 2015b: p. 1-12.
- [100] Sappington, E.N., A. Balasubramani, and H.S. Rifai, "Polychlorinated dibenzo-p-dioxins and polychlorinated dibenzofurans (PCDD/Fs) in municipal and industrial effluents," *Chemosphere*, 2015. 133: p. 82-89.
- [101] Schwarzenbach, R.P., P.M. Gschwend, and D.M. Imboden, "Environmental Organic Chemistry." 2003, Hoboken, NJ: Wiley.
- [102] Howell, N.L., "Bed and suspended sediment as source and transport mechanisms for polychlorinated biphenyls (PCBs) in the Houston Ship Channel estuary system," in Civil and Environmental Engineering 2012, *University of Houston*.
- [103] Halfon, E. and R.J. Allan, "Modelling the fate of PCBs and MIREX in aquatic ecosystems using the TOXFATE model," *Environment International*, 1995. 21(5): p. 557-569.
- [104] Zimmerman, J.R., J.D. Bricker, C. Jones, P.J. Dacunto, R.L. Street, and R.G. Luthy, "The stability of marine sediments at a tidal basin in San Francisco Bay amended with activated carbon for sequestration of organic contaminants," *Water Research*, 2008. 42(15): p. 4133-4145.
- [105] Everaert, G., F. De Laender, K. Deneudt, P. Roose, J. Mees, P.L.M. Goethals, and C.R. Janssen, "Additive modelling reveals spatiotemporal PCBs trends in marine sediments," *Marine Pollution Bulletin*, 2014. 79(1-2): p. 47-53.
- [106] LeBlanc, L.A., J.A. Buckel, D.O. Conover, and B.J. Brownawell, "Tests of bioaccumulation models for polychlorinated biphenyl compounds: A study of young-of-the-year bluefish in the Hudson River Estuary, USA," *Environmental Toxicology and Chemistry*, 2006. 25(8): p. 2067-2076.

- [107] Loizeau, V., A. Abarnou, P. Cugier, A. Jaouen-Madoulet, A.M. Le Guellec, and A. Menesguen, "A model of PCB bioaccumulation in the sea bass food web from the Seine Estuary (Eastern English Channel)," *Marine Pollution Bulletin*, 2001. 43(7-12): p. 242-255.
- [108] Bai, S. and W.S. Lung, "Modeling sediment impact on the transport of fecal bacteria," *Water Research*, 2005. 39(20): p. 5232-5240.
- [109] Liu, X. and W. Huang, "Modeling sediment resuspension and transport induced by storm wind in Apalachicola Bay, USA," *Environmental Modelling and Software*, 2009. 24(11): p. 1302-1313.
- [110] Liu, Z., N.B. Hashim, W.L. Kingery, D.H. Huddleston, and M. Xia, "Hydrodynamic Modeling of St. Louis Bay Estuary and Watershed Using EFDC and HSPF," *Journal of Coastal Research*, 2008: p. 107-116.
- [111] O'Donncha, F., S.C. James, and E. Ragnoli, "Modelling study of the effects of suspended aquaculture installations on tidal stream generation in Cobscook Bay," *Renewable Energy*, 2017. 102, Part A: p. 65-76.
- [112] Ren, H., Y. Tao, and J. Xia, "Characteristics of water environment and response to sudden loads of pollution due to accidents in Shenzhen Bay," *Yingyong Jichu yu Gongcheng Kexue Xuebao/Journal of Basic Science and Engineering*, 2011. 19(1): p. 52-63.
- [113] Tuckey, B.J., M.T. Gibbs, B.R. Knight, and P. Gillespie, "Tidal circulation in Tasman and Golden Bays: Implications for river plume behaviour," *New Zealand Journal of Marine and Freshwater Research*, 2006. 40(2): p. 305-324.
- [114] Zhou, J., R.A. Falconer, and B. Lin, "Refinements to the EFDC model for

- predicting the hydro-environmental impacts of a barrage across the Severn Estuary," *Renewable Energy*, 2014. 62: p. 490-505.
- [115] Gschwend, P.M. and S. Wu, "On the constancy of sediment-water partition coefficients of hydrophobic organic pollutants," *Environmental Science & Technology*, 1985. 19(1): p. 90-96.
- [116] USEPA, "Method 1668, Revision A: Chlorinated Biphenyl Congeners in Water, Soil, Sediment, and Tissue by HRGC/HRMS.," *Washington, D.C: USEPA National Office*, 1999: p. 133.
- [117] USEPA. "Method 8082A, Revision 1, Polychlorinated Biphenyls (PCBs) by Gas Chromatography." 2007 12/02/2015]; Available from:
<http://www3.epa.gov/epawaste/hazard/testmethods/sw846/pdfs/8082a.pdf>.
- [118] Lu, X., A. Skwarski, B. Drake, and D.D. Reible, "Predicting bioavailability of PAHs and PCBs with porewater concentrations measured by solid-phase microextraction fibers," *Environmental Toxicology & Chemistry*, 2011. 30(5): p. 1109-1116.
- [119] Janjic, Z., R. Gall, and M.E. Pyle, "Scientific Documentation for the NMM Solver", R.A. Laboratory, 2010, *National Center for Atmospheric Research (NCAR)*: Colorado. p. 54.
- [120] Ji, Z.-G., "Pathogens and Toxics," in Hydrodynamics and Water Quality: Modeling Rivers, Lakes, and Estuaries. 2008, *Wiley-Interscience*. p. 702.
- [121] Rahman, M.M., M. Lu, and K.H. Kyi, "Seasonality of hydrological model spin-up time: a case study using the Xinanjiang model," *Hydrol. Earth Syst. Sci. Discuss.*, 2016. 2016: p. 1-22.

- [122] Bolzonella, D., F. Fatone, P. Pavan, and F. Cecchi, "Poly-chlorinated dibenzo-p-dioxins, dibenzo-furans and dioxin-like poly-chlorinated biphenyls occurrence and removal in conventional and membrane activated sludge processes," *Bioresource Technology*, 2010. 101(24): p. 9445-9454.
- [123] Guo, L., B. Zhang, K. Xiao, Q.H. Zhang, and M.H. Zheng, "Levels and distributions of polychlorinated biphenyls in sewage sludge of urban wastewater treatment plants," *Journal of Environmental Sciences-China*, 2009. 21(4): p. 468-473.
- [124] Dow. "Dow in Texas - Deer Park." 2009; Available from: <http://www.dow.com/texas/deerpark/about/index.htm>.
- [125] Burkhard, L.P., "Estimating Dissolved Organic Carbon Partition Coefficients for Nonionic Organic Chemicals," *Environmental Science & Technology*, 2000. 34(22): p. 4663-4668.
- [126] Seth, R., D. Mackay, and J. Muncke, "Estimating the Organic Carbon Partition Coefficient and Its Variability for Hydrophobic Chemicals," *Environmental Science & Technology*, 1999. 33(14): p. 2390-2394.
- [127] Hansen, B.G., A.B. Paya-Perez, M. Rahman, and B.R. Larsen, "QSARs for KOW and KOC of PCB congeners: A critical examination of data, assumptions and statistical approaches," *Chemosphere*, 1999. 39(13): p. 2209-2228.

